

Aus dem  
Oscar – Langendorff – Institut für Physiologie  
Gertrudenstraße 9  
18057 Rostock

Direktor: Prof. Dr. R. Köhling

Intrinsische Koordination und nervale Modulation der  
glatten Muskulatur des Gastrointestinaltrakts:  
Vom Organmodell zur klinischen Funktionsstörung

**Habilitationsschrift**

Zur Erlangung des akademischen Grades  
Doctor medicinae habilitatus (Dr. med. habil.)  
der Universitätsmedizin Rostock

Vorgelegt von: Dr. med. Robert Patejdl  
Geboren am: 09.03.1982  
Wohnhaft in: Benitz

Dekan: Prof. Dr. med. Emil Christian Reisinger, Universitätsmedizin Rostock

1. Gutachter: Prof. Dr. Rüdiger Köhling, Universität Rostock, Physiologie
2. Gutachter: Prof. Dr. Michael Schemann, TU München, Humanbiologie
3. Gutachter: Prof. Dr. Lothar Just, Universität Tübingen, Anatomie

Die öffentliche Habilitationsverteidigung fand am 26.04.2021 statt.

Die öffentliche Lehrprobe fand am 26.05.2021 statt.

# Inhaltsverzeichnis

1. EINLEITUNG UND FRAGESTELLUNGEN .....	4
1.1 KOORDINIERUNG UND MODULATION GLATTMUSKULÄRER AKTIVITÄT.....	4
1.2 PATHOPHYSIOLOGIE DER GESTÖRTEN INTESTINALEN MOTILITÄT.....	7
1.3 FRAGESTELLUNGEN DER VORLIEGENDEN ARBEIT .....	7
2. METHODIK .....	10
2.1 EXPERIMENTELLE <i>IN VITRO</i> – EXPERIMENTE (ARBEITEN 1-4).....	10
2.2 HUMANE <i>IN VIVO</i> „ <i>PROOF-OF-CONCEPT</i> “ – STUDIEN (ARBEITEN 5 UND 6).....	10
3. ERGEBNISSE .....	11
3.1 KONFOKALMIKROSKOPISCHE NETZWERKANALYSE.....	11
3.2 KOPPLUNGSHEMMENDE EFFEKTE DES $Na_v$ -BLOCKERS PHENYTOIN.....	12
3.3 KOPPLUNGSFÖRDERNDE EFFEKTE DES $Na_v$ -BLOCKERS AJMALIN.....	13
3.4 GRADUELLE TONISCHE KONTRAKTION DURCH DEN $S1P$ -AGONISTEN FTY720.....	13
3.5 SCHLAGANFÄLLE UND GASTROINTESTINALE MOTILITÄTSSTÖRUNGEN .....	14
3.6 PERIPHERE NEUROMYOPATHIE UND GASTROINTESTINALE MOTILITÄTSSTÖRUNGEN..	16
4. DISKUSSION .....	17
5. ZUSAMMENFASSUNG.....	21
6. LITERATURVERZEICHNIS .....	22
7. VERZEICHNIS DER PUBLIKATIONEN UND VORTRÄGE.....	33
8. EIDESSTATTLICHE ERKLÄRUNG .....	38
9. DANKSAGUNG .....	39

# 1. Einleitung und Fragestellungen

## 1.1 Koordinierung und Modulation glattemuskulärer Aktivität

Die kontraktile Funktion der glatten Muskulatur ist essenziell für die Aufrechterhaltung und Regulation zahlreicher Grundfunktionen des Körpers wie Blutdruck und Durchblutung, Nahrungstransport und Harnausscheidung [1]. Die Kontraktionsmuster glattemuskulärer Gewebe sind in hohem Maße an die organspezifischen physiologischen Funktionen angepasst und können in den drei Dimensionen *Intensität* (Kontraktionskraft), *Zeit* (Kontraktionsdauer und -häufigkeit) und *Ort* (räumliche Ausdehnung der Kontraktion) definiert werden [2, 3]. Auch die Mechanismen der Kontraktionssteuerung variieren von einer direkten und exakten neuronalen Kontrolle einzelner Kontraktionen im Falle der inneren Augenmuskeln [4] bis hin zur reinen Ansteuerung und Modulation lokaler, weitgehend autonom funktionierender Kontraktionsmuster wie im Falle der von lokalen und systemischen Signalen modulierten „basalen organeigenen Rhythmik“ (BOR) in weiten Teilen des Gastrointestinaltrakts [5, 6].

Aufgrund ihrer großen homöostatischen – und damit auch klinischen – Relevanz wird die glatte Muskulatur seit über 100 Jahren unter physiologischen und pathophysiologischen Bedingungen untersucht, um aus experimentellen Befunden Schlussfolgerungen über Erkrankungen, ihre Pathomechanismen und Behandlung abzuleiten.

Weiterhin ist die glatte Muskulatur aufgrund der Komplexität ihrer neuronalen und biochemischen Steuerung ein Gewebe, an dem es sehr häufig zur Ausbildung von unerwünschten Arzneimittelwirkungen oder funktionellen Störungen im Rahmen systemischer Erkrankungen (z.B. Elektrolytstörungen, ZNS-Erkrankungen oder systemischer Inflammation) kommt.

Die vorliegende Arbeit verbindet experimentelle Befunde zur Kontraktionssteuerung isolierter glatter Muskulatur mit klinischen Untersuchungen zu gastrointestinalen Funktionsstörungen bei Patienten. Damit soll nicht nur das große analytische Potenzial der Untersuchungen isolierter glatter Muskulatur, sondern auch deren Relevanz und ihre Vorhersagekraft für klinische *in vivo* - Szenarien gezeigt werden.

Neben fluoreszenzmikroskopischen Methoden, digitalen Datenprozessierungstechniken und klinischer Elektrophysiologie kommt dabei der traditionellen Organbadtechnik zur Analyse des Kontraktionsverhaltens intakter nativer Gewebepreparate eine zentrale Rolle zu. Diese leitet sich aus dem Erkenntnisgewinn der letzten Jahre zur Physiologie der interzellulären Koordination gastrointestinaler glatter Muskulatur und zur Bedeutung des Nervensystems für die Modulation der glatten Muskulatur des Gastrointestinaltrakts ab. Frühere Organbadstudien gingen von grundsätzlich anderen Prämissen, z.B. zur Rolle der ICC und des ENS aus [7]. In den letzten Jahren haben sich daher neue

Fragestellungen und methodische Ansätze für Organbadexperimente ergeben. Diese Arbeit stellt dabei die Koordination und Steuerung des Kontraktionsverhaltens der glatten Muskulatur des Magens und der Portalvene in den Mittelpunkt.

Die unmittelbare Kontraktion glatter Muskelzellen wird durch eine vermehrte Phosphorylierung der regulatorischen leichten Kette des Myosins ausgelöst, für die eine Erhöhung der Aktivität der Myosin-Leichkettenkinase (MLCK) oder eine Hemmung der Myosin-Leichkettenphosphatase (MLCP) nötig ist [8]. Zahlreiche Signalwege beeinflussen die glattnuskuläre Kontraktibilität, zentral für die dynamische Steuerung der MLCK-Aktivität sind jedoch Anstiege der zyttoplasmatischen Kalziumkonzentration ( $[Ca^{2+}]_i$ ) [9–14]. Diese erfolgen entweder als Ergebnis eines Kalziumeinstroms über spannungsabhängige Kalziumkanäle (VDCC) vom L-Typ oder infolge einer Kalziumfreisetzung aus intrazellulären Speichern [15].

Die glatte Muskulatur des Magens zerfällt funktionell in zwei Anteile: die des stark dehnbaren proximalen Fundus und die des rhythmisch kontrahierenden distalen Magenanspruchs. Der Fundus dient als Reservoir und die ihn umschließende Muskelschicht entwickelt einen stabilen Tonus, welcher die aufgenommene Nahrung stetig in Richtung des Antrums drückt [16–19]. Der vom Fundus entwickelte stetige Druck in Richtung auf den Magenausgang schafft die Voraussetzung dafür, dass die im Antrumbereich stattfindenden phasisch-rhythmischen Kontraktionen den Speisebrei effektiv weiter durchmischen und zerkleinern können [20–22].

Nachdem das Verhalten der spontanaktiven gastrointestinalen Muskulatur lange Zeit als intrinsisch von Myozyten generiert und vom autonomen Nervensystem moduliert aufgefasst worden war, entwickelten sich seit den 80er Jahren des 20. Jahrhunderts weitaus differenzierte Konzepte [7, 23–25]. Vereinfachend kann das aktuelle Konzept wie folgt zusammengefasst werden:

Sowohl die tonische Kontraktion des Magenfundus als auch die phasischen Kontraktionen des Magenanspruchs basieren auf der Generierung, Ausbreitung und nervalen Modulation elektrischer Erregungen im Gewebe [25, 26]. Verantwortlich für die Erzeugung der rhythmischen Depolarisationen, in deren Folge es zur Öffnung der VDCC in elektrisch über Gap Junctions angekoppelten glatten Muskelzellen kommt, sind im Gastrointestinaltrakt spezifische Schrittmacherzellen, die zur Gruppe der interstitiellen Zellen nach Cajal (*interstitial cells of Cajal*, ICC) gehören [27–30]. Die rhythmischen Potenzialschwankungen der zwischen Ring- und Längsmuskelschicht im Plexus myentericus lokalisierten ICC (ICC-My) laufen ununterbrochen ab, der Bedarf für mechanische Aktivität ist jedoch nicht ständig gegeben, sondern im Gegenteil

diskontinuierlich und in verschiedenen Regionen sequenziell vorhanden. Ob die spontanen Depolarisationen der ICC-My zu Kontraktionen führen, hängt einerseits von deren Amplitude (also der Stärke der in den ICC-My generierten Einwärtsströme), andererseits vom Bahnungszustand, also der Erregbarkeit der glatten Muskelzellen selbst ab [23, 24, 31–35]. Beide Faktoren werden durch das enterische Nervensystem (ENS) reguliert, welches die übergroße Mehrzahl der Neurone des Plexus myentericus bildet und sowohl mit den ICC-My als auch mit den die Erregbarkeit der Myozyten modulierenden „intramuskulären ICC“ (ICC-IM) zahlreiche synaptische Verbindungen unterhält [36–39].

Das ENS wird nach gegenwärtiger Ansicht neben dem zentralen, dem somatisch-peripheren und dem vegetativen Nervensystem als eine eigenständige Komponente anerkannt [40, 41]. Es integriert luminale chemische und mechanische Signale mit hormonellen Einflüssen und den Steuersignalen des klassischen vegetativen (autonomen) Nervensystems (Parasympathikus/Sympathikus) und koordiniert die gastrointestinale Motilität über Steuersignale, die es indirekt über eine Modulation der ICC an die glatte Muskulatur übermittelt [42]. Die synaptischen Netzwerke des ENS ermöglichen – ähnlich wie im Rückenmark – den autonomen Ablauf einfacher Programme (z.B. des peristaltischen Reflexes [43–46]), welche auch nach Abkopplung vom vegetativen und zentralen Nervensystem die Erhaltung einer basalen Motilität sichern [47–51]. Wie spezifisch und wie effektiv die letztlich von den ICC generierten Steuersignale die Muskulatur erregen, hängt wesentlich von der interzellulären Kopplung zwischen beiden ab, deren Charakterisierung daher einen besonderen Schwerpunkt in der vorliegenden Arbeit einnimmt.

Historisch wurde die phasisch aktive glatte Muskulatur des Gastrointestinaltrakts und der Portalvene dem Single-unit-Typ zugeordnet [52–54]. Das Single-Unit-Konzept postuliert eine starke und stabile elektrische Kopplung der Myozyten im Synzytium des Gewebes und die Ausbreitung lokal entstehender Erregungen über viele Zellen hinweg [55–58]. Variationen der Kopplungsstärke als mögliche weitere Modulationsebene (bzw. als Ziel für andere Modulatoren wie Innervation und hormonelle Steuerung) für die Aussteuerung der Kraft wurden außerhalb pathologischer Situationen mit gestörter zellulärer Netzwerkintegrität entsprechend bislang nur vereinzelt für die glatte Muskulatur arterieller Gefäße und des Uterus, nicht jedoch für die des Gastrointestinaltrakts berücksichtigt [59–63]. Die experimentelle Charakterisierung der interzellulären Kopplung im phasisch aktiven glatten Muskel unter spontanen Bedingungen, unter pharmakologischem Agonisteneinfluss sowie unter Einwirkung klinisch relevanter Ionenkanalblocker erscheint daher besonders geeignet, unser Verständnis gastrointestinaler Motilitätsstörungen zu verbessern [63–68].

## **1.2 Pathophysiologie der gestörten intestinalen Motilität**

Die Funktion der Motilität des Gastrointestinaltrakts besteht vereinfachend darin, trotz einer diskontinuierlichen Nahrungsaufnahme den nachgeschalteten Darmabschnitten eine stets an die lokale Kapazität für Resorption und osmotischen Ausgleich angepasste Menge und Form von Nahrungsbrei zuzuführen [69, 70]. Abgeleitet daraus können Störungen in zwei Richtungen auftreten:

Eine zu schnelle Entleerung überfordert die Resorptionskapazität, so dass Nährstoffe verlorengehen und in den nachfolgenden Darmabschnitten durch die Interaktion mit dem intestinalen Mikrobiom zu Flatulenz und mikrobiellen Fehlbesiedlungen führen. Weiterhin kann es insbesondere nach Gastrektomien durch osmotische Ausgleichsphänomene zu Flüssigkeitsverlagerungen kommen, die herausfordernd für die Kreislaufregulation sind („Dumping-Syndrom“) [71].

Eine Hypomotilität (in Abwesenheit eines mechanischen Hindernisses) wird im Fall des Magens als Gastroparese bzw. sonst allgemein als Darmträgheit („Konstipation“) bezeichnet. Sie ist regelhaft mit einer Reduktion der koordinierten phasischen Aktivität der glatten Muskulatur verbunden [72]. Neben subjektiven Beschwerden wie frühzeitiger Sättigung, Gewichtsverlust, Oberbauchschmerzen und Übelkeit stellt die Gastroparese insbesondere in älteren Patientenpopulationen und unter den häufig betroffenen Diabetikern durch die geänderte Resorptionsdynamik von oral applizierten Medikamenten bzw. die Verzögerung der Glukoseaufnahme nach Insulininjektion ein teils erhebliches medizinisches Komplikationsrisiko dar. Bei kritisch kranken Patienten kann sie zu Problemen in der Enteralisierung der Ernährung führen [73–76].

Schätzungen zur Prävalenz der Gastroparese liegen zwischen 13 und 50 Fälle pro 100.000 in der Allgemeinbevölkerung. Da ca. ein Drittel der Fälle auf einen Diabetes mellitus zurückgeführt wird, ist die Prävalenz unter Diabetikern entsprechend größer [77–79]. Die patientenspezifische Pathophysiologie hinsichtlich der betroffenen Signalwege oder Zellpopulationen ist oft unbekannt, bestehende Therapieverfahren haben oft nur eine unbefriedigende Wirksamkeit [76].

## **1.3 Fragestellungen der vorliegenden Arbeit**

Medizinisch relevante Motilitätsstörungen treten stark gehäuft in Situationen auf, in denen potenziell mehrere Ebenen der glattmuskulären Modulation verändert sind, da bei schweren Allgemeinerkrankungen gleichzeitig sowohl eine intensive Polypharmazie als auch Störungen der Funktion des Nervensystems auftreten [80–83]. So können zahlreiche klinisch eingesetzte Pharmaka oder endogen im Rahmen von Erkrankungen gebildete Mediatoren mit Ionenkanälen auf Neuronen, ICC und Myozyten interagieren und auf diesem Weg – insbesondere bei Patienten mit ohnehin erhöhtem Risiko, z.B.

durch das Vorliegen eines Diabetes mellitus – zu Störungen der Magenmotilität führen [84, 85]. Dennoch existieren bezogen auf die Funktion der Magenmuskulatur kaum klinische oder experimentelle Studien darüber, in welchem Ausmaß und über welche Mechanismen einzelne Substanzen die lokalen Kontraktionsmuster beeinflussen.

Gegenstand der vorliegenden Arbeit sind daher zum einen die Kontraktionsmuster isolierter Magen- und Portalvenenmuskulatur sowie ihre Veränderung durch exogene- und endogene Substanzen. Im Fokus stehen dabei Ionenkanalblocker mit bekannter antiepileptischer bzw. antiarrhythmischer Wirkung sowie die immunmodulatorische Substanz FTY720, welche potenzielle „Drug-targets“ in Gestalt spannungs- und rezeptorgesteuerter Ionenkanäle der Myozyten, der ANS- und ENS- Neurone sowie der ICC beeinflussen [86–91]. Zum anderen wird der Frage nachgegangen, inwieweit speziell Schlaganfälle und akute Neuromyopathien an der Entstehung der intensivmedizinisch häufig vorkommenden Motilitätsstörungen des Gastrointestinaltrakts beteiligt sind [73, 92].

Schematisch fasst Abbildung 1 den analytischen Ansatz der vorliegenden Arbeit zusammen.

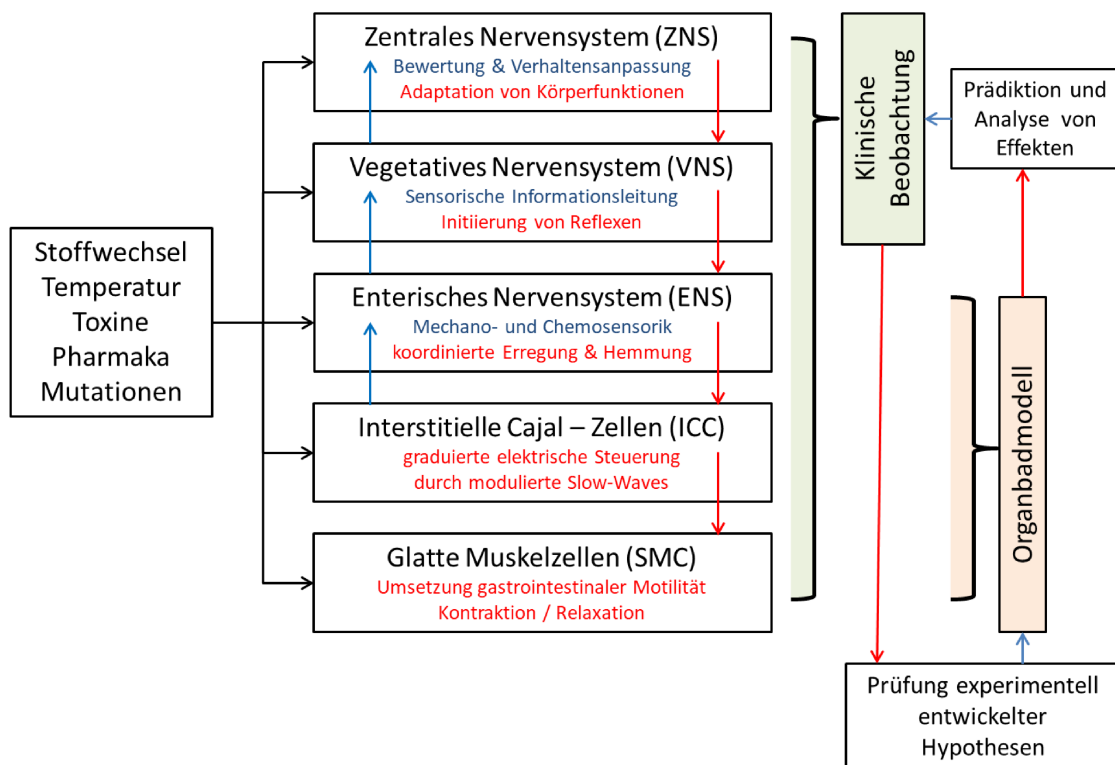


Abbildung 1: Anatomisch-funktionell relevante Instanzen für die Generierung und Modulation gastrointestinaler Motilität. Im Organbad sind gezielte, modellhafte Analysen von Einflussfaktoren auf motorische Muster unter Beteiligung von ENS, ICC und SMC möglich. Die klinisch beobachtbaren funktionellen Änderungen zeigen hingegen die summierten Wirkungen von Einflussfaktoren auf allen Ebenen vom ZNS bis hin zur glatten Muskulatur an. Sie besitzen unmittelbare Relevanz, die an ihrer Entstehung beteiligten Systeme und Mechanismen sind jedoch ohne komplementäre wissenschaftliche Ansätze nicht sicher zuzuordnen.

Konkret werden in den nachfolgend referierten Arbeiten einerseits die räumlich-zeitlichen Eigenschaften der Kraftentwicklung im glatten Muskel von Magen und Portalvene unter physiologischen Bedingungen und unter Einwirkung von Substanzen mit direkten und indirekten Wirkungen auf Ionenkanäle und die glattmuskuläre Erregbarkeit in vitro analysiert (**Arbeiten 1-4, [93–96]**). Weiterhin werden die Auswirkungen von Läsionen des zentralen Nervensystems (ZNS) bei Schlaganfällen sowie des peripheren Nervensystems (PNS) im Rahmen schwerer Allgemeinerkrankungen auf Surrogatparameter der intestinalen Motilität untersucht (**Arbeiten 5 und 6, [97, 98]**). Die genannten Untersuchungen können auf drei zentrale Forschungsfragen kondensiert werden:

- Wie ausgeprägt ist die interzelluläre Kopplung der intrazellulären Kalziumkonzentration in einem typischen phasisch aktiven glattmuskulären Gewebe (Portalvene)?
- Welche Wirkungen haben die Klasse-I-Antiarrhythmika Phenytoin und Ajmalin auf die mechanische phasische Aktivität und Kopplung der glatten Muskulatur?
- Wie wichtig ist die vom zentralen und peripheren Nervensystem ausgehende Steuerung für die Aufrechterhaltung der gastrointestinalen Motilität?

## 2. Methodik

Die eingesetzten experimentellen und statistischen Methoden werden in den Originalarbeiten ausführlich dargelegt. Im Rahmen der *in vitro* – Experimente wurden ausschließlich Experimente an Geweben nach der Tötung der Versuchstiere zu wissenschaftlichen Zwecken im Sinne des §4 Abs 2 TierschG durchgeführt.

### 2.1 Experimentelle *in vitro* – Experimente (Arbeiten 1-4)

Die zeitlichen Kontraktionsmuster von Streifenpräparaten verschiedener glattmuskulärer Gewebe der Ratte wurden isometrisch im Organbad registriert. In den **Arbeiten 1-3** [93–95] erfolgte zudem eine Registrierung der extrazellulären elektrischen Feldpotentiale, in den **Arbeiten 1 und 2** zudem eine fluoreszenzbasierte Messung der freien intrazellulären Kalziumkonzentration. In allen *in vitro* – Arbeiten wurden pharmakologische Agonisten- / Antagonistenexperimente mit quantitativen Auswertungen vorgenommen.

### 2.2 Humane *in vivo* „proof-of-concept“ – Studien (Arbeiten 5 und 6)

Zur Frage, ob Schlaganfälle oder periphere akute Polyneuropathien im Vergleich zu schweren Allgemeinerkrankungen ohne ZNS- bzw. PNS-Schädigung signifikant mit dem Auftreten gastrointestinaler Motilitätsstörungen assoziiert sind, wurden zwei verschiedene Kohortenstudien konzipiert und durchgeführt, von denen die **Arbeiten 5 und 6** klinische Surrogatparameter nutzten, während **Arbeit 6** zusätzlich eine apparative elektroneurographische Untersuchung zur Quantifizierung der PNS - Schädigung beinhaltete.

### 3. Ergebnisse

#### 3.1 Konfokalmikroskopische Netzwerkanalyse

Die glatte Muskulatur der Portalvene ist ein prototypisches Modell für intrinsisch generierte mechanische Spontanaktivität und zeigt hinsichtlich ihres Kontraktionsverhaltens, ihrer Innervation und des Vorhandenseins von ICC eine große Ähnlichkeit mit phasisch aktiver gastrointestinaler Muskulatur. Allerdings ist sie wesentlich dünnwandiger und somit für vitalmikroskopische Untersuchungen besser zugänglich [99–103].

Um die Stärke der Aktivitätskopplung des Gewebes im Rahmen der Spontanaktivität zu untersuchen, wurde das Gewebe als homogenes zelluläres Netzwerk betrachtet und über dieses ein  $20 \times 20 \mu\text{m}$  messendes Raster an diskreten Orten gelegt. Über die Rasterpunkte hinweg wurde die Synchronizität der Kalziumoszillationen als Maß für die lokale Aktivität analysiert. Die so bestimmte funktionelle Kopplung überwindet Limitationen früherer Methoden, da mittels klassischer elektrischer Ableitmethoden nur entweder die Aktivität einzelner Zellen oder aber die summierten Feldpotenziale einer großen und letztlich unbekanntem Zahl von Myozyten registriert werden konnte. Farbstoffdiffusionsstudien bilden hingegen rein passive Diffusionsphänomene ab und sind nicht zur Beschreibung zeitlich-räumlicher Aktivitätsmuster geeignet [104]. Daher blieb unbekannt, welches Ausmaß die lokalen Unterschiede zwischen eng benachbarten Regionen des Gewebes haben und über welche Strecken sich Unterschiede im Verlauf von  $[\text{Ca}^{2+}]_i$  als dem eigentlichen Steuersignal für die Muskelkontraktion zeigen.

Mathematisch wurde zur Quantifizierung der Kopplungsstärke die Kreuzkorrelationsanalyse von Zeitreihen genutzt, welche neben der Kopplungsstärke Informationen über den Phasenversatz zweier Signale liefert. Die Analyse spontaner Kalziumsignale sowie deren Modulation durch Noradrenalin ergab, dass die Signale in alle Richtungen ausgehend vom Referenzpunkt bereits in Abständen von wenigen Mikrometern Abweichungen vom Referenzsignal aufweisen. Noradrenalin vermindert die Signaldämpfung als Zeichen einer verbesserten interzellulären Kopplung.

Zusammenfassend wurde gezeigt, dass die lokalen Oszillationen von  $[\text{Ca}^{2+}]_i$  im Rahmen der Spontanaktivität bereits über kurze Distanzen nur unvollständig gekoppelt sind. Physiologische Signalsubstanzen können zu einer Synchronisierung beitragen und so eine Anpassung der Organfunktion an variable physiologische Anforderungen bewirken. Die beschriebene Methode der Netzwerkanalyse ermöglicht es somit, unabhängig von detaillierten Informationen über die morphologische Konnektivität eines Gewebes spezifische Aussagen über dessen Aktivitätsmuster zu machen.

Referenz: **Patejdl R, Noack T.** Calcium movement in smooth muscle and evaluation of graded functional intercellular coupling. *Chaos*. 2018 Oct;28(10):106311. PMID: 30384639.

### 3.2 Kopplungshemmende Effekte des Na<sub>v</sub>-Blockers Phenytoin

Die Bedeutung von Änderungen der Kopplungsstärke innerhalb der glatten Muskulatur liegt in ihren Auswirkungen auf die mechanische Aktivität begründet. Unter Beteiligung zahlreicher Ionenkanäle werden hierfür mehr oder weniger synchrone elektrische Erregungen erzeugt, welche die Grundlage für diese Aktivierung darstellen. In klinisch-therapeutischen Kontexten werden Ionenkanalblocker z.B. im Rahmen der pharmakologischen Behandlung epileptischer Anfälle eingesetzt, um elektrische Synchronisation zu hemmen. Da jedoch Ionenkanalblocker nicht nur glatte Muskelzellen, sondern alle in Abb. 1 genannten Strukturen funktionell beeinflussen können, ist eine Analyse ihrer Wirkungen auf die unterschiedlichen Systeme wesentlich für das Verständnis ihrer Gesamteffekte.

In dieser Arbeit wurden Zeitreihen spontaner und neurogen evozierter Kontraktionen glatter Muskulatur des Gastrointestinaltrakts sowie der Portalvene und ihre Beeinflussung durch Phenytoin untersucht. Phenytoin bewirkte eine konzentrationsabhängige Abnahme der Frequenz und der Amplitude spontaner phasischer Kontraktionen. Eine spezifische Blockade von Na<sub>v</sub>-Kanälen mit Tetrodotoxin ergab keine vergleichbaren Effekte, womit eine Na<sub>v</sub>-Blockade als zugrundeliegender Mechanismus unwahrscheinlich wurde. Da sich aber in ratiometrischen Fura2-Fluoreszenzmessungen Reduktionen der Kalziumsignale nach kaliuminduzierter Depolarisation sowie eine Antagonisierung der Phenytoineffekte durch BAYK8644 zeigten, konnte eine Hemmung des Kalziumeinstroms durch Phenytoin angenommen werden. Da Kalziumströme die dominante spannungsabhängige Einwärtsstromkomponente der untersuchten glattmuskulären Gewebe darstellen, erklärt sich hieraus die in Feldpotenzialmessungen nachgewiesene reduzierte elektrische Erregungskopplung im Organverband. Diese wiederum erklärt unmittelbar die beobachtete Reduktion der Kontraktionskraftentwicklung sowie – im Falle von Schrittmacheraktionen, die sich aufgrund fehlender Verstärkung durch Kalziumströme nicht ausbreiten können – die beobachtete Frequenzreduktion. Weiterhin inhibiert Phenytoin im Rahmen seiner Na<sub>v</sub>-blockierenden Wirkung neurogene Kontraktionen der Fundusmuskulatur und somit potenziell auch die in vivo ablaufenden neuronale Einflüsse auf die Motilität.

Zusammenfassend wurde gezeigt, dass Phenytoin nicht durch seine klassische Wirkung auf Natriumkanäle in ZNS, VNS und ENS, sondern durch eine Hemmung des Kalziumanstiegs in verschiedenen glattmuskulären Geweben Stärke und Frequenz der Spontanaktivität sowie die Neurotransmission hemmt.

Referenz: *Phenytoin inhibits contractions of rat gastrointestinal and portal vein smooth muscle by inhibiting calcium entry.* **Patejdl R**, Leroux AC, Noack T. *Neurogastroenterol Motil.* 2015 Oct;27(10):1453-65. PMID: 26265316

### 3.3 Kopplungsfördernde Effekte des Na<sub>v</sub>-Blockers Ajmalin

Aus den unter 3.2 genannten Ergebnissen kann die These abgeleitet werden, dass klassische Na<sub>v</sub>-Blocker in Abhängigkeit ihres Interaktionsprofils mit weiteren Ionenkanälen grundsätzlich sowohl hemmend als auch verstärkend auf die interzelluläre Kopplung wirken können, je nachdem, ob sie de- oder repolarisierende Ströme hemmen. Diesbezügliche Untersuchungen ergaben, dass die als Klasse-I-Antiarrhythmikum bekannte Substanz Ajmalin an Magen und Portalvene der Ratte deutliche Steigerungen der Amplitude spontaner Kontraktionen bewirkt. Demgegenüber war die Kraftentwicklung durch exogene cholinerge Stimulation oder kaliuminduzierte Depolarisation in Gegenwart von Ajmalin kaum verändert, wodurch relevante Effekte auf Kalziumströme im Gewebe unwahrscheinlich waren. Ebenfalls kam es zu keiner messbaren Verschiebung des Grundtonus der Präparate, so dass eine basale Depolarisation, z.B. durch die Blockade einwärts-gleichrichtender Kaliumkanäle ebenfalls unwahrscheinlich war. Ajmalin reduzierte weiterhin elektrisch induzierte neurogene Dilatationen. Dennoch konnte pharmakologisch weitgehend ausgeschlossen werden, dass z.B. eine Disinhibition der Muskulatur durch eine Hemmung konstitutiver hemmender Neurotransmission oder aber eine Aktivierung cholinergischer Transmitterausschüttung der Steigerung der Spontanaktivität zugrunde liegt, da weder eine Vorbehandlung mit TTX noch mit L-NAME oder Atropin die Wirkung von Ajmalin relevant veränderte. Allerdings ergaben Untersuchungen zur Manipulation der interzellulären Kopplung, dass Ajmalin die Wirkung des Gap-Junction-Blockers Carbenoxolon antagonisiert.

Auf dieser Datengrundlage konnte zusammenfassend eine Hemmung spannungsaktivierter Kaliumströme mit nachfolgender Entthemung der Erregungsausbreitung im Gewebe als zugrundeliegender Mechanismus der starken aktivierenden Wirkung von Ajmalin auf die kontraktile Aktivität von Magenantrum und Portalvene postuliert werden.

Referenz: *Effects of ajmaline on contraction patterns of isolated rat gastric antrum and portal vein smooth muscle strips and on neurogenic relaxations of gastric fundus.*

**Patejdl R**, Gromann A, Bänsch D, Noack T. *Pflugers Arch.* 2019 Jul;471(7):995-1005. PMID: 31044280

### 3.4 Graduelle tonische Kontraktion durch den S1P-Agonisten FTY720

Während die gegensinnige Veränderung der Kontraktionen phasisch aktiver Gewebe durch die Hemmung spannungsabhängiger Kalzium- bzw. Kaliumkanälen methodisch sehr robust dargestellt werden kann, ist die Analyse von graduellen Veränderungen des

Kontraktionszustandes tonisch aktiver Muskulatur z.B. durch artifizielle Driftphänomene wesentlich störanfälliger. Unsere Untersuchungen zeigten, dass neben bekannten Mediator- und Neurotransmittersystemen (z.B. Prostaglandinen oder Cholinergika) auch der Sphingosin-1-Phosphat (S1P) – Agonist FTY720 den Tonus der Fundusmuskulatur des Rattenmagens graduell zu steigern vermag. Auffällig war eine zeitliche Verzögerung zwischen Substanzapplikation und Wirkeintritt von mehreren Minuten. Die durchschnittliche FTY720-induzierte Kontraktion erreichte unter Standardbedingungen im Mittel 8,9% der Amplitude einer durch 50 mmol/l Kaliumchlorid induzierten Referenzkontraktion, in Anwesenheit von Indometacin sogar 31,2%. Die Verstärkung des Effekts durch Indometacin war unerwartet, da die einzigen zuvor bekannten Studien zu Effekten von FTY720 auf glattmuskuläre Gewebe Gefäßpräparate untersucht und dort eine Aufhebung der Kontraktion durch Indometacin beschrieben hatten.

Da es sich um die erstmalige Beschreibung der Wirkungen von S1P-Agonisten am nativen intestinalen glatten Muskel des Magens handelte, wurde in weitergehenden Experimenten der Wirkmechanismus untersucht: Die Wirkung von FTY720 wurde in Gegenwart des VDCC-Blockers Nifedipin sowie in kalziumfreier Lösung nahezu vollständig aufgehoben und war nach Gabe von Antagonisten für die S1P-Rezeptorsubtypen 2 und 3 stark reduziert, woraus eine rezeptorvermittelte Depolarisation mit nachfolgender VDCC-Aktivierung als Mechanismus der FTY720-induzierten Kontraktion abgeleitet werden konnte.

Zusammenfassend wurde erstmalig die Wirkung eines Sphingosinanalogs auf ein intaktes glattmuskuläres Gewebe charakterisiert und eine Beteiligung spannungsabhängiger Ionenkanäle am Wirkmechanismus nachgewiesen.

Referenz: *The sphingosine analog fingolimod (FTY720) enhances tone and contractility of rat gastric fundus smooth muscle.* Kraft M, Zettl UK, Noack T, **Patejdl R.** *Neurogastroenterol Motil.* 2018 Oct;30(10):e13372. PMID: 29740911

### **3.5 Schlaganfälle und gastrointestinale Motilitätsstörungen**

Schlaganfälle stellen ein häufiges und vor allem durch seine zahlreichen Komplikationen oftmals vital bedrohliches Krankheitsbild dar [105]. Aus theoretischen Erwägungen ergeben sich mögliche Interaktionen zwischen gestörter vegetativer Steuerfunktion des ZNS und Alterationen der gastrointestinalen Funktion, z.B. durch Läsionen wichtiger vegetativer Integrations- und Steuerzentren wie der Kerne des N. vagus im Hirnstamm, des Hypothalamus oder der Inselregion [106]. Dennoch existieren jenseits der Analyse von Schluckstörungen und allgemeiner Ernährungsempfehlungen kaum Daten über Art und Häufigkeit gastrointestinaler Komplikationen bei betroffenen Patienten. Wir unterzogen eine Kohorte von 76 Patienten mit Verweildauern von mehr als 14 Tagen auf der neurologischen Intensivstation einer retrospektiven Analyse. Hierbei wurden

Patienten mit (n=57, Schlaganfallgruppe, SG) und ohne (n=19) Schlaganfall miteinander verglichen. Die nicht-Schlaganfallgruppe (NSG) bestand zu großen Teilen aus Patienten mit epileptischen Anfällen und peripheren Neuropathien. Die gastrointestinale Funktion wurde durch die tageweise Analyse des Residualvolumens des Magens, von Erbrechen, Dysphagie, Obstipation, Prokinetika- und Laxantienbedarf sowie der Toleranz gegenüber enteraler Nahrungszufuhr erfasst. Die Vergleiche der Patienten erfolgten nach Adjustierung hinsichtlich der allgemeinen Krankheitsschwere, der Abhängigkeit von invasiver Beatmung und dem Vorliegen schwerer systemischer Infektionen bzw. Inflammationsreaktionen (Sepsis/SIRS). Dabei zeigte sich für die gesamte Kohorte, dass sowohl Patienten der SG als auch der NSG mit 58% bzw. 79% eine hohe Wahrscheinlichkeit für das Auftreten gastrointestinaler Symptome hatten. Die weitere Analyse nach Adjustierung der jeweiligen Gruppen zur Berücksichtigung der o.g. Störgrößen zeigte, dass das Vorliegen eines Schlaganfalles per se im Vergleich zu Patienten mit anderen neurologischen Erkrankungen kein erhöhtes Risiko für das Vorliegen gastrointestinaler Symptome bedeutete, sondern dass im Gegenteil in der betrachteten NSG ein signifikant höheres Risiko für das Vorliegen zumindest eines Symptoms gastrointestinaler Dysfunktion vorliegt. Da auch die Grunderkrankungen der Patienten der NSG mit Störungen der Innervation des Gastrointestinaltraktes einhergehen können, steht dieser Befund nicht im Widerspruch zur allgemein akzeptierten These einer Beteiligung von ZNS und PNS an der Motilität. Er zeigt lediglich, dass diesbezüglich Schlaganfälle in der betrachteten Kohorte neurologischer Intensivpatienten nicht per se zu schwereren gastrointestinalen Komplikationen führen. Aufgrund der geringen Patientenzahl war diese Studie nicht geeignet zu klären, ob insbesondere Infarkte von Hirnstamm oder Inselregion mit spezifisch erhöhten Risiken für Motilitätsstörungen verbunden sind.

Zusammenfassend belegte diese Studie erstmalig die hohe Wahrscheinlichkeit für das Auftreten gastrointestinaler Funktionsstörungen bei kritisch kranken Schlaganfallpatienten und gab gleichzeitig Hinweise auf eine insgesamt möglicherweise sogar noch größere Häufigkeit entsprechender Komplikationen unter kritisch kranken Patienten mit anderen, größtenteils weniger stark lokalisierten neurologischen Erkrankungen (z.B. Status epilepticus oder Polyneuropathien).

Referenz: *Clinical nutrition and gastrointestinal dysfunction in critically ill stroke patients.* **Patejdl R, Kästner M, Kolbaske S, Wittstock M. Neurol Res. 2017 Nov;39(11):959-964. PMID: 28828964**

### 3.6 Periphere Neuromyopathie und gastrointestinale Motilitätsstörungen

Neben dem zentralen ist auch das periphere Nervensystem an der Regulation der gastrointestinalen Motilität und ihrer Koordination mit den jeweiligen Sekretionsprozessen wesentlich beteiligt. Zu nennen sind neben den efferenten Fasern des Parasympathikus und Sympathikus des VNS hierbei auch afferente Fasern intestinaler Chemo- und Mechanosensoren sowie Inter- und Motoneurone des ENS. Motilitätsstörungen bei chronischen PNS-Schädigungen wie der diabetischen Polyneuropathie führen jedoch auch zum Verlust von Schrittmacherzellen (ICC), so dass der reine Beitrag der direkten Steuerungsfunktion des PNS zur Pathophysiologie der Motilitätsstörungen nur schwer abgeschätzt werden kann. Wenn akute PNS-Schädigungen einen relevanten Risikofaktor für gastrointestinale Dysmotilität darstellen, ist im Umkehrschluss ein erhöhtes Risiko für PNS-Schädigungen bei anderweitig nicht erklärba­ren gastrointestina­len Motilitätsstörungen zu erwarten. Beispielhaft wurde in der vorliegenden Arbeit untersucht, ob Patienten mit schwerer Allgemeinerkrankung und ausgeprägtem intensivmedizinischen Behandlungsbedarf häufiger Zeichen gastrointestinaler Dysfunktion zeigen, wenn bei ihnen frühzeitig im Erkrankungsverlauf elektrophysiologisch eine Polyneuromyopathie (Critical Illness Polyneuro- bzw. Polyneuromyopathie, CINM) nachweisbar ist. Hierfür wurden Patienten mit einem einheitlich definierten Grad an Krankheitsschwere (SOFA-Score >8 über drei Tage) elektroneurographisch untersucht und entsprechend des erhobenen Befundes in Patienten mit- und ohne Zeichen der frühen Schädigung des PNS gruppiert. Da die apparative Testung von VNS und ENS in der betreffenden Kohorte durch die Analgosedierung erheblich eingeschränkt war, wurde stellvertretend als Surrogatparameter eine elektrophysiologische Diagnostik des somatischen PNS vorgenommen. Hierbei zeigte sich, dass Patienten mit entsprechendem Schädigungsnachweis ein erhöhtes Residualvolumen des Magens aufwiesen und nur verzögert den oralen Kostaufbau vollziehen konnten. Eine umfangreiche Analyse möglicher Störfaktoren ergab, dass dieser Unterschied zwischen Patienten mit- und ohne CINM nicht durch Gruppenunterschiede in der Behandlung mit Opioiden, Sedativa oder dem Vorliegen weiterer Risikofaktoren erklärbar war. Obwohl also die gastrointestinalen Motilitätsstörungen bei kritisch kranken Patienten weiterhin als multifaktoriell und ätiologisch komplex anzusehen sind, liefert die vorliegende Studie erstmals Hinweise darauf, dass eine sehr früh stattfindende Schädigung des PNS einen relevanten Risikofaktor darstellt, der in die prognostische Beurteilung und die Behandlungskonzepte der Patienten einbezogen werden kann.

Referenz: *Relations Between Early Neuromuscular Alterations, Gastrointestinal Dysfunction and Clinical Nutrition in Critically Ill Patients: An Exploratory Single-center Cohort Study.* Klawitter F, Ehler J, Reuter DA, **Patejdl R.** *Neurocrit Care. Epub ahead of print. PMID: 32246438*

## 4. Diskussion

Eine auf die Bedürfnisse des Gesamtorganismus abgestimmte Motilität der glatten Muskulatur ist eine homöostatische Grundfunktion. Neben biochemischen Prozessen auf der Ebene der einzelnen glatten Muskelzelle wird sie von verschiedenen Typen der ICC, intestinalen Neuronen sowie lokalen und systemischen Signalen (u.a. aus der intestinalen Mukosa, aus verschiedenen Regionen des ZNS) beeinflusst [6]. All diese Ebenen können im Rahmen von Erkrankungen verändert sein. Gleichzeitig existiert ein immer größeres Repertoire an Pharmaka mit potenziellen Wirkungen auf lokale Signalwege, Transporter, Ionenkanäle oder neuronale Strukturen. Ein besseres Verständnis der Bedeutung der verschiedenen Ebenen der Regulation ist eine Voraussetzung dafür, valide pathophysiologische Konzepte und damit effektive und sichere Behandlungsstrategien für Störungen der gastrointestinalen Motilität entwickeln zu können. Die Ergebnisse der vorgelegten Arbeiten versuchen zu den diesbezüglich eingangs formulierten Fragen einen Beitrag zu leisten.

Für die **Kopplung des Aktivitätszustandes** zwischen glatten Muskelzellen gelten niederohmige Verbindungen („Gap-junctions“) zwischen benachbarten Myozyten sowie zwischen Myozyten und ICC als Schlüsselemente, obwohl auch alternative physikalische Mechanismen vorgeschlagen wurden [104, 107–109]. Unabhängig vom konkreten Mechanismus wurde das Konzept eines „synzytialen Charakters“ vieler glattmuskulärer Gewebe bereits in den 30er Jahren des 20. Jahrhunderts von Bozler eingeführt, später auf den „phasischen Typ“ glatter Muskulatur übertragen und ist bis heute ein verbreitetes Modell zur Beschreibung der elektrischen Eigenschaften glatter Muskulatur [52, 110, 111]. Untersuchungen extrazellulärer Feldpotenziale ergaben jedoch, dass in der Portalvene als klassischem Single-Unit-Gewebe durchaus starke räumliche Heterogenitäten vorliegen, so dass mehrere nur wenige Millimeter entfernte Schrittmacherzentren unabhängig voneinander Aktivitätsmuster erzeugen können [112]. Quantitative experimentelle Analysen der zeitlichen Kopplungseigenschaften auf mikroskopischer Ebene fehlen bislang, die Effekte von strukturell beschriebenen Heterogenitäten auf Erregungsprozesse wurden bislang nur für die Uterusmuskulatur mathematisch modelliert [113]. Die unsererseits entwickelte Methode der mathematischen Kreuzkorrelationsanalyse von Kalziumsignalen in spontanaktiven Geweben bestätigte auch auf der damit zugänglichen räumlichen Auflösungsebene das Vorliegen von einer vorhandenen, aber imperfekten Kopplung im spontanaktiven glatten Muskel sowie die Modulierbarkeit der Kopplung durch physiologische Agonisten [93].

Geht man von einer unter basalen Bedingungen nicht-perfekten Kopplung der Myozytenaktivität aus, so ergibt sich unmittelbar, dass in glattmuskulären Geweben die

erzeugte Kraft abhängig vom Kopplungsgrad ist. Dies ist insbesondere wegen des passiven elektrotonischen Charakters der Signalfortleitung naheliegend: Änderungen der Erregbarkeit der Zellen können die Geschwindigkeit der Ausbreitung und die Reichweite lokal erzeugter Signale bestimmen [114, 115]. Obwohl die Auswirkungen unterschiedlicher Aktivierungsgrade einzelner Gewebe – z.B. des Kolons – auf die Kraftentwicklung ein bekanntes Phänomen sind [116], existieren keine experimentellen Arbeiten, die systematisch die **Bedeutung von Kopplungsverstärkung und – abschwächung für die Kraftentwicklung** gastrointestinaler Gewebe untersucht haben. Auch wurde die physiologische Relevanz von Ionenkanälen im gastrointestinalen glatten Muskel aus methodischen Gründen meist nur unter zellulären Aspekten und kaum im Hinblick auf die Kopplung der Erregungsmuster des intakten Organs diskutiert [117–119], obwohl hemmende und stimulierende Effekte zahlreicher Ionenkanalblocker auf die phasische Aktivität der glatten Muskulatur durchaus bekannt und beschrieben worden sind [120–122]. Unsere Untersuchungen zu den stimulierenden bzw. hemmenden Effekten der klassischen Ionenkanalblocker Phenytoin und Ajmalin zeigten eine Verringerung bzw. Steigerung der Kraft spontaner Kontraktionen in gastrointestinalen glatten Muskeln, die jeweils über die Effekte auf exogene Aktivierungen durch globale Depolarisation oder muskarinerge Agonisten hinausging [94, 95]. Wesentlich ist hierbei, dass auch ohne jegliche Änderungen der Gap Junction – Funktion eine Beeinflussung der de- und repolarisierenden Ströme der Myozyten die funktionelle Kopplung sehr wirkungsvoll beeinflusst: Während Phenytoin über Hemmungen der erregungsverstärkenden Kalziumströme zu einer geringeren Kopplung und damit unvollständigeren Rekrutierung von krafterzeugenden Myozyten durch die spontane Depolarisation führt, kommt es in Gegenwart von Ajmalin und anderen Blockern spannungsabhängiger Kaliumkanäle zu einer „ungebremsteren“ und damit vollständigeren Ankopplung des Gewebes.

Die unsererseits erstmalig beschriebene kontraktionsfördernde Wirkung des S1P-Agonisten FTY720 auf intakte Gewebepräparate des Magenfundus kann ebenfalls als Beleg für die kritische Rolle des Erregungszustands der glatten Muskelzellen für die Kraftentwicklung interpretiert werden, da unsererseits eine Abhängigkeit der Kraftentwicklung von der Verfügbarkeit von spannungsabhängigen Kalziumkanälen nachgewiesen wurde, der depolarisierende Effekt von FTY720 selbst jedoch offenbar nur vergleichsweise schwach ausfällt, wie an der auch nach FTY720-Zugabe weiterhin starken Reaktion auf extrazelluläre Kaliumerhöhungen ablesbar ist [96].

Angesichts der Stärke dieser Kopplungsänderungen könnte die pharmakologische Beeinflussung der Kopplung ein bisher wenig beachtetes, aber sehr attraktives Ziel für die Behandlung bei hypo- und hypomotilen Störungen sein.

Ob und wie das **Nervensystem** an der Generierung der physiologischen GI-Motilität beteiligt ist, wurde historisch sehr unterschiedlich bewertet: Anfang des 20. Jahrhunderts gab es Befunde, die einen neuronalen Ursprung der gesamten Darmmotilität nahelegen schienen [123]. Diese sind rückblickend auf die enge räumliche Nähe von Neuronen des ENS und ICC zurückzuführen [124–126]. Nach heutigem Stand des Wissens gilt eine große Bedeutung des ENS für eine intakte GI-Motilität als gesichert [40, 127, 128]. Über die Rollen des peripheren bzw. autonomen Nervensystems sowie des ZNS existieren hingegen vergleichsweise wenige humanphysiologische bzw. klinische Daten, obwohl beide durch Verfahren der klinischen Routinediagnostik (z.B. Kernspintomographie oder Elektroneurographie) deutlich leichter zugänglich sind als das ENS. Beinahe alle Publikationen zu gastrointestinalen Funktionsstörungen bei Schlaganfällen beziehen sich auf experimentelle Beobachtungen oder auf nicht-rein glattmuskuläre Funktionen wie den Schluckakt sowie auf Einzelfallberichte [106, 129–131]. Die unsererseits erhobene Häufigkeit von Zeichen einer gastrointestinalen Funktionsstörung bei 58% der Schlaganfallpatienten und 79% der Patienten mit anderen schweren neurologischen Erkrankungen liefert somit erstmalig einen Anhalt für die besonders starke Verbreitung dieses Problems in der neurologischen Intensivmedizin und damit indirekt auch für die Relevanz ZNS- und PNS-vermittelter Einflüsse für die Erhaltung der physiologischen Motilität. Studien zur Häufigkeit gastrointestinaler Störungen unter Patienten mit gemischten intensivpflichtigen Erkrankungen sind aus methodischen Gründen oft schwer vergleichbar, berichten jedoch überwiegend geringere Zahlen im Bereich zwischen 10 und 20% [132–135]. Dass die Häufigkeit von Symptomen in der Schlaganfallgruppe, also unter Patienten mit isolierten, lokalisierten ZNS-Schäden, sogar eher geringer war als im gemischten Patientengut der Kontrollgruppe, kann als Hinweis auf eine besondere Bedeutung von diffusen Schädigungen von ZNS und PNS angesehen werden [97].

Die funktionelle Relevanz des somatischen peripheren Nervensystems konnte hingegen in der von uns durchgeführten Untersuchung an Patienten mit kritischer Allgemeinerkrankung nachgewiesen werden. Ob die an peripheren motorischen und sensorischen Nerven nachgewiesene Schädigung ein valider Surrogatparameter für eine Schädigung von VNS und ENS ist, bleibt letztlich aufgrund der fehlenden Option einer direkten Testung in der untersuchten Population ungeklärt. Im Gegensatz hierzu ist die Durchführung der apparativen Testung somatischer Nerven gut standardisiert und selbst im Kontext der Intensivstation mit entsprechendem logistischem Aufwand gut durchführbar.

Spezifische funktionsdiagnostische Tests des enterischen Nervensystems existieren bislang nicht, selbst hoch entwickelte Testverfahren wie die hochauflösende Manometrie

des Ösophagus oder des Anorektums bilden die *gemeinsame* Funktion der zellulären Komponenten des jeweiligen Abschnitts des Verdauungskanals ab [136]. Im Gegensatz zur überwiegenden Zahl der bisherigen Studien [137–140] betrachtete diese Untersuchung erstmalig einen akuten, binnen weniger Tage eintretenden neuronalen Schaden, so dass hier im Gegensatz zur chronischen Situation keine komplexen Kompensations- oder Folgereaktionen, sondern die unmittelbare Wirkung der PNS-Läsion auf die gastrointestinale Funktion beobachtet werden konnte.

## 5. Zusammenfassung

In den hier zusammengefassten Arbeiten wurden die Mechanismen der interzellulären Koordinierung für die Steuerung der Kraft- bzw. Druckentwicklung glattmuskulärer Organe sowie ihre Relevanz im Kontext von Erkrankungen des Nervensystems untersucht. Die dabei erhobenen experimentellen Befunde sind mit dem tradierten Konzept eines „single-unit“-Verhaltens phasisch aktiver glatter Muskulatur nicht vereinbar: Bereits die Aktivität direkt benachbarter Muskelzellen kann sich relevant unterscheiden, und auch in größeren Gewebesegmenten erfasst der organeigene Schrittmacherprozess im Rahmen der basalen Spontanaktivität nicht alle Muskelzellen gleichermaßen. Die erhobenen Befunde belegen weiterhin, dass Veränderungen der Synchronisation innerhalb des Gewebes drastische Änderungen der Kraftentwicklung bewirken.

Die experimentell dargestellte Fragilität der interzellulären Kopplung legt nahe, dass die Abschwächung kopplungsfördernder Einflüsse des zentralen sowie des somatischen Nervensystems auch im klinischen Kontext gastrointestinale Funktionen beeinträchtigt. Tatsächlich bestätigten unsere Untersuchungen an Patienten die Häufigkeit von Störungen der gastrointestinalen Motilität infolge von Läsionen des zentralen sowie des peripheren Nervensystems. Trotz vieler weiterhin unbekannter Einflussfaktoren und unzureichend charakterisierter Mechanismen belegen die Ergebnisse dieser Arbeit die Bedeutung eines integrativen, auf die Organfunktion zentrierten experimentellen Vorgehens für ein besseres Verständnis der gastrointestinalen Motilität. Darüber hinaus unterstreichen sie die Bedeutung experimenteller Untersuchungen nativer Gewebe als Modellsysteme für die Vorhersage und Interpretation klinischer Funktionsstörungen.

## 6. Literaturverzeichnis

- 1 Kim HR, Appel S, Vetterkind S, et al. Smooth muscle signalling pathways in health and disease. *J Cell Mol Med* 2008;12(6a):2165–80.
- 2 Golenhofen K, Loh D von, Milenov K. Elektrophysiologische Untersuchungen zur Spontanaktivität isolierter Muskelpräparate aus verschiedenen Abschnitten des Meerschweinchen-Magens. *Pflugers Arch* 1970;315(4):336–56.
- 3 Eddinger TJ. Smooth muscle – protein translocation and tissue function. *Anat Rec (Hoboken)* 2014;297(9):1734–46.
- 4 Kriechbaum K, Findl O, Koepl C, et al. Stimulus-driven versus pilocarpine-induced biometric changes in pseudophakic eyes. *Ophthalmology* 2005;112(3):453–59.
- 5 Golenhofen K, Mandrek K. Phasic and tonic contraction processes in the gastrointestinal tract. *Dig Dis* 1991;9(6):341–46.
- 6 Huizinga JD. Gastrointestinal peristalsis: joint action of enteric nerves, smooth muscle, and interstitial cells of Cajal. *Microsc Res Tech* 1999;47(4):239–47.
- 7 Drumm BT, Baker SA. Teaching a changing paradigm in physiology: a historical perspective on gut interstitial cells. *Adv Physiol Educ* 2017;41(1):100–09.
- 8 Adelstein RS, Sellers JR, Conti MA, et al. Regulation of smooth muscle contractile proteins by calmodulin and cyclic AMP. *Fed Proc* 1982;41(12):2873–78.
- 9 Murthy KS. Signaling for contraction and relaxation in smooth muscle of the gut. *Annu Rev Physiol* 2006;68:345–74.
- 10 Ganitkevich V, Hasse V, Pfitzer G. Ca<sup>2+</sup>-dependent and Ca<sup>2+</sup>-independent regulation of smooth muscle contraction. *J Muscle Res Cell Motil* 2002;23(1):47–52.
- 11 Harnett KM, Cao W, Biancani P. Signal-transduction pathways that regulate smooth muscle function I. Signal transduction in phasic (esophageal) and tonic (gastroesophageal sphincter) smooth muscles. *American journal of physiology. Gastrointestinal and liver physiology* 2005;288(3).  
<https://pubmed.ncbi.nlm.nih.gov/15701619/>.
- 12 Perrino BA. Calcium Sensitization Mechanisms in Gastrointestinal Smooth Muscles. *J Neurogastroenterol Motil* 2016;22(2):213–25.
- 13 Li B, Wang R, Wang Y, et al. Regulation of smooth muscle contraction by monomeric non-RhoA GTPases. *Br J Pharmacol* 2020.

- 14 Kuo IY, Ehrlich BE. Signaling in muscle contraction. *Cold Spring Harb Perspect Biol* 2015;7(2):a006023.
- 15 Hill-Eubanks DC, Werner ME, Heppner TJ, et al. Calcium signaling in smooth muscle. *Cold Spring Harb Perspect Biol* 2011;3(9):a004549.
- 16 Heading RC. Role of motility in the upper digestive tract. *Scand J Gastroenterol Suppl* 1984;96:39–44.
- 17 Schemann M, Rohn M, Michel K. Motor control of the stomach. *Eur Rev Med Pharmacol Sci* 2008;12 Suppl 1:41–51.
- 18 Goyal RK, Guo Y, Mashimo H. Advances in the physiology of gastric emptying. *Neurogastroenterol Motil* 2019;31(4):e13546.
- 19 Tack J. The physiology and the pathophysiology of the gastric accommodation reflex in man. *Verh K Acad Geneeskd Belg* 2000;62(3):183-207; discussion 207-10.
- 20 Camilleri M, Malagelada JR, Brown ML, et al. Relation between antral motility and gastric emptying of solids and liquids in humans. *Am J Physiol* 1985;249(5 Pt 1):G580-5.
- 21 Indireshkumar K, Brasseur JG, Faas H, et al. Relative contributions of "pressure pump" and "peristaltic pump" to gastric emptying. *American journal of physiology. Gastrointestinal and liver physiology* 2000;278(4):G604-16.
- 22 Pal A, Brasseur JG, Abrahamsson B. A stomach road or "Magenstrasse" for gastric emptying. *J Biomech* 2007;40(6):1202–10.
- 23 Kito Y. The functional role of intramuscular interstitial cells of Cajal in the stomach. *J Smooth Muscle Res* 2011;47(2):47–53.
- 24 Ward SM, McLaren GJ, Sanders KM. Interstitial cells of Cajal in the deep muscular plexus mediate enteric motor neurotransmission in the mouse small intestine. *J Physiol (Lond )* 2006;573(Pt 1):147–59.
- 25 Sanders KM. Spontaneous Electrical Activity and Rhythmicity in Gastrointestinal Smooth Muscles. *Adv Exp Med Biol* 2019;1124:3–46.
- 26 van Helden DF, Laver DR, Holdsworth J, et al. Generation and propagation of gastric slow waves. *Clin Exp Pharmacol Physiol* 2010;37(4):516–24.
- 27 Thuneberg L. Interstitial cells of Cajal: intestinal pacemaker cells? *Adv Anat Embryol Cell Biol* 1982;71:1–130.
- 28 Sanders KM, Ward SM, Koh SD. Interstitial cells: regulators of smooth muscle function. *Physiol Rev* 2014;94(3):859–907.
- 29 Foong D, Zhou J, Zarrouk A, et al. Understanding the Biology of Human

- Interstitial Cells of Cajal in Gastrointestinal Motility. *Int J Mol Sci* 2020;21(12).
- 30 Dickens EJ, Edwards FR, Hirst GD. Selective knockout of intramuscular interstitial cells reveals their role in the generation of slow waves in mouse stomach. *J Physiol (Lond)* 2001;531(Pt 3):827–33.
- 31 Horiguchi K, Semple GS, Sanders KM, et al. Distribution of pacemaker function through the tunica muscularis of the canine gastric antrum. *J Physiol (Lond)* 2001;537(Pt 1):237–50.
- 32 Iino S, Ward SM, Sanders KM. Interstitial cells of Cajal are functionally innervated by excitatory motor neurones in the murine intestine. *J Physiol (Lond)* 2004;556(Pt 2):521–30.
- 33 Edwards FR, Hirst GDS. An electrical analysis of slow wave propagation in the guinea-pig gastric antrum. *J Physiol (Lond)* 2006;571(Pt 1):179–89.
- 34 Sanders KM. A case for interstitial cells of Cajal as pacemakers and mediators of neurotransmission in the gastrointestinal tract. *Gastroenterology* 1996;111(2):492–515.
- 35 Hirst GD, Edwards FR. Generation of slow waves in the antral region of guinea-pig stomach—a stochastic process. *J Physiol (Lond)* 2001;535(Pt 1):165–80.
- 36 Beckett EAH, Takeda Y, Yanase H, et al. Synaptic specializations exist between enteric motor nerves and interstitial cells of Cajal in the murine stomach. *J Comp Neurol* 2005;493(2):193–206.
- 37 Daniel EE. Communication between interstitial cells of Cajal and gastrointestinal muscle. *Neurogastroenterol Motil* 2004;16 Suppl 1:118–22.
- 38 Horiguchi K, Sanders KM, Ward SM. Enteric motor neurons form synaptic-like junctions with interstitial cells of Cajal in the canine gastric antrum. *Cell Tissue Res* 2003;311(3):299–313.
- 39 Blair PJ, Bayguinov Y, Sanders KM, et al. Relationship between enteric neurons and interstitial cells in the primate gastrointestinal tract. *Neurogastroenterol Motil* 2012;24(9):e437-49.
- 40 Schneider S, Wright CM, Heuckeroth RO. Unexpected Roles for the Second Brain: Enteric Nervous System as Master Regulator of Bowel Function. *Annu Rev Physiol* 2019;81:235–59.
- 41 Spencer NJ, Hu H. Enteric nervous system: sensory transduction, neural circuits and gastrointestinal motility. *Nat Rev Gastroenterol Hepatol* 2020;17(6):338–51. <https://pubmed.ncbi.nlm.nih.gov/32152479/>.
- 42 Bertrand PP, Thomas EA. Multiple levels of sensory integration in the intrinsic

- sensory neurons of the enteric nervous system. *Clin Exp Pharmacol Physiol* 2004;31(11):745–55.
- 43 Bayliss WM, Starling EH. The movements and innervation of the small intestine. *J Physiol (Lond)* 1899;24(2):99–143.
- 44 Bayliss WM, Starling EH. The movements and the innervation of the large intestine. *J Physiol (Lond)* 1900;26(1-2):107–18.
- 45 Bayliss WM, Starling EH. The movements and innervation of the small intestine. *J Physiol (Lond)* 1901;26(3-4):125–38.
- 46 Schemann M, Reiche D, Michel K. Enteric pathways in the stomach. *Anat. Rec.* 2001;262(1):47–57.
- 47 Costa M, Furness JB. The peristaltic reflex: an analysis of the nerve pathways and their pharmacology. *Naunyn Schmiedebergs Arch Pharmacol* 1976;294(1):47–60.
- 48 Meneghelli UG. Chagas' disease: a model of denervation in the study of digestive tract motility. *Braz J Med Biol Res* 1985;18(3):255–64.
- 49 Furness JB, Johnson PJ, Pompolo S, et al. Evidence that enteric motility reflexes can be initiated through entirely intrinsic mechanisms in the guinea-pig small intestine. *Neurogastroenterol Motil* 1995;7(2):89–96.
- 50 Furness JB, Callaghan BP, Rivera LR, et al. The enteric nervous system and gastrointestinal innervation: integrated local and central control. *Adv Exp Med Biol* 2014;817:39–71.
- 51 Oliveira RB, Meneghelli UG, Godoy RA de, et al. Abnormalities of interdigestive motility of the small intestine in patients with Chagas' disease. *Dig Dis Sci* 1983;28(4):294–99.
- 52 Bozler E. Physiological Evidence for the Syncycital Character of Smooth Muscle. *Science* 1937;86(2238):476.
- 53 Holman ME, Kasby CB, Suthers MB, et al. Some properties of the smooth muscle of rabbit portal vein. *J Physiol (Lond)* 1968;196(1):111–32.
- 54 Vogalis F, Ward SM, Sanders KM. Correlation between electrical and morphological properties of canine pyloric circular muscle. *Am J Physiol* 1991;260(3 Pt 1):G390-8.
- 55 Hara Y, Ito Y. The electrical activity recorded from smooth muscle of the circular layer of the human stomach. *Pflugers Arch* 1979;382(2).  
<https://pubmed.ncbi.nlm.nih.gov/574265/>.
- 56 Ito Y, Kuriyama H. Membrane properties of the smooth-muscle fibres of the

- guinea-pig portal vein. *J Physiol (Lond)* 1971;214(3):427–41.
- 57 Dewey MM, Barr L. Intercellular Connection between Smooth Muscle Cells: the Nexus. *Science* 1962;137(3531). <https://pubmed.ncbi.nlm.nih.gov/17770946/>.
- 58 Barr L, Dewey MM, Berger W. Action potentials can propagate along small strands of smooth muscle. *Pflugers Arch* 1979;380(2):165–70.
- 59 O'Grady G, Angeli TR, Du P, et al. Abnormal initiation and conduction of slow-wave activity in gastroparesis, defined by high-resolution electrical mapping. *Gastroenterology* 2012;143(3). <https://pubmed.ncbi.nlm.nih.gov/22643349/>.
- 60 Matchkov VV. Mechanisms of cellular synchronization in the vascular wall. Mechanisms of vasomotion. *Dan Med Bull* 2010;57(10):B4191.
- 61 Hermsmeyer K. Excitation of vascular muscles by norepinephrine. *Annals of biomedical engineering* 1983;11(6). <https://pubmed.ncbi.nlm.nih.gov/6680276/>.
- 62 Christ GJ, Spray DC, el-Sabban M, et al. Gap junctions in vascular tissues. Evaluating the role of intercellular communication in the modulation of vasomotor tone. *Circ Res* 1996;79(4):631–46.
- 63 Sims SM, Daniel EE, Garfield RE. Improved electrical coupling in uterine smooth muscle is associated with increased numbers of gap junctions at parturition. *J Gen Physiol* 1982;80(3):353–75.
- 64 Mello WC de. Cell-to-cell coupling assayed by means of electrical measurements. *Experientia* 1987;43(10):1075–79.
- 65 Carbone SE, Wattchow DA, Spencer NJ, et al. Loss of responsiveness of circular smooth muscle cells from the guinea pig ileum is associated with changes in gap junction coupling. *American journal of physiology. Gastrointestinal and liver physiology* 2012;302(12):G1434-44.
- 66 Sanders KM, Koh SD, Ordög T, et al. Ionic conductances involved in generation and propagation of electrical slow waves in phasic gastrointestinal muscles. *Neurogastroenterol Motil* 2004;16 Suppl 1:100–05.
- 67 Takeda Y, Ward SM, Sanders KM, et al. Effects of the gap junction blocker glycyrrhetic acid on gastrointestinal smooth muscle cells. *American journal of physiology. Gastrointestinal and liver physiology* 2005;288(4):G832-41.
- 68 van Helden DF, Imtiaz MS. Ca<sup>2+</sup> phase waves: a basis for cellular pacemaking and long-range synchronicity in the guinea-pig gastric pylorus. *J Physiol (Lond)* 2003;548(Pt 1):271–96.
- 69 Papacocea T, Papacocea R, Rădoi M, et al. Stomach 'tastes' the food and adjusts its emptying: A neurophysiological hypothesis (Review). *Exp Ther Med*

- 2020;20(3):2392–95.
- 70 Tack J, van den Houte K, Carbone F. Gastroduodenal motility disorders. *Curr Opin Gastroenterol* 2018;34(6):428–35.
- 71 Rostas JW, Mai TT, Richards WO. Gastric motility physiology and surgical intervention. *Surg Clin North Am* 2011;91(5):983–99.
- 72 Grover M, Farrugia G, Stanghellini V. Gastroparesis: a turning point in understanding and treatment. *Gut* 2019;68(12):2238–50.
- 73 Ladopoulos T, Giannaki M, Alexopoulou C, et al. Gastrointestinal dysmotility in critically ill patients. *Ann Gastroenterol* 2018;31(3):273–81.
- 74 Marathe CS, Marathe JA, Rayner CK, et al. Hypoglycaemia and gastric emptying. *Diabetes, obesity & metabolism* 2019;21(3).  
<https://pubmed.ncbi.nlm.nih.gov/30378748/>.
- 75 Singh PJ, Santella RN, Zawada ET. Gastrointestinal prokinetic agents for enhancing drug response in gastroparesis. *Am J Health Syst Pharm* 1997;54(22):2609–12.
- 76 Camilleri M, Chedid V, Ford AC, et al. Gastroparesis. *Nat Rev Dis Primers* 2018;4(1):41.
- 77 Jung H-K, Choung RS, Locke GR, et al. The incidence, prevalence, and outcomes of patients with gastroparesis in Olmsted County, Minnesota, from 1996 to 2006. *Gastroenterology* 2009;136(4):1225–33.
- 78 Syed AR, Wolfe MM, Calles-Escandon J. Epidemiology and Diagnosis of Gastroparesis in the United States: A Population-based Study. *Journal of clinical gastroenterology* 2020;54(1). <https://pubmed.ncbi.nlm.nih.gov/31135630/>.
- 79 Ye Y, Jiang B, Manne S, et al. Epidemiology and outcomes of gastroparesis, as documented in general practice records, in the United Kingdom. *Gut* 2020.
- 80 Rubinos C, Ruland S. Neurologic Complications in the Intensive Care Unit. *Curr Neurol Neurosci Rep* 2016;16(6):57.
- 81 Kane-Gill SL, Jacobi J, Rothschild JM. Adverse drug events in intensive care units: risk factors, impact, and the role of team care. *Crit Care Med* 2010;38(6 Suppl):S83-9.
- 82 Voils SA, Human T, Brophy GM. Adverse neurologic effects of medications commonly used in the intensive care unit. *Crit Care Clin* 2014;30(4):795–811.
- 83 Ali I, Bazzar A, Hussein N, et al. Potential drug-drug interactions in ICU patients: a retrospective study. *Drug Metab Pers Ther* 2020.
- 84 Philpott HL, Nandurkar S, Lubel J, et al. Drug-induced gastrointestinal disorders.

- Frontline Gastroenterol* 2013;5(1):49–57.
- 85 Jonderko K, Kwiecień J, Kasicka-Jonderko A, et al. The effect of drugs and stimulants on gastric myoelectrical activity. *Prz Gastroenterol* 2014;9(3):130–35.
- 86 Beyder A, Farrugia G. Targeting ion channels for the treatment of gastrointestinal motility disorders. *Therap Adv Gastroenterol* 2012;5(1):5–21.
- 87 Huizinga JD, Thuneberg L, Vanderwinden JM, et al. Interstitial cells of Cajal as targets for pharmacological intervention in gastrointestinal motor disorders. *Trends Pharmacol Sci* 1997;18(10):393–403.
- 88 Tack J. Receptors of the enteric nervous system: potential targets for drug therapy. *Gut* 2000;47(Suppl 4):iv20-2.
- 89 Scholz A. Mechanisms of (local) anaesthetics on voltage-gated sodium and other ion channels. *Br J Anaesth* 2002;89(1):52–61.
- 90 Lirk P, Hollmann MW, Strichartz G. The Science of Local Anesthesia: Basic Research, Clinical Application, and Future Directions. *Anesth Analg* 2018;126(4):1381–92.
- 91 Watterson KR, Ratz PH, Spiegel S. The role of sphingosine-1-phosphate in smooth muscle contraction. *Cell Signal* 2005;17(3):289–98.
- 92 Deane AM, Chapman MJ, Reintam Blaser A, et al. Pathophysiology and Treatment of Gastrointestinal Motility Disorders in the Acutely Ill. *Nutr Clin Pract* 2019;34(1):23–36.
- 93 Patejdl R, Noack T. Calcium movement in smooth muscle and evaluation of graded functional intercellular coupling. *Chaos* 2018;28(10):106311.
- 94 Patejdl R, Leroux A-C, Noack T. Phenytoin inhibits contractions of rat gastrointestinal and portal vein smooth muscle by inhibiting calcium entry. *Neurogastroenterol Motil* 2015;27(10):1453–65.
- 95 Patejdl R, Gromann A, Bänsch D, et al. Effects of ajmaline on contraction patterns of isolated rat gastric antrum and portal vein smooth muscle strips and on neurogenic relaxations of gastric fundus. *Pflugers Arch* 2019;471(7):995–1005.
- 96 Kraft M, Zettl UK, Noack T, et al. The sphingosine analog fingolimod (FTY720) enhances tone and contractility of rat gastric fundus smooth muscle. *Neurogastroenterol Motil* 2018;30(10):e13372.
- 97 Patejdl R, Kästner M, Kolbaske S, et al. Clinical nutrition and gastrointestinal dysfunction in critically ill stroke patients. *Neurol Res* 2017;39(11):959–64.
- 98 Klawitter F, Ehler J, Reuter DA, et al. Relations Between Early Neuromuscular

- Alterations, Gastrointestinal Dysfunction, and Clinical Nutrition in Critically Ill Patients: An Exploratory Single-center Cohort Study. *Neurocrit Care* 2020.
- 99 Sutter MC. The mesenteric-portal vein in research. *Pharmacol Rev* 1990;42(4):287–325.
- 100 Mancinelli R. L-propionylcarnitine and synchronization of spontaneous activity in rat isolated portal vein. *Arch Ital Biol* 1993;131(2-3):245–54.
- 101 Povstyan OV, Gordienko DV, Harhun MI, et al. Identification of interstitial cells of Cajal in the rabbit portal vein. *Cell Calcium* 2003;33(4):223–39.
- 102 Harhun MI, Gordienko DV, Povstyan OV, et al. Function of interstitial cells of Cajal in the rabbit portal vein. *Circ Res* 2004;95(6):619–26.
- 103 Funaki S, Bohr DF. Electrical and Mechanical Activity of Isolated Vascular Smooth Muscle of the Rat. *Nature* 1964;203:192–94.
- 104 Daniel EE, Wang YF. Gap junctions in intestinal smooth muscle and interstitial cells of Cajal. *Microsc Res Tech* 1999;47(5):309–20.
- 105 Walter U, Kolbaske S, Patejdl R, et al. Insular stroke is associated with acute sympathetic hyperactivation and immunodepression. *Eur J Neurol* 2013;20(1):153–59.
- 106 Schaller BJ, Graf R, Jacobs AH. Pathophysiological changes of the gastrointestinal tract in ischemic stroke. *Am J Gastroenterol* 2006;101(7):1655–65.
- 107 Vigmond EJ, Bardakjian BL, Thuneberg L, et al. Intercellular coupling mediated by potassium accumulation in peg-and-socket junctions. *IEEE Trans Biomed Eng* 2000;47(12):1576–83.
- 108 Sperelakis N. Combined electric field and gap junctions on propagation of action potentials in cardiac muscle and smooth muscle in PSpice simulation. *J Electrocardiol* 2003;36(4):279–93.
- 109 Seki K, Komuro T. Immunocytochemical demonstration of the gap junction proteins connexin 43 and connexin 45 in the musculature of the rat small intestine. *Cell Tissue Res* 2001;306(3):417–22.
- 110 Himpens B, Matthijs G, Somlyo AV, et al. Cytoplasmic free calcium, myosin light chain phosphorylation, and force in phasic and tonic smooth muscle. *J Gen Physiol* 1988;92(6):713–29.
- 111 Boberg L, Szekeres FLM, Arner A. Signaling and metabolic properties of fast and slow smooth muscle types from mice. *Pflugers Arch* 2018;470(4):681–91.
- 112 Hermsmeyer K. Multiple pacemaker sites in spontaneously active vascular

- muscle. *Circ Res* 1973;33(2):244–51.
- 113 Sheldon RE, Baghdadi M, McCloskey C, et al. Spatial heterogeneity enhances and modulates excitability in a mathematical model of the myometrium. *J R Soc Interface* 2013;10(86):20130458.
- 114 Tomita T. Spread of excitation in smooth muscle. *Prog Clin Biol Res* 1990;327:361–73.
- 115 Manchanda R, Appukuttan S, Padmakumar M. Electrophysiology of Syncytial Smooth Muscle. *J Exp Neurosci* 2019;13:1179069518821917.
- 116 Sarna SK. Colonic Motility: From Bench Side to Bedside. San Rafael (CA) 2010.
- 117 Farrugia G, Rich A, Rae JL, et al. Calcium currents in human and canine jejunal circular smooth muscle cells. *Gastroenterology* 1995;109(3):707–17.
- 118 Farrugia G. Ion channels as targets for treatment of gastrointestinal motility disorders. *Eur Rev Med Pharmacol Sci* 2008;12 Suppl 1:135.
- 119 Noack T, Deitmer P, Lammel E. Characterization of membrane currents in single smooth muscle cells from the guinea-pig gastric antrum. *J Physiol (Lond)* 1992;451:387–417.
- 120 Biamino G, Wessel HJ, Nöring J. Ajmaline-induced changes in mechanical and electrical activity of vascular smooth muscle. *Blood Vessels* 1975;12(1):68–80.
- 121 Ferrari M, Furlanut M, Maragno I. Effects of quinidine and ajmaline on the mechanical and electrical activity of smooth muscle. *Arch Int Pharmacodyn Ther* 1972;200(1):64–69.
- 122 Lammel E, Golenhofen K. Selektive Unterdrückung einzelner Komponenten der Spontanaktivität glatter Muskulatur durch Iproveratril. *Pflugers Arch* 1972;332:Suppl 332:R76.
- 123 Magnus R. Versuche am überlebenden Dünndarm von Säugetieren. *Pflugers Arch* 1904;103(11-12):515–24.
- 124 Herzog W. Zur Autonomie des Magens. *Acta Neuroveg (Wien)* 1957;16(1-4):166–75.
- 125 Wang X-Y, Paterson C, Huizinga JD. Cholinergic and nitrenergic innervation of ICC-DMP and ICC-IM in the human small intestine. *Neurogastroenterol Motil* 2003;15(5):531–43.
- 126 Ward SM, Sanders KM. Interstitial cells of Cajal: Primary targets of enteric motor innervation. *Anat. Rec.* 2001;262(1):125–35.
- 127 Romański KW. Importance of the enteric nervous system in the control of the migrating motility complex. *Physiol Int* 2017;104(2):97–129.

- 128 Furness JB. The enteric nervous system and neurogastroenterology. *Nat Rev Gastroenterol Hepatol* 2012;9(5):286–94.
- 129 Liff JM, Labovitz D, Robbins MS. Profound gastroparesis after bilateral posterior inferior cerebellar artery territory infarcts. *Clin Neurol Neurosurg* 2012;114(6):789–91.
- 130 Browning KN, Travagli RA. Central nervous system control of gastrointestinal motility and secretion and modulation of gastrointestinal functions. *Compr Physiol* 2014;4(4):1339–68.
- 131 Crome P, Rizeq M, George S, et al. Drug absorption may be delayed after stroke: results of the paracetamol absorption test. *Age Ageing* 2001;30(5):391–93.
- 132 Padar M, Starkopf J, Uusvel G, et al. Gastrointestinal failure affects outcome of intensive care. *J Crit Care* 2019;52:103–08.
- 133 Reintam A, Parm P, Redlich U, et al. Gastrointestinal failure in intensive care: a retrospective clinical study in three different intensive care units in Germany and Estonia. *BMC Gastroenterol* 2006;6:19.
- 134 Reintam Blaser A, Poeze M, Malbrain MLNG, et al. Gastrointestinal symptoms during the first week of intensive care are associated with poor outcome: a prospective multicentre study. *Intensive Care Med* 2013;39(5):899–909.
- 135 McClave SA, Gualdoni J, Nagengast A, et al. Gastrointestinal Dysfunction and Feeding Intolerance in Critical Illness: Do We Need an Objective Scoring System? *Curr Gastroenterol Rep* 2020;22(1):1.
- 136 Wood JD. Enteric Nervous System: Neuropathic Gastrointestinal Motility. *Dig Dis Sci* 2016;61(7):1803–16.
- 137 Lubomski M, Davis RL, Sue CM. Gastrointestinal dysfunction in Parkinson's disease. *J Neurol* 2020;267(5):1377–88.
- 138 Wegeberg A-ML, Brock C, Ejskjaer N, et al. Gastrointestinal symptoms and cardiac vagal tone in type 1 diabetes correlates with gut transit times and motility index. *Neurogastroenterol Motil* 2020:e13885.
- 139 Wood JD. Neuropathy in the brain-in-the-gut. *Eur J Gastroenterol Hepatol* 2000;12(6):597–600.
- 140 Parkman HP, Wilson LA, Farrugia G, et al. Delayed Gastric Emptying Associates With Diabetic Complications in Diabetic Patients With Symptoms of Gastroparesis. *Am J Gastroenterol* 2019;114(11):1778–94.



## 7. Verzeichnis der Publikationen und Vorträge

### Originalarbeiten mit Impact-Faktor

1. Klawitter F, Ehler J, Reuter DA, **Patejdl R**. Relations Between Early Neuromuscular Alterations, Gastrointestinal Dysfunction, and Clinical Nutrition in Critically Ill Patients: An Exploratory Single-center Cohort Study. *Neurocrit Care*. 2020 *Online ahead of print*. PMID: 32246438 IF: 2,72
2. **Patejdl R**, Gromann A, Bänsch D, Noack T. Effects of ajmaline on contraction patterns of isolated rat gastric antrum and portal vein smooth muscle strips and on neurogenic relaxations of gastric fundus. *Pflugers Arch*. 2019 PMID: 31044280. IF: 3,16
3. **Patejdl R\***, Walter U, Rosener S, Sauer M, Reuter DA, Ehler J. Muscular Ultrasound, Syndecan-1 and Procalcitonin Serum Levels to Assess Intensive Care Unit-Acquired Weakness. *Can J Neurol Sci*. 2019 Mar;46(2):234-242. PMID: 30739614. IF: 1,71
4. Tscherpel C, **Patejdl R**, Kisters K, Noack T. Calcium channels and effects of aliskiren on vascular smooth muscle. *Trace Elements and Electrolytes*. 2019;36(4):180-189 DOI: 10.5414/TEX01590 IF: 0,44
5. **Patejdl R**, Noack T. Calcium movement in smooth muscle and evaluation of graded functional intercellular coupling. *Chaos*. 2018 Oct;28(10):106311. PMID: 30384639. IF: 2,83
6. Kraft M, Zettl UK, Noack T, **Patejdl R**. The sphingosine analog fingolimod (FTY720) enhances tone and contractility of rat gastric fundus smooth muscle. *Neurogastroenterol Motil*. 2018 Oct;30(10):e13372. PMID: 29740911. IF: 3,80
7. **Patejdl R**, Kästner M, Kolbaske S, Wittstock M. Clinical nutrition and gastrointestinal dysfunction in critically ill stroke patients. *Neurol Res*. 2017 Nov;39(11):959-964. PMID: 28828964. IF: 1,45
8. **Patejdl R**, Leroux AC, Noack T. Phenytoin inhibits contractions of rat gastrointestinal and portal vein smooth muscle by inhibiting calcium entry. *Neurogastroenterol Motil*. 2015 Oct;27(10):1453-65. PMID: 26265316. IF: 3,31

9. Ludwig M, Skorska A, Tölk A, Hopp HH, **Patejdl R**, Li J, Steinhoff G, Noack T. Characterization of ion currents of murine CD117(pos) stem cells in vitro and their modulation under AT2 R stimulation. *Acta Physiol (Oxf)*. 2013 Jul;208(3):274-87. PMID: 23648269. IF: 4,25
10. Walter U, Kolbaske S, **Patejdl R**, Steinhagen V, Abu-Mugheisib M, Grossmann A, Zingler C, Benecke R. Insular stroke is associated with acute sympathetic hyperactivation and immunodepression. *Eur J Neurol*. 2013 Jan;20(1):153-9. PMID: 22834894 IF: 3,85
11. Rommer PS, **Patejdl R**, Winkelmann A, Benecke R, Zettl UK. Rituximab for secondary progressive multiple sclerosis: a case series. *CNS Drugs*. 2011 Jul;25(7):607-13. PMID: 21699272 IF: 4,79

#### Übersichtsartikel mit Impact-Faktor

1. **Patejdl R**, Zettl UK. Spasticity in multiple sclerosis: Contribution of inflammation, autoimmune mediated neuronal damage and therapeutic interventions. *Autoimmun Rev*. 2017 Sep;16(9):925-936. PMID: 28698092. IF: 8,74
2. **Patejdl R**, Winkelmann A, Ehler J, Zettl H, Meister S, Zettl UK. [Diagnostic Workup and Treatment of Antibody-Related Encephalomyelitis]. *Fortschr Neurol Psychiatr*. 2016 Oct;84(S 02):S88-S91. PMID: 27806422. IF: 0,71
3. Zettl UK, Dudesek A, Rimmele F, Zettl H, **Patejdl R**. [Autoimmune-Mediated Encephalomyelitis: a Heterogeneous Entity in Between Neurology and Psychiatry]. *Fortschr Neurol Psychiatr*. 2016 Oct;84(S 02):S84-S87. PMID: 27806421. IF: 0,71
4. Zettl UK, Rommer P, Hipp P, **Patejdl R**. Evidence for the efficacy and effectiveness of THC-CBD oromucosal spray in symptom management of patients with spasticity due to multiple sclerosis. *Ther Adv Neurol Disord*. 2016 Jan;9(1):9-30. PMID: 26788128 IF: 4.12
5. **Patejdl R**, Penner IK, Noack TK, Zettl UK. Multiple sclerosis and fatigue: A review on the contribution of inflammation and immune-mediated neurodegeneration. *Autoimmun Rev*. 2016 Mar;15(3):210-20. PMID: 26589194. IF: 8,96

6. **Patejdl R**, Penner IK, Noack TK, Zettl UK. [Fatigue in patients with multiple sclerosis-  
-pathogenesis, clinical picture, diagnosis and treatment]. *Fortschr Neurol Psychiatr*.  
2015 Apr;83(4):211-20. PMID: 25893494. IF: 0,80
7. **Patejdl R**, Tesar S, Zettl UK. [Multiple sclerosis, neuromyelitis optica and spasticity:  
control of specific symptoms and quality of life]. *Fortschr Neurol Psychiatr*. 2014  
Jul;82(7):373-85. PMID: 25014200. IF: 0,63
8. **Patejdl R**, Mix E, Zettl UK. Editorial: keeping track of an expanding subject--recent  
trends in immunology and their clinical implications. *Curr Pharm Des*.  
2012;18(29):4441-2. PMID: 22873750. IF: 3,31
9. Rommer PS, **Patejdl R**, Zettl UK. Monoclonal antibodies in the treatment of  
neuroimmunological diseases. *Curr Pharm Des*. 2012;18(29):4498-507. PMID:  
22612751 IF: 3,31
10. **Patejdl R**, Zettl UK. Animal models in neurology: drawbacks and opportunities. *Curr  
Pharm Des*. 2012;18(29):4443-52. PMID: 22612747 IF: 3,31
11. Zettl UK, Stüve O, **Patejdl R**. Immune-mediated CNS diseases: a review on  
nosological classification and clinical features. *Autoimmun Rev*. 2012 Jan;11(3):167-  
73. PMID: 21619943 IF: 7,98

#### Korrespondenz und Kasuistiken mit Impact-Faktor

1. **Patejdl R**, Wittstock M, Zettl UK, Jost K, Grossmann A, Prudlo J. Neuromyelitis optica  
spectrum disorder coinciding with hematological immune disease: A case report. *Mult  
Scler Relat Disord*. 2016 Sep;9:101-3. PMID: 27645353. IF: 2,35
2. **Patejdl R**, Krohn S, Murua Escobar H, Zettl UK. Fatal Acute Myeloid Leukemia With  
11q23 MLL Gene Rearrangement Following Mitoxantrone Treatment in a Case of  
Childhood-onset Multiple Sclerosis. *J Pediatr Hematol Oncol*. 2015 Jul;37(5):413-4.  
PMID: 25851557. IF: 1,15
3. **Patejdl R**, Markmann S, Benecke R, Wittstock M. Severe acute motor neuropathy  
after treatment with triple tyrosine kinase inhibitor BIBF 1120 (Nintedanib). *Clin Neurol  
Neurosurg*. 2013 Sep;115(9):1851-2. PMID: 23414813. IF: 1,25

4. Ehler J, **Patejdl R**, Junghanss C, Lehmitz R, Pahnke J, Großmann A, Vogelgesang S, Brüggemann M, Benecke R, Zettl UK. Intrathecal large granular lymphocytes as an unusual presentation of a small cell T cell lymphoma. Clin Neurol Neurosurg. 2012 Sep;114(7):1102-3. doi: 10.1016/j.clineuro.2012.02.029 PMID: 22421252 IF: 1,23
5. **Patejdl R**, Borchert K, Pagumbke H, Benecke R, Grossmann A, Prall F, Kahl C, Freund M, Schmitt M, Walter U. Posterior reversible encephalopathy syndrome (PRES): an unusual primary manifestation of a diffuse large B-cell lymphoma. Clin Neurol Neurosurg. 2011 Nov;113(9):819-21. PMID: 21924823 IF: 1,58
6. **Patejdl R**, Winkelmann A, Benecke R, Zettl UK Muscle rupture caused by exacerbated spasticity in a patient with multiple sclerosis. J Neurol. 2008 Dec;255 Suppl 6:115-8. PMID: 19300971 IF: 2,54
7. Winkelmann A, **Patejdl R**, Wagner S, Benecke R, Zettl UK. Cerebral MRI lesions and anti-tumor necrosis factor-alpha therapy. J Neurol. 2008 Dec;255 Suppl 6:109-14. PMID: 19300970 IF: 2,54

#### Buchbeiträge

**Patejdl R**, Zettl UK. Immunpathologie und Pathogenese in: Fatigue bei Multipler Sklerose. Penner IK (Hrsg). 2008, S. 39-52. ISBN 978-3-936817-32-4

#### Kongressbeiträge / Vorträge

1. **Patejdl R**, Schulz B, Freitag V, Noack T: Wirkungen von Methylenblau auf die Kontraktionsmuster der murinen Magenmuskulatur. 27. Jahrestagung der Deutschen Gesellschaft für Neurogastroenterologie und Motilität, Freising, 29.02.2020
2. **Patejdl R**: AWMF Update: Fallstricke der neuen Approbationsordnung-Curriculum Neurogastroenterologie. 27. Jahrestagung der Deutschen Gesellschaft für Neurogastroenterologie und Motilität, Freising, 01.03.2020
3. **Patejdl R**, Schulz B, Noack T: Erstellung und Charakterisierung eines photodynamisch induzierbaren murinen ex vivo Modells der Gastroparese. 26. Jahrestagung der Deutschen Gesellschaft für Neurogastroenterologie und Motilität, Berlin, 23.03.2019

4. **Patejdl R:** Präsenz der Neurogastroenterologie in der Lehre 26. Jahrestagung der Deutschen Gesellschaft für Neurogastroenterologie und Motilität, Berlin, 24.03.2019
5. **Patejdl R:** Funktion begreifen: Das „Herzpraktikum“ in der Humanmedizin.im Rahmen des „Didactic Workshop“, 98. Jahrestagung der Deutschen Physiologischen Gesellschaft, Ulm, 29.09.2019
6. **Patejdl R, Zanaty K, Ehler J, Noack T:** Neurotransmission and contractility of human colon muscle as bioassay to predict critical illness polyneuropathy (CIP). 25. Jahrestagung der Deutschen Gesellschaft für Neurogastroenterologie und Motilität, Freising, 03.03.2018
7. **Patejdl R, Zanaty K, Noack T et al:** Neurotransmission and Contractility of Human Colon Smooth Muscle as a Predictive Bioassay for Critical Illness Neuromyopathy (CINM). Hauptstadtkongress der Deutschen Gesellschaft für Anästhesiologie & Intensivmedizin, Berlin, 20.09.2018
8. **Patejdl R, Gromann A, Zanaty K, Noack T:** Enhanced giant contractions and inhibited neurotransmission are independent effects of ajmaline in smooth muscle from rat distal colon. 24. Jahrestagung der Deutschen Gesellschaft für Neurogastroenterologie und Motilität, Berlin, 12.03.2017
9. **Patejdl R, Rustenbeck L, Heinrich HH:** Neurogenic control of venous smooth muscle: a functional component analysis. 6<sup>th</sup> Symposium of the German Young Physiologists, Jena, 28.9.2017
10. **Patejdl R, Kraft M, Noack T:** The sphingosine analogue FTY720 increases tone and contractility of gastric smooth muscle. 9. Lübeck Workshop on Smooth Muscle Function, Lübeck, 04.12.2017
11. **Patejdl R:** Gastroparese bei Neurologischen Intensivpatienten. 33. Arbeitstagung der NeuroIntensivMedizin, Berlin, 30.01.2016
12. **Patejdl R, Leroux AC, Gromann A, Noack T:**Klasse Ia – Antiarrhythmika und ihre stimulierenden Effekte auf die gastrointestinale Motilität. 23. Jahrestagung der Deutschen Gesellschaft für Neurogastroenterologie und Motilität, Freising, 06.02.2016
13. **Patejdl R, Brüggemann T:** smooth and sighted - optogenetic control of stomach and bladder contractions. 4<sup>th</sup> Symposium of the German Young Physiologists, Jülich, 06.09.2016
14. **Patejdl R, Heinrich HH, Rustenbeck L:** Tetanization and relaxation in venous smooth muscle exposed to electric field stimulation. 7. Lübeck Workshop on Smooth Muscle Function, Lübeck, 9.11.2015
15. **Patejdl R, Leroux AC, Noack T:** Pacemaking in extraintestinal phasic smooth muscle – what about TRPs? 3rd Symposium of the German Young Physiologists, Bonn, 28.9.2014

## 8. Eidesstattliche Erklärung

Hiermit erkläre ich an Eides statt, dass die vorliegende Arbeit von mir selbstständig und ohne fremde Hilfe sowie nur unter Benutzung der angegebenen Quellen und Hilfsmittel erstellt worden ist.

Ich versichere weiterhin, dass diese Arbeit nicht vorher und auch nicht gleichzeitig bei einer anderen als der genannten Fakultät zur Eröffnung des Habilitationssverfahrens eingereicht worden ist.

Weiterhin erkläre ich an Eides statt, dass ich die deutsche Staatsbürgerschaft besitze und mir die Bestimmungen der Habilitationsordnung bekannt sind.

Rostock, 08.09.2020

Dr. Robert Patejdl

## 9. Danksagung

Herr Prof. Dr. Thomas K. Noack hat meinen wissenschaftlichen Werdegang über viele Jahre hinweg unermüdlich mit seinen anregenden Ideen und seinen unbestechlich klaren Analysen begleitet. Ihm gebührt mein besonderer Dank für seine fachliche und Unterstützung und Förderung.

Weiterhin bedanke ich mich bei meinen klinischen und grundlagenwissenschaftlichen Kooperationspartnern sowie meinen gegenwärtigen und früheren Kolleginnen und Kollegen an der Universitätsklinik für Neurologie sowie am Oscar-Langendorff-Institut für Physiologie für die Möglichkeit zum Lernen und zu anregenden Diskussionen. Insbesondere gedankt sei Herrn Prof. Dr. Uwe K. Zettl für seine vorbildhafte Vermittlung ärztlicher Haltung und eines naturwissenschaftlich fundierten klinischen Denkens.

Ebenfalls bedanken möchte ich mich bei den Studentinnen und Studenten, die ich im Rahmen meiner akademischen und wissenschaftlichen Tätigkeit auf ihrem Weg begleiten konnte. Es war eine inspirierende Erfahrung, gemeinsam mit und von ihnen zu lernen.

Möglich und mit Sinn erfüllt wurde diese Arbeit erst durch die Unterstützung und Motivation vonseiten meiner Eltern, meiner Frau Sophia und meinen Kindern Hanna und Jakob Patejdl, bei denen ich mich besonders herzlich bedanken möchte.

## Calcium movement in smooth muscle and evaluation of graded functional intercellular coupling

R. Patejdl, and T. Noack

Citation: *Chaos* **28**, 106311 (2018); doi: 10.1063/1.5035168

View online: <https://doi.org/10.1063/1.5035168>

View Table of Contents: <http://aip.scitation.org/toc/cha/28/10>

Published by the [American Institute of Physics](#)

---

### Articles you may be interested in

[Differentiating resting brain states using ordinal symbolic analysis](#)

*Chaos: An Interdisciplinary Journal of Nonlinear Science* **28**, 106307 (2018); 10.1063/1.5036959

[Harnessing stochasticity: How do organisms make choices?](#)

*Chaos: An Interdisciplinary Journal of Nonlinear Science* **28**, 106309 (2018); 10.1063/1.5039668

[Spiking patterns and synchronization of thalamic neurons along the sleep-wake cycle](#)

*Chaos: An Interdisciplinary Journal of Nonlinear Science* **28**, 106314 (2018); 10.1063/1.5039754

[Evolutionary dynamics in the public goods games with switching between punishment and exclusion](#)

*Chaos: An Interdisciplinary Journal of Nonlinear Science* **28**, 103105 (2018); 10.1063/1.5051422

[System-size expansion of the moments of a master equation](#)

*Chaos: An Interdisciplinary Journal of Nonlinear Science* **28**, 106303 (2018); 10.1063/1.5039817

[Propagation delays determine neuronal activity and synaptic connectivity patterns emerging in plastic neuronal networks](#)

*Chaos: An Interdisciplinary Journal of Nonlinear Science* **28**, 106308 (2018); 10.1063/1.5037309

---



**Don't** let your writing  
keep you from getting  
published!

**AIP** | Author Services

Learn more today!

# Calcium movement in smooth muscle and evaluation of graded functional intercellular coupling

R. Patejdl<sup>a)</sup> and T. Noack<sup>b)</sup>

Department of Physiology, University of Rostock, Universitätsmedizin, Oscar-Langendorff Institut für Physiologie, Gertrudenstr. 9, D-18057 Rostock, Germany

(Received 13 April 2018; accepted 3 July 2018; published online 10 October 2018)

Spontaneous activity of vascular smooth muscle is present in small arteries and some venous tissues like the hepatic portal vein. Whereas the ability to generate rhythmic membrane potential changes is expressed in a high number of primary oscillators, the generation of physiological tone and phasic activity requires synchronization of specialized pacemaker activity (Interstitial Cajal-like cells) by intercellular propagation and regeneration of excitation or a strong coupling mechanism of smooth muscle cells. The aim of this study was to deduce oscillator coupling by analyzing the spatiotemporal homogeneity of calcium oscillations within a native tissue preparation. Portal vein tissue was loaded with a calcium-sensitive dye (Fluo-3). By combining confocal microscopy and computation of spatial auto- and cross-correlation of the calcium signals, temporal and spatial coupling between cells was characterized. Spontaneous oscillations of calcium signals were measured at different predefined regions of interest. Cross-correlation analysis of these signals revealed that their damping was very similar in all directions of the investigated z-plane. In single experiments, improved cell-to-cell coupling was seen when noradrenaline (1–10  $\mu\text{M}$ ) was added to the bath-solution. With the chosen parameters of frame refresh, the velocity of signal propagation was faster than the maximum detectable velocity, but it could be estimated to exceed 0.1 mm/s. Correlative Network Analysis is a new and very useful tool to determine the functional coupling parameters of quasi-homogenous biological networks and their temporal changes. The action and significance of pharmacological modulators can be well studied on cellular and functional aspects with this newly introduced technique in biological sciences. *Published by AIP Publishing.* <https://doi.org/10.1063/1.5035168>

**In multicellular tissues, excitation and calcium signaling is dependent on structural and functional tissue properties which have many determinants. Total activity, coupling, and action of the tissue cannot be estimated easily. Using confocal microscopy to determine the temporal changes of the intracellular calcium concentrations, the calculation of the two or three-dimensional cross correlation, facilitates a measure of functional cellular coupling and changes of the coupling by the action of hormones or transmitters. In cellular networks, where the cell types are non-homogenous, this network-analysis provides insights about the geometrical signal flow by inverting and non-inverting cells.**

## I. INTRODUCTION

Spontaneous activity of vascular smooth muscle is present in small arteries and some venous tissues like the hepatic portal vein.<sup>1–4</sup> The generation and propagation of electrical signals is a key element of physiological function in these excitable tissues. The basic oscillatory process underlying spontaneous activity in smooth muscle is complex and not yet fully elucidated.<sup>3,5</sup> The ability to generate oscillations is considered to be an intrinsic function of cells and

subcellular domains distributed all over the smooth muscle tissue. In gastric smooth muscle, it is accepted that different types of specialized oscillating and transmitting cells exist. These cells are termed as “Interstitial cells of Cajal” or ICC. The oscillating “pacemaker cells” are connected morphologically amongst each other and to smooth muscle cells. In vascular smooth muscle, the existence of such specialized cells is discussed controversially.<sup>1–4</sup> In portal vein smooth muscle, ICC have been morphologically and physiologically identified. In mesenteric arterial smooth muscle, such cells were not found and spontaneous activity was explained by strong cellular coupling and calcium release mechanisms. The degree of coupling between the elementary oscillators (ICCs and smooth muscle or smooth muscle cells solely) is largely unknown and has formerly been estimated indirectly in most studies from observations of the contractile patterns of the tissue or by measuring electrical or diffusive conductivities between cells (Table I).

In most vascular tissues, the mechanical activity results from “minute-rhythm” oscillations of membrane potential and can be increased in amplitude and frequency up to a “tetanic tone” under stimulation with the sympathetic agonist noradrenaline.<sup>6,7</sup> Under physiologic conditions, a part of vascular tone<sup>8</sup> and, especially, phasic contractions depend on changes of intracellular calcium levels that are controlled by intercellular propagation and regeneration of excitation. Both processes involve a variety of biophysical mechanisms

<sup>a)</sup>Electronic mail: robert.patejdl@uni-rostock.de

<sup>b)</sup>Author to whom correspondence should be addressed: thomas.noack@uni-rostock.de. Tel.: +49 381 494 8010

TABLE I. Experimental approaches to intercellular coupling in smooth muscle.

Technique	Advantage	Disadvantage
Extracellular electrical recordings <sup>a</sup>	No tissue damage High temporal resolution	Poor spatial resolution No direct information on cell to cell communication
Sharp microelectrodes and microinjection <sup>b</sup>	Determination of signal velocity Determination of important parts in the cascade Good temporal resolution	Restricted spatial resolution No direct information on cell to cell communication
Multi-cell patch clamp <sup>c</sup>	Direct measurement of intercellular connections High temporal resolution	Incalculable alteration of cells and intercellular communication by enzymatic and mechanical preparation
Dye-diffusion <sup>d</sup>	Possible without tissue damage	No information on dynamic electrical tissue properties and excitation Unknown interactions with cellular metabolism
Confocal microscopy <sup>e</sup>	No tissue damage necessary visualization of dynamic changes in Ca-Concentration Wide tissue areas observable at once	Only semi-quantitative, indirect information on excitation

<sup>a</sup>Refs. 24 and 25.<sup>b</sup>Ref. 26.<sup>c</sup>Ref. 27.<sup>d</sup>Refs. 10 and 28.<sup>e</sup>Refs. 2 and 29.

and cellular structures, which have been the subject of a number of investigations, including measurements of cell-to-cell coupling and analysis of connexins.<sup>9–11</sup> Furthermore, the generation and propagation of electrical activity is difficult to describe in a mathematical and physiological way yet since the determination of cell-to-cell coupling is not a simple resistive behavior.<sup>12–16</sup> Taking all these items together, the aim of this study was to provide an elegant phenomenological characterization of the spatiotemporal properties of functional intercellular coupling of such a complicated network, rather than giving detailed estimates on the mechanisms and parameters of cell-to-cell connectivity.

For some tissues, e.g., nerves or skeletal muscle, the processes underlying coordinated behavior have been thoroughly characterised and integrated into mathematical and biophysical models.<sup>17–19</sup> In smooth muscle, several cell types with a wide range of largely unknown active and passive bioelectrical properties contribute to the bioelectrical activity, giving too many dark horses to yet allow for its mathematical description or physiological modeling. In the early 20th century, the term of “single-unit” and “multi-unit” type smooth muscles has been formed which categorizes the variety of smooth muscle tissues into those with “higher” and “lower” cell to cell coupling and, correspondingly, different patterns of neuronal control.<sup>20,21</sup> This, however, was made up by the observation of spontaneous myogenic activity in some smooth muscle tissues (single unit type). Until today, electrical coupling of smooth muscle cells and the interconnection to other cell types like endothelial cells, nerve tissue, and interstitial cells of Cajal (ICC) is of great interest. One physiological

feature of endogenous or hormonal modulation of tissue function could be the modulation of gap junctions.<sup>10,22,23</sup>

Table I gives a synopsis on experimental techniques that have been employed to elucidate the function and interaction of smooth muscle cells, neural structures, ICC, and endothelial cells, which are assumed to be the key elements in the regulation of smooth muscle tone.<sup>30</sup> Recording electrical activity is the most intuitive way of establishing a representation of excitation, but its utility is strongly restricted by the risk of producing artificial signals by cellular damage during isolation procedures and by the technical restrictions of simultaneous multicellular measurements. Confocal microscopy has extensively been employed in studies on excitation contraction coupling and calcium movements in smooth muscle cells.<sup>31,32</sup> However, only a small number of studies by now have addressed the issue of functional coupling behavior in smooth muscle tissues. Since functional coupling consists of electrotonic depolarization of the surrounding cells leading to opening of voltage dependent calcium channels, it is much more than a simple comparison of resistive conductances. The results of former studies on the coordination of contraction and electrical activity in the rat portal vein have been discussed in Ref. 25. In brief, it can be assumed that there are multiple coupled pacemaker sites that generate complex action potentials that then spread along the vessel wall. However, the degree of synchronization of neighbouring smooth muscle cells has not been studied systematically yet. In the present work, we therefore studied the degree of spatial coupling in the subendothelial smooth muscle layer of the rat portal vein by using a Correlative Network Analysis that

extends conventional fast confocal microscopy for calcium imaging by subsequent algorithms for mathematical Signal- and Network Analysis. Cross correlation of time- or space-dependent signals is a widely used mathematical algorithm in signal detection, image processing, and being used in neurobiological applications. Even in neuronal networks, such a technique is used to determine the connectivity of structures and the delay between signals mostly in event-driven experiments.<sup>33,34</sup> For our best knowledge, this is the first study which uses consequently multidimensional, spatial, and temporal cross correlations in spontaneously active smooth muscle to determine the tissue parameters in terms of signal damping or amplification.

## II. METHODS

**Tissue preparation and dye loading:** The portal veins of 23 Wistar rats were dissected and cleaned from fat and connective tissue. Afterward, they were cut into pieces of  $2 \times 2$  mm size, mounted on a silicon slide, and incubated with Fluo-3 AM-E  $5 \mu\text{mol/l}$  (Sigma-Aldrich, USA) and non-cytotoxic detergent (Pluronic P-123®, BASF, Germany) in Krebs solution at  $22^\circ\text{C}$  in the dark. After 2 h, the mounted tissue was placed into a special organ bath chamber with a bottom made of high quality glass at a thickness of  $160 \mu\text{m}$  with the endothelial side of the preparation faced downwards. The temperature was kept at  $29^\circ\text{C}$  by a thermostat (Temperature Controller TC-344B, Warner Instrument Corporation) and the bathing chamber was perfused with Krebs solution continuously supplied with carbogen gas (95%  $\text{O}_2$ , 5%  $\text{CO}_2$ ). In the course of the experiments, noradrenaline (Sigma-Aldrich, USA) was added at a concentration of 1 up to  $10 \mu\text{M}$ . **Microscopy:** A confocal laser microscope (Eclipse TE 2000-S, Nikon Instruments Inc.) with an integrated scanning unit (CSU-10, Yokogawa) was used for image acquisition via an immersion oil object lens with a magnification factor of 60. An Argon laser (643 Ion Laser, CVI Melles Griot) was used for excitation at 488 nm. An image of the scanned area was gained each 500 ms and the processed with UltraView (Windows-based) software by PerkinElmer. Figure 1 gives a schematic overview of the experimental setup.

### A. Measurements

After 20 min of settling and equilibration in the chamber, the optical plane was positioned in the second subendothelial cell layer. Recordings of fluorescence emission were made at intervals of 10 min in an area of  $120 \times 160 \mu\text{m}$  with a resolution of  $1344 \times 1024$  dots for 120 s. During these 120 s, one image was generated every 500 ms.

### B. Data processing

Areas of interest were defined in the acquired image series, consisting of a central reference area surrounded by 8 central and 8 peripheral areas at horizontal and vertical distances of 2 and  $25 \mu\text{m}$ , respectively, as shown in Fig. 2(a). The local fluorescence values measured in the series of 240 images of one recording were transformed to give the time course of

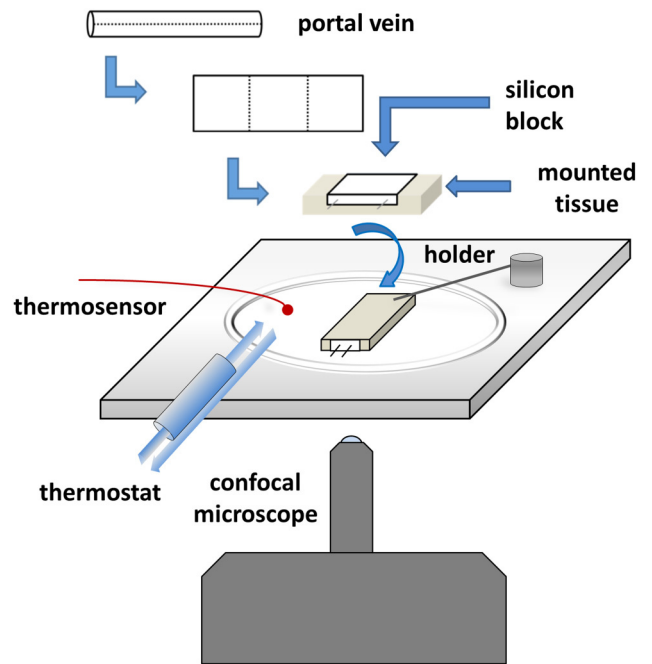


FIG. 1. Setup and tissue preparation for Correlative Network Analysis. The portal vein is split longitudinally and cut into pieces of  $2 \times 2$  mm which are then mounted onto a silicon block and placed in a measuring chamber for confocal microscopy superperfused with physiological salt solution. The tissue bath has a volume of 2 ml and is thermally controlled by the supplying solution and a thermosensor placed near the preparation.

relative fluorescence intensity ( $I_t$ ) at the previously defined areas. **Correlative Network Analysis:** This method uses the myogenic activity of portal vein smooth muscle with the corresponding periods of excitation and rest. During excitation, the intracellular calcium levels are high when compared with resting periods.

If this signal is of high regularity and periodicity, the degree of correlation of the signal  $x$  with signal  $y$  (each from a different location) as a function of their lag (when signal  $x$  follows the course of  $y$ ) or lead (when signal  $x$  anticipates  $y$ ) interval  $\tau$  is given by the cross-correlation function (1) as a dependent variable of  $\tau$ . The minimum distance of  $\tau$  is given by the time duration of each frame—and was chosen here as 500 ms.

$$\Psi_{xy}(\tau) = \lim_{T \rightarrow \infty} \frac{1}{2T} \int_{-T}^T [x(t) - \bar{x}] \times [y(t + \tau) - \bar{y}] dt. \quad (1)$$

Division of (1) by the square root of the product of the auto-correlations of  $x$  and  $y$  gives the normalized cross-correlation function (2):

$$\hat{\Psi}_{xy}(\tau) = \frac{\Psi_{xy}(\tau)}{\sqrt{\Psi_{xx}(\tau) \times \Psi_{yy}(\tau)}}. \quad (2)$$

From pairs of calcium signals from the center region of interest and all other regions at distances of  $2 \mu\text{m}$  and  $25 \mu\text{m}$ , cross correlations were calculated as shown in Fig. 2(a) using Microsoft Excel with the WinStat extension (R.K. Fitch, Germany, 2006). The algorithm used by the software subtracted means from both signals prior to calculating normalized correlation coefficients. Values for cross correlation

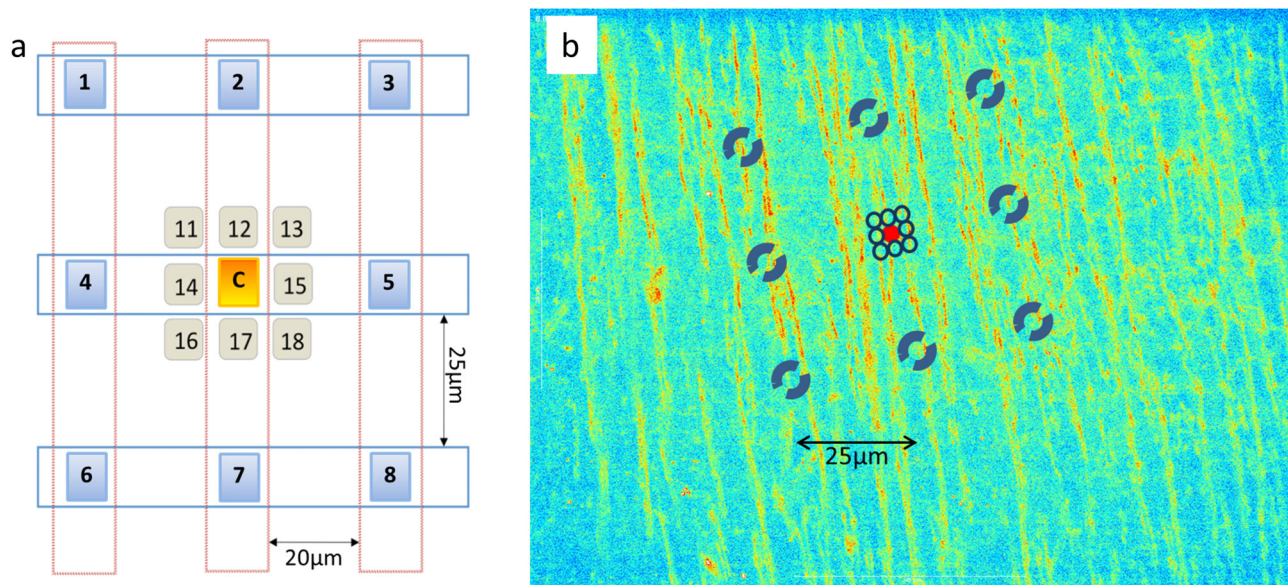


FIG. 2. Areas of interest and schema. (a) For cellular coupling, fluorescence signals are measured in the regions numbered from 1 to 18 and correlated to the signal from the central region “c.” (b) Total scan of calcium signals in the vascular wall. Since oscillation frequency is in the range of 0.05–0.1 Hz (typical minute-rhythm) and signal propagation velocity in  $x$ - or  $y$ -plane is low, all the cells of this scan seem to oscillate in the same phase. To investigate cellular coupling, regions of interest defined for the recording of calcium-dependent fluorescence signals in rat portal vein using confocal microscopy is shown schematically.

were calculated with four decimals. Data are expressed as mean  $\pm$  SEM.  $P$ -values were calculated using a paired  $t$ -test (two sided).

Since the cross correlation between two signals is not dependent on absolute values of the detected signals (i.e., calcium signals), the cross correlation equals 1 if signals from two distinct regions are perfectly in-phase (auto-correlation); if they have a phase-shift of  $180^\circ$ , the scaled cross correlation equals  $-1$ .

For periodic signals, when  $\Psi$  is plotted against  $\tau$ , the value of  $\Psi$  gives peaks at the specific lag or lead interval  $\tau_{xy}$  of the signals and other peaks for multiples of the signal period duration  $T$  added or subtracted from  $\tau_{xy}$ . Therefore, it is possible to determine the degree of similarity between calcium signals from different regions of the tissue, the period length and frequency of the calcium oscillations, the time lag between signals (phase shift) at different given distances and thus the velocity of calcium signal, and finally, spatial differences in the signal-to-noise ratio. With increasing noise, the second and third order maxima and minima of  $\Psi$  will be strongly reduced. In the continuous layer of excited smooth muscle cells, the detected calcium signals can be measured continuously, indicating that the cells are functionally connected to each other. Furthermore, it is a well-accepted fact that between smooth muscle cells, the electrical cellular activity propagates but the parameters of coupling are not yet unequivocally determined (Table I). Being aware that a correlation is not an analytic proof of a direct physical connection, we use the term of functional network analysis in this context.

### III. RESULTS

*Confocal microscopy of portal vein:* After mounting the preparation on the silicone block and placing it in the

organ bath, an appropriate  $z$ -plane was selected for confocal imaging. Figure 2(b) shows a typical example of such a preparation. The smooth muscle cells are vertically orientated in this picture. Some of the regions which are yellow/red colored, indicating higher levels of intracellular calcium, show blotchy areas of calcium accumulation. During the first hour of warming-up, the calcium signal started to change with time and low amplitude oscillations of the signal were observed [Figs. 3(a) and 3(b)].

These wavelike oscillations of fluorescence could be observed for more than 120 min in all preparations. The observed frequency of steady calcium oscillations was 1–2 per minute. Figure 3(a) gives an example of signals from two different regions of interest, namely, those of the center field “C” and the region “4,” lying  $20 \mu\text{m}$  apart in the transversal plane of the tissue. Especially, the center field “C” was chosen to be placed outside the areas where the calcium signal exceeded the normal level. The calcium signal typically declined during the oscillation. This damping was dependent on the laser intensity and due to bleaching of the dye. From the recordings in Fig. 3(a), one can roughly obtain that for both regions the calcium intensity signal is going up and down simultaneously, suggesting that they are in-phase-signals. A more sophisticated method of analysis was performed by applying the temporal cross-correlation function ( $\Psi$ ) on these irregular intensity-time plots.

The spontaneously occurring calcium oscillations had time courses with a high degree of similarity among one another. As can be seen in Fig. 3(a), the cross-correlation function of signals from the included regions has its maximum value at a lag near to zero seconds. This indicates that the temporal offset between the signals observed  $20 \mu\text{m}$  apart in the horizontal direction (center region “C” vs. region 4) was in or below the range of the temporal resolution of the image acquisition. Furthermore, the scaled cross correlation between

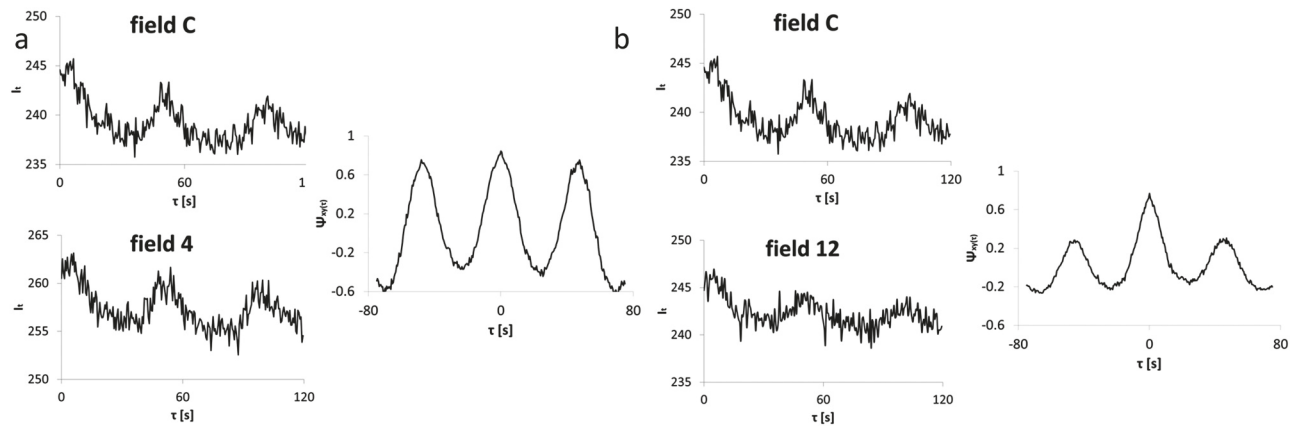


FIG. 3. Time course of the calcium signals and processed cross correlation. (a) Fluorescence signals from the central region “c” and a peripheral region “4.” The according cross correlation has a maximum at the time lag  $\tau$  near zero. (b) Fluorescence signals from a region being  $2\ \mu\text{m}$  apart in the vertical position (field 12) to the central region “c” and their cross correlation which has a similar maximum at  $\tau = 0$  (time lag) but smaller maxima of first order (peaks left and right to the center peak) than in Fig. 3(a).

these signals was close to 0.9, a very high value of correlation. In the example of Fig. 3(b), the center signal was cross correlated with the temporal signal being only  $2\ \mu\text{m}$  apart in the longitudinal direction of the cell orientation. The scaled cross correlation had its maximum also close to 0.8 and close to a tau of 0. The maxima of the second order were smaller than those of Fig. 3(a). This fact indicates that, in addition to the periodic calcium signal, a stochastic noise signal was detected which must have been larger in Fig. 3(b) than in Fig. 3(a). In the following, the first maxima of the scaled cross correlation and their individual  $\tau$  (time when the maxima occurred) were measured subsequently at four positions by shifting the “frame of interest” [Fig. 2(a)] in steps of  $2\ \mu\text{m}$  into the diagonal direction. This procedure of data evaluation was chosen to reduce noise from individual measurements.

Using these algorithms, it was possible to estimate the functional coupling in spontaneous active, vascular smooth muscle. The amplitudes of the maximum values of  $\Psi$  from the regions of interest designated in Fig. 2(a) were plotted against their spatial distances and directions. An example of the results is shown in Fig. 4(a).

The maximum values of  $\Psi$  from regions  $2\ \mu\text{m}$  apart from the center region “C” were higher than those from regions of interest  $20\ \mu\text{m}$  or  $25\ \mu\text{m}$  apart from the center region “C,” indicating a spatial “damping” of the signal. Moreover, the functional damping was relatively large during the first  $2\ \mu\text{m}$  (91.2%,  $n = 16$ , SEM = 2%) and was less expressed from 2 to  $20\ \mu\text{m}$  (84.8%,  $n = 16$ , SEM = 3.7%). As can be obtained from the graph in Fig. 4(a), functional propagation in transversal and longitudinal directions was not significantly different from each other ( $p > 0.1$ ;  $n = 16$ ).

When noradrenaline (NA) was added to the bathing solution, the calcium signals became larger and the part of the oscillating amplitude increased. However, after increasing the bath concentration of NA above  $3\ \mu\text{M}$ , the oscillatory component of the calcium signal decreased and remained on a higher level afterward. The functional coupling of the signals under NA was calculated using the same procedures as described above. The set of data was then condensed and is presented in Fig. 4(b). Compared to the control conditions, the functional coupling was increased at both  $2\ \mu\text{m}$  and  $20/25\ \mu\text{m}$  distances. Such an improvement is due to a more regular spontaneous

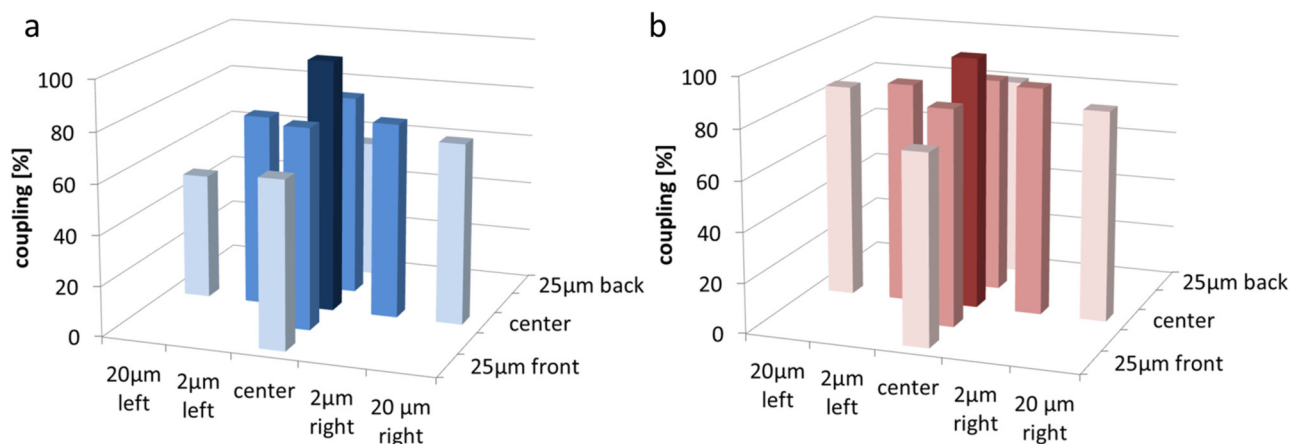


FIG. 4. Example for functional spatial coupling under normal conditions and noradrenaline stimulation. (a) Spatial coupling of calcium waves in rat portal vein: control conditions. z axis: coupling in per cent; x- and y-axes: distance of measured regions from central region. (b) Spatial coupling of calcium waves in rat portal vein: effects of noradrenaline. z axis: coupling in per cent; x- and y-axes: distance of measured regions from central region. Each point is the mean of four samples. For clarity, different shading of the bars was used (central—dark; short distance—medium; and longer distance—light).

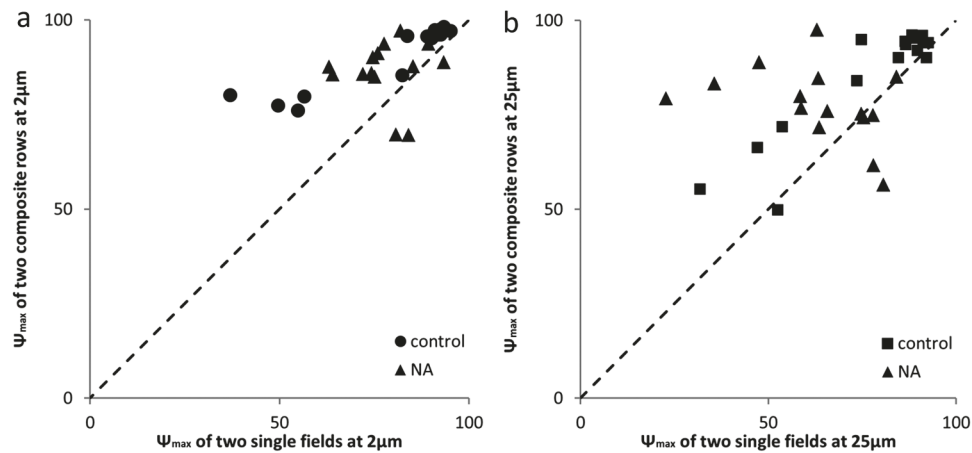


FIG. 5. Influence of sample field size and noradrenaline (NA) on signal similarity. The dashed line represents expected values at theoretical conditions of noise-free homogeneity and complete synchronicity of regions at equal distances from the central region. The points in this figure are obtained by averaging three signals from sites of equal distance in “composite fields.” Points lying above the dashed line represent values increased by increasing field size by averaging due to improved signal-to-noise ratio. Points lying below the level of the dashed line can only occur when there is phase drift and reduced synchronization of signals from fields at equal distance to the central region. Coupling values obtained from single field calculations compared to those from composite fields. (a) Results for composite fields formed from single fields  $2\ \mu\text{m}$  apart from each other. (b) Results for composite fields formed from single fields  $25\ \mu\text{m}$  apart from each other.

activity and a smaller amount of irregular and non-periodic calcium events.

When the NA concentration was further increased to  $10\ \mu\text{M}$ , the functional coupling virtually decreased. Since cross correlation is vitally dependent on the presence of cyclic oscillations, a change of frequency or reduction of the oscillating part of the signal will virtually decrease the functional coupling. Choosing an appropriate size of the regions of interest is important for stability and noise reduction during network-analysis. If the fields were chosen larger than  $10\ \mu\text{m}$  in diameter, the chance to detect a mixed area (in phase and  $180^\circ$  turned phase, see above) became significantly larger than in situations when a circle area of interest with a diameter of only  $2\ \mu\text{m}$  was used. To overcome this problem and to further reduce noise, three raw signals from single fields at the same plane and distance to the each other were summed up, normalized, and cross correlated as “composite fields” [Figs. 5(a) and 5(b)].

In situations of zero noise and without any phase difference, there would be no difference between cross-correlation values from single and “composite fields” which then would exactly cover the dashed lines shown in Figs. 5(a) and 5(b). Data points above this line indicate higher cross-correlation maxima caused by an improved signal to noise ratio. Such a reduction of noise to estimate the coupling properties in smooth muscle tissue can be well performed on the “shorter” distances of  $2\ \mu\text{m}$  [Fig. 5(a)] and on the longer distances of  $25\ \mu\text{m}$  [Fig. 5(b)].

The ambiguous effects of NA on coupling were also seen when single and composite field values were compared: whereas the formation of composite fields for cross correlation gave improved values for coupling under control conditions in all the experiments, adding NA to the solution produced both increased and decreased coupling in different experiments [Figs. 5(a) and 5(b)] due to NA-induced heterogeneity of calcium oscillations.

#### IV. DISCUSSION

In this paper, we have described the measurement of functional cell to cell coupling in an intact portal vein that shows spontaneous activity as it is also present in small arteries and some venous tissues. Its typical minute-rhythm is very sensitive in amplitude and frequency and dies out frequently during *in vitro* experiments. It can be increased in amplitude and frequency to a “tetanic tone” under stimulation with the sympathetic agonist noradrenaline or during stimulation with high potassium solution. Tone and phasic activity depend on intercellular propagation and regeneration of excitation. For determination of functional cell to cell coupling, it is of vital importance that this minute rhythm is present and stable; otherwise, a cross correlation would not make any sense.

The propagation of rhythmical excitation involves a variety of biophysical mechanisms and cellular structures, which have been the subject of a number of investigations, including measurements of cell-to-cell coupling<sup>23</sup> or dye injection.<sup>35</sup> Furthermore, generation and propagation of electrical cellular activity is difficult to describe in a mathematical and physiological way to give a clear picture of the propagation yet, since the determination of cell-to-cell coupling is not a simple ohmic behavior.<sup>25</sup> It is much more the functional character of coupling that has to be determined, since it necessarily includes electrotonic conduction of excitation and reaching the threshold of the L-type calcium channel system (or other voltage dependent current components).<sup>36</sup> The aim of this study was to determine tissue and cellular properties without disturbing the cellular syncytial tissue properties. From organ bath experiments, it is known that the activation of spontaneous activity is often non-gradual; it is either present or absent and from a certain level, small depolarizations rather suddenly evoke spontaneous activity. Such a behavior can be explained by a positive feedback mechanism that is activated when the threshold is reached and which is known as the “all

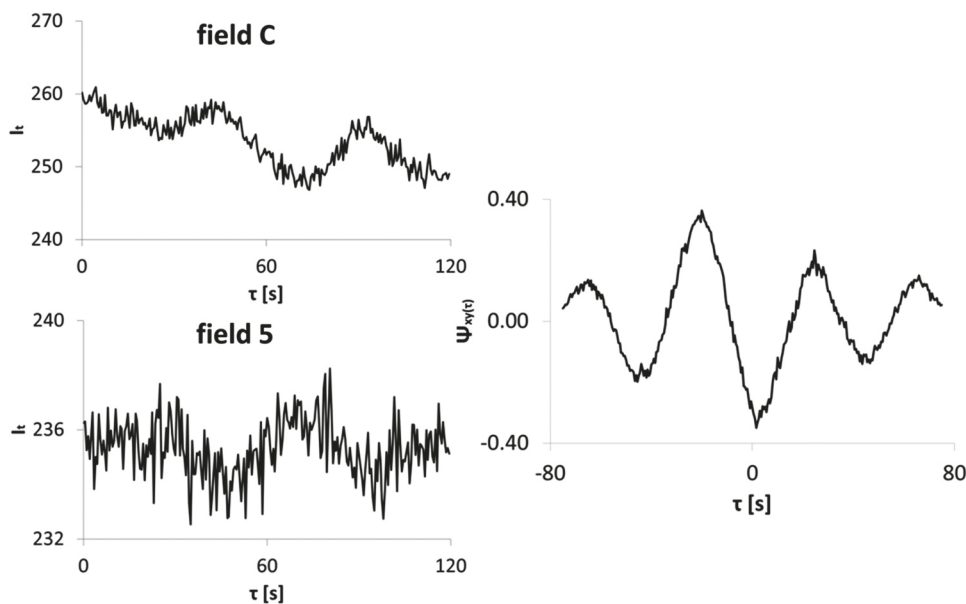


FIG. 6. Example of a signal from a distinct sample region showing antiphase behavior in relation to the circumjacent vascular smooth cells. Despite the only modest signal-to-noise ratio, the antiphase character is clearly depicted in the raw signal from region “S” when compared to that from the central region “C.” In accordance with both, the antiphase character and the low signal power, the cross correlation on the right side of the figure has a negative first order peak (see arrow) and significantly reduced second order maxima.

or nothing” mechanism of excitation in nervous tissues. Such a mechanism is strongly dependent on the positive feedback and the circuit’s forward amplification. In the term of excitation of a whole tissue, this feedback and amplification are due to the coupling between the cells and the size of de- and repolarizing currents.<sup>36</sup> If these factors are large, the “functional reserve” of cellular coupling is also large and small changes of excitation parameters (e.g., inward currents or potassium channel modulation) will not dramatically change the amplitude or frequency of the smooth muscle tone.

### A. Effects of noradrenaline

Noradrenaline, the transmitter of the sympathetic nervous system, increases tone in various vascular beds via alpha receptor binding. This increase of tone is often accompanied by an increase of the intracellular calcium level. Since the vessels contract along the whole circumferential wall, all smooth muscle cells are more or less involved in this activation process. It has been shown in rat mesenteric arteries that the intracellular calcium becomes more homogenous in different smooth muscle cells with increasing concentration of noradrenaline.<sup>37</sup> The underlying mechanism is a better electrotonic coupling via gap junctions which can be modulated in their coupling behavior by various hormones or transmitters. On a longer time scale, an improved cell-to-cell coupling can be maintained by a higher expression of connexin proteins.<sup>23</sup> Such an improvement of cell-to-cell coupling by noradrenaline seems, however, not to be the only mechanism of excitation and propagation in spontaneously active vascular smooth muscle. In rat portal vein, during noradrenaline action, phases of activity fuse more and more and at high concentrations, they fuse completely and contraction does not reach the baseline like it can be observed in pure phasically active smooth muscle (i.e., gastric antrum). Up to a certain concentration (1–3  $\mu\text{M}$ ), portal vein reacts to NA increase with an improved synchronization of the activity kernels, an increased amplitude of their calcium oscillations, and

an increase of coupling between these kernels so that it might look like as the contraction of a “single unit” preparation.<sup>20,21</sup>

In some of our measurements, we observed a slight decrease of cellular coupling, when a NA concentration was used up to 10  $\mu\text{M}$ . This virtual contradiction is due to the fact that the intrinsic, endogenous oscillatory behavior of the tissue was used to perform the Correlative Network Analysis. When noradrenaline causes tetanic contractions as described above, it does so by increasing the intracellular calcium concentration to a plateau-level. This, in turn, would decrease the overall-amplitude of calcium oscillations of single kernels. The resulting cross-correlation function would, however, not be influenced by this process, since it uses an inherent normalization procedure. Nevertheless, if the phasic activity is not changed homogeneously so that in some kernels distinct activations fuse to a single one in some kernels, whereas in others, they remain separated, an apparent inhomogeneity of the oscillation frequency may occur that then, in turn, would decrease the cross-correlation maximum. As can be shown with model simulations, a temporal change of the frequency by only 10% can result in a reduced functional coupling of up to 50% (depending on the duration of the observed interval and the duration of the apparent frequency change).

### B. Spatial and temporal decline of the cross-correlated signal

As stated above, the maximum of the cross-correlated signals declines with distance from each center region. Such a behavior is due to other excitatory or inhibitory signals which influence the determined signal with increasing distance. Stronger coordination between the cells and the signals lead to a better all-over functional coupling. Beside this decrease of the maximal spatial cross correlation, the maxima of the second or third order tend to decrease more or less faster [cf. Figs. 3(a) and 3(b), right side]. The reason for the decrease of the maxima of higher order to a different extend is due to a different signal to noise ratio of the detected signals; noise sources may be due to the dye, the

coupling noise, and the noise induced by fluid movement. The wanted signal is the periodically changing calcium signal caused by periodical excitation. Although cross correlation of time- or space-dependent signals is a widely used mathematical algorithm in biological sciences, this paper is for our best knowledge the first which consequently uses multidimensional, spatial, and temporal cross correlation of intracellular calcium signals in spontaneous active smooth muscle tissues to determine the tissue parameters in terms of signal damping or amplification.

### C. Perspectives

Apart from the specific coupling behavior under NA is the fact that changes of cellular coupling at the threshold can be well detected by the use of this method and technique. As stated above, we sometimes observed 180° phase shifted calcium signals only some  $\mu\text{m}$  apart from spots which were in-phase to the smooth muscle tissue as the whole (Fig. 6).

Such 180° phase shifts were observed when regions of interests were located in areas displaying structural features distinct from the homogenous smooth muscle cell layer. In gastrointestinal preparations, phase shifted signals were prominent in areas containing small blood vessels. From these observations, it might be deduced that also in the vascular wall, signal inverting cells must exist apart from endothelial and smooth muscle cells. Maybe that the structural difference between venous, arterial, and gastric smooth muscle is the numeric occurrence of ICCs and the grade of coupling.<sup>1-4</sup> The physiological role of such anti-phase cells has yet to be determined. Converse calcium signals are known to occur in smooth muscle and endothelial cells during acetylcholine induced endothelial activation.<sup>38</sup> They have also been reported to occur spontaneously in smooth muscle and endothelial cells.<sup>39</sup> By now, it only can be speculated that the phenomenon observed in our preparations in the absence of external agonists might contribute to adapt vascular resistance by lowering calcium in smooth muscle cells of intramural resistance vessels to compensate for luminal compression occurring in periods of increased intramural pressure caused by extravascular smooth muscle contraction. This, however, will be the subject of further studies that hopefully will help to integrate the described phenomena into existing theories of pacemaker activity and signal propagation in the vascular wall and lead to a better understanding of the temporal patterns of intercellular communication in general.<sup>2,40-42</sup>

### ACKNOWLEDGMENTS

The authors declare that they have no conflict of interest.

All experiments of this study comply with the regulations and rules as defined by the ethics commission of the University of Rostock and with German laws.

<sup>1</sup>Th. Noack, P. Deitmer, and K. Golenhofen, *Pflügers Arch.* **416**, 467 (1990).

- <sup>2</sup>T. B. Bolton, D. V. Gordienko, O. V. Povstyan, M. I. Harhun, and V. Pucovsky, *Cell Calcium* **35**, 643 (2004).
- <sup>3</sup>C. Aalkjaer and H. Nilsson, *Br. J. Pharmacol.* **144**, 605 (2005).
- <sup>4</sup>V. V. Matchkov, A. Rahman, H. Peng, H. Nilsson, and C. Aalkjaer, *Br. J. Pharmacol.* **142**, 961 (2004).
- <sup>5</sup>R. Lees-Green, P. Du, G. O'Grady, A. Beyder, G. Farrugia, and A. J. Pullan, *Front. Physiol.* **2**, 29 (2011).
- <sup>6</sup>K. Golenhofen and D. von Loh, *Pflügers Arch.* **314**, 312 (1970).
- <sup>7</sup>K. Golenhofen and N. Hermstein, *J. Physiol.* **231**, 14P–15P (1973).
- <sup>8</sup>L. T. Lubomirov, K. Reimann, D. Metzler, V. Hasse, R. Stehle, M. Ito, D. J. Hartshorne, H. Gagov, G. Pfitzer, and R. Schubert, *Circ. Res.* **98**, 1159 (2006).
- <sup>9</sup>N. M. Rummery and C. E. Hill, *Clin. Exp. Pharmacol. Physiol.* **31**, 659 (2004).
- <sup>10</sup>D. Begandt, A. Bader, L. Dreyer, N. Eisert, T. Reeck, and A. Ngezhahayo, *J. Cell Commun. Signal.* **7**, 151 (2013).
- <sup>11</sup>A. Kapela, J. Parikh, and N. M. Tsoukias, *Biophys. J.* **102**, 211 (2012).
- <sup>12</sup>S. P. Parsons and J. D. Huizinga, *Front. Neurosci.* **10**, 19 (2016).
- <sup>13</sup>A. Corrias, P. Pathmanathan, D. J. Gavaghan, and M. L. Buist, *Integr. Biol.* **4**, 192 (2012).
- <sup>14</sup>T. M. Griffith and D. H. Edwards, *Am. J. Physiol.* **266**, H1801–H1811 (1994).
- <sup>15</sup>M. Z. Malik, S. Ali, M. J. Alam, G. R. Devi, Ravins, R. Ishrat, and R. K. B. Singh, *J. Nanosci. Nanotechnol.* **12**, 8303 (2012).
- <sup>16</sup>J. D. Huizinga, S. P. Parsons, J.-H. Chen, A. Pawelka, M. Pistilli, C. Li, Y. Yu, P. Ye, Q. Liu, M. Tong, Y. F. Zhu, and D. Wei, *Am. J. Physiol. Cell Physiol.* **309**, C403–C414 (2015).
- <sup>17</sup>A. L. Hodgkin and A. F. Huxley, *J. Physiol.* **117**, 500 (1952).
- <sup>18</sup>A. L. Hodgkin and A. F. Huxley, *Proc. R. Soc. Lond. B Biol. Sci.* **140**, 177 (1952).
- <sup>19</sup>T. Kiyosue, M. Arita, H. Muramatsu, A. J. Spindler, and D. Noble, *J. Physiol.* **468**, 85 (1993).
- <sup>20</sup>E. Bozler, *Science* **86**, 476 (1937).
- <sup>21</sup>E. Bozler, *Am. J. Physiol.* **122**, 614 (1938).
- <sup>22</sup>M. Imamura, Y. Sugino, X. Long, O. J. Slivano, N. Nishikawa, N. Yoshimura, and J. M. Miano, *J. Cell. Physiol.* **228**, 1819 (2013).
- <sup>23</sup>A. Salameh, C. Frenzel, A. Boldt, B. Rassler, I. Glawe, J. Schulte, K. Mühlberg, H.-G. Zimmer, D. Pfeiffer, and S. Dhein, *FASEB J.* **20**, 365 (2006).
- <sup>24</sup>K. Hermsmeyer, *Circ. Res.* **33**, 244 (1973).
- <sup>25</sup>R. Patejdl and T. Noack, *Trace Elem. Electrolytes* **27**, 202 (2010).
- <sup>26</sup>C. de Wit, F. Roos, S. S. Bolz, S. Kirchhoff, O. Krüger, K. Willecke, and U. Pohl, *Circ. Res.* **86**, 649 (2000).
- <sup>27</sup>S. Verheule, M. J. van Kempen, P. H. te Welscher, B. R. Kwak, and H. J. Jongasma, *Circ. Res.* **80**, 673 (1997).
- <sup>28</sup>E. E. Daniel and Y. F. Wang, *Microsc. Res. Tech.* **47**, 309 (1999).
- <sup>29</sup>J. D. Huizinga, L. W. Liu, M. G. Blennerhassett, L. Thuneberg, and A. Molleman, *Experientia* **48**, 932 (1992).
- <sup>30</sup>R. Wei, S. P. Parsons, and J. D. Huizinga, *Exp. Physiol.* **102**, 329 (2017).
- <sup>31</sup>M. J. Berridge, *Biochim. Biophys. Acta* **1793**, 933 (2009).
- <sup>32</sup>M. D. Bootman and M. J. Berridge, *Curr. Biol.* **6**, 855 (1996).
- <sup>33</sup>R. T. Dean and W. T. M. Dunsmuir, *Behav. Res. Methods* **48**, 783 (2016).
- <sup>34</sup>S. F. Farmer, D. M. Halliday, B. A. Conway, J. A. Stephens, and J. R. Rosenberg, *J. Neurosci. Methods* **74**, 175 (1997).
- <sup>35</sup>D. G. Welsh and S. S. Segal, *Am. J. Physiol.* **274**, H178–H186 (1998).
- <sup>36</sup>R. Patejdl, P. Noack, H. H. Hopp, A. Weston, and T. Noack, *Trace Elem. Electrolytes* **22**, 248 (2005).
- <sup>37</sup>M. Sell, W. Boldt, and F. Markwardt, *Cell Calcium* **32**, 105 (2002).
- <sup>38</sup>S. S. Bolz, C. de Wit, and U. Pohl, *Br. J. Pharmacol.* **128**, 124 (1999).
- <sup>39</sup>A. Schuster, H. Oishi, J. L. Bény, N. Stergiopoulos, and J. J. Meister, *Am. J. Physiol.* **280**, H1088–H1096 (2001).
- <sup>40</sup>C. Depry, S. Mehta, and J. Zhang, *Pflügers Arch.* **465**, 373 (2013).
- <sup>41</sup>M. I. Harhun, V. Pucovsky, O. V. Povstyan, D. V. Gordienko, and T. B. Bolton, *J. Cell. Mol. Med.* **9**, 232 (2005).
- <sup>42</sup>H. Peng, V. Matchkov, A. Ivarsen, C. Aalkjaer, and H. Nilsson, *Circ. Res.* **88**, 810 (2001).

# Phenytoin inhibits contractions of rat gastrointestinal and portal vein smooth muscle by inhibiting calcium entry

R. PATEJDL, A.-C. LEROUX & T. NOACK

Institut für Physiologie, Universitätsmedizin Rostock, Rostock, Germany

## Key Messages

- This study investigated the effects of phenytoin, a widely used anticonvulsant drug, on gastrointestinal tissue function using an *in vitro* model of smooth muscle preparations from rats by combining registrations of pharmacological effects on mechanical contractions, electric field potentials, and dynamic intravital fluorescence microscopy.
- Strong inhibitory effects of phenytoin on the spontaneous and stimulated contractile activity of smooth muscles from both upper and lower gastrointestinal tract were observed.
- The inhibitory effects of phenytoin were not related to its sodium channel blocking activity, but are rather caused by an inhibition of calcium entry through voltage dependent L-type calcium channels.
- The results of this study should raise vigilance to gastrointestinal complications in patients treated with phenytoin.

## Abstract

**Background** Phenytoin is widely used as a second-line treatment for status epilepticus. Besides its well-known cardiac pro-arrhythmogenicity, side effects on other organ systems have received less attention.

**Methods** This study investigates the effects of phenytoin on gastrointestinal tissue function using an *in vitro* model of smooth muscle preparations from rats by combining registrations of pharmacological effects on mechanical contractions, electric field potentials, and dynamic intravital fluorescence microscopy. **Key Results** When added to the bathing solution at a concentration of 30  $\mu\text{M}$ , phenytoin reduced the frequency of spontaneous activity significantly in antrum and portal vein preparations to  $72.2 \pm 36.5\%$  ( $p = 0.022$ ) and  $80.7 \pm 24.4\%$  ( $p = 0.037$ ) of control

values, respectively. At a concentration of 100  $\mu\text{M}$ , the height of spontaneous contractions declined to  $9.8 \pm 19.6\%$  ( $p = 0.005$ ) (antrum),  $15.7 \pm 28.2\%$  ( $p = 0.004$ ) (portal vein), and  $31.8 \pm 31.3\%$  ( $p = 0.005$ ) (colon) in comparison to the control conditions before the application of phenytoin. Depolarization triggered increases in calcium dependent fluorescence signals were reduced by  $52.8 \pm 39.1\%$  ( $p = 0.012$ ). The inhibition of spontaneous activity caused by phenytoin was reduced in the presence of the L-type calcium channel agonist BAY K8644(-). **Conclusions & Inferences** Phenytoin exerts strong inhibitory effects on the spontaneous and stimulated contractile activity of smooth muscles from both the upper and lower gastrointestinal tract. The mechanism underlying this effect is not related to the sodium channel blocking activity of phenytoin, but is rather caused by an inhibition of calcium entry through voltage dependent L-type calcium channels. The results of this study should raise vigilance to gastrointestinal complications in patients treated with phenytoin.

**Keywords** BAYK 8644, intestinal smooth muscle, phenytoin, status epilepticus, vascular smooth muscle.

## Address for Correspondence

Robert Patejdl, Oscar-Langendorff-Institut für Physiologie, Universitätsmedizin Rostock, Gertrudenstraße 9, Rostock 18047, Germany.

Tel: +49 381 494 8006; fax: +49 381 494 8002; e-mail: robert.patejdl@uni-rostock.de

Received: 2 December 2014

Accepted for publication: 7 July 2015

**Abbreviations:** ACh, acetylcholine; CAP, compound action potential; ECR, electromechanical coupling ratio; EFS, electrical field stimulation; PB, preparation buffer; TTX, tetrodotoxin.

## INTRODUCTION

Status epilepticus most frequently occurs in children and in the elderly. Especially within the latter, prognosis of the affected patients is often poor due to prior multimorbidity, delayed diagnosis, and age-specific complications of treatment. The reported incidences of status epilepticus in elderly persons range from 22 to 54 per 100 000 depending on group definition and study, which underlines the need for appropriate, knowledge-based treatment strategies in the aging western societies.<sup>1–3</sup>

Despite the growing number of other available anti-convulsive drugs, phenytoin is still widely used as an approved second-line treatment for status epilepticus that is not responsive to benzodiazepines.<sup>4–6</sup> It exerts its inhibitory effects on neuronal excitability by binding to and hindering activation of voltage dependent sodium channels while they are in their inactivated state, thereby producing a use-dependent type of block.<sup>7</sup> Via the same mechanism, phenytoin acts on cardiac sodium channels, which is the basis for its historical use as an antiarrhythmic drug and for its well-known proarrhythmogenic potential. Side effects of phenytoin on other organ systems have received less attention. Disturbances in gastrointestinal motility are known to occur frequently in patients receiving antiepileptic drugs, including phenytoin, and in patients in need for critical care.<sup>8,9</sup> Refractory seizures with prolonged losses of consciousness may cause secondary complications as pneumonia that may then lead to critical care measures as mechanical ventilation and to extensive engagement of motility-disturbing drugs as catecholamines and opioids, leading to a further increase in the risk to develop gastrointestinal hypomotility.<sup>10</sup> The resulting intolerance to enteral feeding contributes to the poor prognosis of the affected patients.<sup>11,12</sup>

This study investigates the effects of phenytoin on gastrointestinal function using an *in vitro* model of smooth muscle preparations from rats. As the functions of upper and lower parts of the alimentary tract, namely gastric emptying and colonic propulsion, are most frequently affected, it was chosen to study preparations from gastric antrum, gastric fundus, and the left colon flexure, reflecting the phasic and tonic component of the gastric motility and colonic function. Furthermore, effects on the motor patterns of the hepatic portal vein were studied, as changes in the

intestinal hemodynamics may bring forward gastrointestinal failure during critical illness.

## MATERIALS AND METHODS

### Preparation of tissues and tissue bath experiments

Twenty-nine Wistar rats of both sexes were killed by decapitation after anesthesia according to German national law and the regulations and ethical standards of the University of Rostock.

The intact stomach, the portal vein, and part of the distal colon (1 cm distal to the left flexure) were excised, transferred to cooled preparation buffer (PB), and stored at 4 °C. The tissues were then pinned to Sylgard dishes and fat and connective tissues were removed by sharp dissection. Longitudinal smooth muscle strips of an *in situ* length of 5–10 mm were excised from antrum, fundus, and colon without opening the stomach. The mucosa of the colon preparations was carefully removed by blunt dissection. Portal veins were split longitudinally. All types of tissue preparations were mounted in an organ bath, each filled with 20 mL of Krebs solution and equilibrated with 95% O<sub>2</sub> and 5% CO<sub>2</sub> at a temperature of 36 °C and a pH of 7.4. They were then connected to mechanoelectrical transducers coupled to a bridge amplifier (both World Precision Instruments, Sarasota, FL, USA), digitized by a PowerLab8/32 at 100/s, digitally low-pass filtered with 0.5 Hz (ADInstruments, Bella Vista, Australia), and then stored for further processing on a conventional computer using LabCart 5 (ADInstruments) and MSExcel (Microsoft, Redmond, WA, USA). Prior to the initiation of experiments, the tissues were adjusted to a prestrain of 3 mN and left in the bathing solution for at least 1 h to ensure sufficient equilibration time for developing their specific motor pattern.

In time control experiments, we could ensure that the specific pattern of activity was stable over at least 6 h under the stated conditions, with minor shifts in frequency and amplitude. To fully compensate for the time-dependent variance, the frequency effects and the effects of pharmacological or other interventions on the amplitude of spontaneous contractions measured in this study were always related to the situation immediately before the intervention. All contractions evoked by elevations of [K<sup>+</sup>] or adding ACh in the course of an experiment were related to a standard control contraction evoked by these substances in the same experiment prior to any other substance application unless stated otherwise.

### Simultaneous registration of electrical and mechanical activity

In a small series of experiments, electrical and mechanical activity of portal veins was measured simultaneously. The portal vein was connected to a force transducer and placed in a plastic capillary of 2.5 mm width that was continuously perfused with Krebs solution from a reservoir. The spontaneously occurring contractions of portal vein smooth muscle are preceded and accompanied by compound action potentials (CAP) that have been described in detail by.<sup>13</sup> They consist of a depolarization with a duration of several seconds with superimposed fast spikes of only 50 ms duration. These CAP were measured as extracellular electric field potentials using ring-shaped platinum electrodes fixed on the inside of a small tube that is continuously perfused with Krebs solution and kept at a constant temperature. The small tube with the fixed electrodes is named 'perfused

capillary'. The portal vein is placed inside this capillary. One end is fixed to the apparatus and the other is connected to an isometric force transducer of the same type that was used for the conventional organ bath experiments. Electrical signals were amplified, filtered with a 10–65 Hz bandpass, digitized at 1000/s (AnimalBioAmp, PowerLab4/32; ADInstruments) and then stored as stated above. Mechanical force was recorded simultaneously, low-pass filtered at 1 Hz and then stored. Substances were applied directly into the organ bath or into the reservoir of the capillary.

## Electric field stimulation

Strips of the fundus muscle were mounted on special holders with inserted platinum wires in the same organ baths as described above. The wires had contact to the bathing medium in close proximity to the position where the smooth muscle tissue was connected to the holder. Stimulus current was generated by a Stimulator (Grass Technologies, Warwick, RI, USA) that was lined to the wires in the holder in a way that ensured that alternating electrode polarities could produce a homogeneous depolarization of the tissue piece. Stimuli were applied subsequently with frequencies of 5, 10 and 20 Hz over 10 s. Each single pulse had an amplitude of 80 V and a duration of 1 ms.

## Intravital fluorescence microscopy

To test for changes in intracellular calcium signals caused by phenytoin, portal vein preparations were loaded with the ratio-metric dye Fura-2-AM at room temperature for 2 h in the presence of 0.1% Pluronic-F127. Afterward, preparations were mounted in an organ bat with a thin bottom suitable for fluorescence microscopy. Excitation was alternately applied at 340 and 380 nm and emission at 510 nm was recorded using a Nikon 200 diaphot microscope (Nikon, Tokyo, Japan) photomultiplier combined with a 714-PTI-photomultiplier (PTI, Edison, NJ, USA). The signal was recorded and stored for further processing using the Felix 1.1 – software (PTI, Edison, NJ, USA). Increases in intracellular calcium are reflected by an increase in the 510-nm emission triggered by the excitation of Fura-2 at 340 nm and a decrease in the 510-nm emission triggered by the excitation at 380 nm. The ratio of the emission caused by 340 and 380 nm excitation is calculated instantaneously to give an intuitive measure of changes in intracellular calcium concentration.

## Drugs and solutions

The solutions used had the following compositions: PB: NaCl 145 mM, KCl 4.5 mM, NaH<sub>2</sub>PO<sub>4</sub> 1.4 mM, MgSO<sub>4</sub> 1 mM CaCl<sub>2</sub>, Ethylenediaminetetraacetic acid (EDTA) 0.025 mM, 4-(2-hydroxyethyl)-1-piperazineethanesulfonic acid (HEPES) 5 mM. Krebs solution: NaCl 112 mM, NaHCO<sub>3</sub> 25 mM, KH<sub>2</sub>PO<sub>4</sub> 1.2 mM, KCl 4.7 mM, MgCl<sub>2</sub> 1.2 mM, CaCl<sub>2</sub> 2.5 mM, Glucose 11.5 mM. Potassium-rich, calcium-free Krebs solution: KCl 116.7 mM, NaHCO<sub>3</sub> 25 mM, KH<sub>2</sub>PO<sub>4</sub> 1.2 mM, MgCl<sub>2</sub> 3.7 mM, Glucose 11.5 mM. The pH was 7.4 at 36.6 °C with continuous carbogen gas bubbling during all experiments (95% O<sub>2</sub>, 5% CO<sub>2</sub>). All salts were purchased from Sigma-Aldrich (St. Louis, MO, USA).

Fura-2-AM and Pluronic F-127 were purchased from Life Technologies (Carlsbad, CA, USA). Effects of phenytoin (Desitin, Hamburg, Germany), tetrodotoxin (TTX, Tocris Bioscience, Bristol, UK), lidocaine (Mibe, Sandersdorf-Brehna, Germany) and BAY K8644(-) (Bayer, Leverkusen, Germany) were tested. Amplitudes of

contractions evoked by increasing the potassium concentration to 40 mM or by adding 10 μM acetylcholine (ACh; Sigma-Aldrich) were normalized against amplitude of contractions evoked by 70 mM potassium unless stated otherwise.

## Data presentation and statistics

Values are given as mean values ± standard deviation of mean. Error bars indicate standard error. The data were analyzed using SPSS (SPSS Inc. Chicago, IL, USA). For statistical testing, the Wilcoxon test for dependent samples and the Mann–Whitney test for independent samples were applied. All tests of significance were performed at  $\alpha = 0.05$ .

## RESULTS

### Spontaneous activity under control conditions

We investigated the changes in rhythm and force development of antrum, colon, and portal vein preparations ( $n = 17$  for each). Under standard conditions (36.6 °C, pH 7.4), the tissue preparations developed their organ-specific pattern of activity which is shown in the leftmost part of the panel Fig. 1A–C and in the Fig. S1. In gastric antrum, it consists of regular, phasic oscillations of tone (Fig. 1A, Fig. S1A). In contrast, portal veins show periods of quiescence with a constant basal tone (Fig. 1B, Fig. S1B). The frequencies were within a range of 3–5 per min for gastric antrum and portal veins preparations, respectively. Strips of gastric fundus smooth muscle exhibited a purely tonic contraction without relevant oscillations of force in the absence of external stimulants. Preparations of colonic smooth muscle exhibited small, irregular contractions of high frequency (>10/min), on which larger 'giant' contractions with a several-fold higher magnitude and duration imposed at a frequency of 1–2 per min (Fig. 11C, Fig. S1C).

### Effects of phenytoin on frequency of spontaneous activity

When added to the bathing solution at a concentration of 30 μM, phenytoin changed the pattern of spontaneous activity in all tissues, as can be seen in representative recordings (Fig. 1A–C). The frequency of spontaneous activity was reduced significantly in antrum and portal vein preparations to  $72.2 \pm 36.5\%$  ( $p = 0.022$ ) and  $80.7 \pm 24.4\%$  ( $p = 0.037$ ) of control values, respectively (Fig. 1D). The effect was dose dependent with a further reduction when phenytoin was raised to 100 μM ( $23.1 \pm 46.1\%$  and  $30.2 \pm 39.0\%$  of control), as can also be seen in the representative traces from Fig. 1A–C. Colonic preparations responded to phenytoin with a decrease in the amplitude of giant

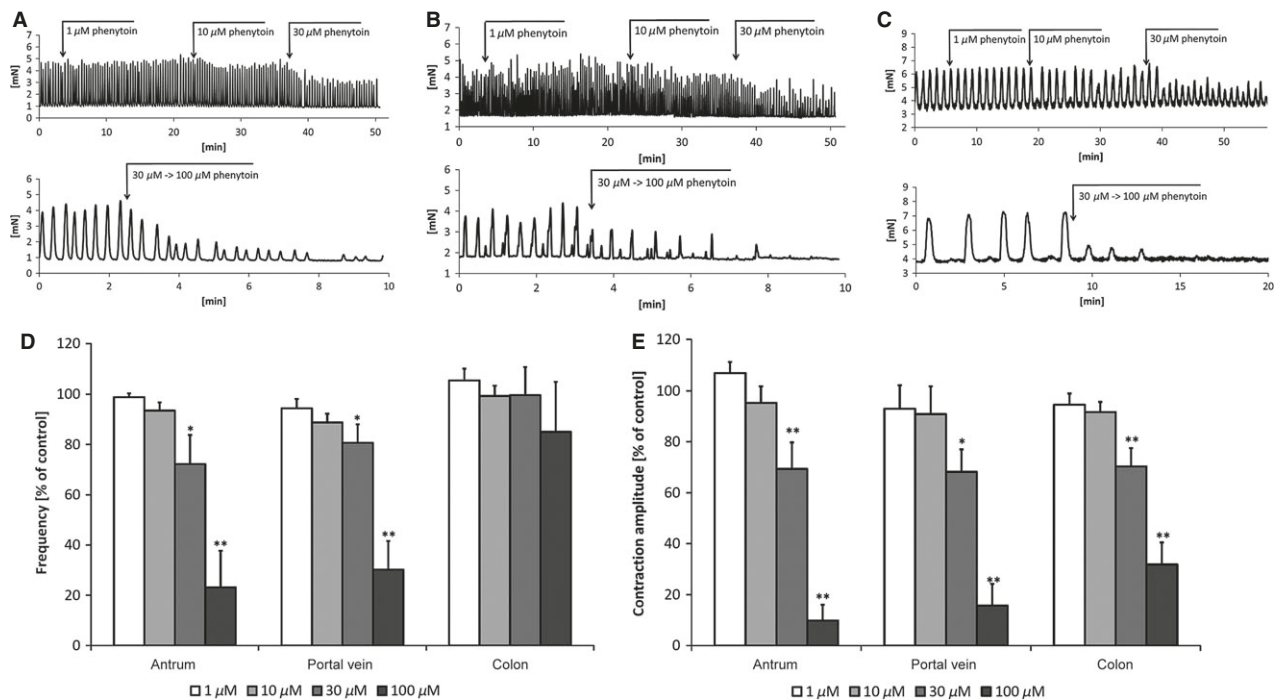


**Figure 1** (A–C) Representative recording traces of a spontaneously active smooth muscle preparations exposed to increasing concentrations of up to 30  $\mu\text{M}$  (upper part) and, finally, a final step from 30 to 100  $\mu\text{M}$  phenytoin. The panel figures show (A) longitudinal strip of gastric antrum; (B) longitudinal strip of smooth muscle from the portal vein; (C) smooth muscle from the descending colon. Changes in phenytoin concentration are indicated by arrows. (D and E) Effects of increasing concentrations of phenytoin on frequency (D) and contraction amplitude (E) of spontaneous contractions of gastric antrum, portal vein, and colon, given as percentage of control values measured prior to adding phenytoin to the bathing solution. Error bars indicate SEM, \* $p < 0.05$ , \*\* $p < 0.01$ ; antrum:  $n = 10$ ; portal vein  $n = 11$ ; colon:  $n = 13$ ).

contractions, as will be depicted later in greater detail. As long as the amplitude was sufficient to produce clearly identifiable contraction events, the frequency of these events persisted largely unchanged over the whole range of tested concentrations. At concentrations of 100  $\mu\text{M}$ , however, contractile activity was completely lost in 4 of the 14 tested preparations, thus formally giving a frequency of zero. Statistically, this behavior is reflected by a small reduction in the arithmetic mean value of frequency, which did not reach significance due to the very high standard deviation ( $85.0 \pm 71.8\%$ ,  $p = 0.798$ ). The small baseline contractions of colonic strips occurring in between the giant contractions were likewise not changed by phenytoin (Fig. S2).

The onset of the action of phenytoin was similar between the different tissues. The maximum effect was attained within less than 5 min independently from the chosen concentration. The inhibitory effect was fully reversible after washout of phenytoin within 25 min in all tissues. Five of the nine antrum preparations showed full recovery (defined as more than 85% of control) within 5–10 min, whereas the remaining four fully recovered within 20 min. In few

instances, colonic smooth muscle showed a persistent inhibition of activity which could be usually overcome by a short and transient stimulation with 1  $\mu\text{M}$  ACh.

### Effects of phenytoin on the amplitude of spontaneous contractions

Phenytoin significantly diminished the height of spontaneously occurring contractions in antrum, colon, and portal vein preparations (Fig. 1E) at concentrations greater than or equal to 30  $\mu\text{M}$  in a dose dependent manner. At a concentration of 100  $\mu\text{M}$ , the mean contraction amplitude declined to  $9.8 \pm 19.6\%$  ( $p = 0.005$ ) (antrum),  $15.7 \pm 28.2\%$  ( $p = 0.004$ ) (portal vein), and  $31.8 \pm 31.3\%$  ( $p = 0.005$ ) (colon) in comparison to the control values obtained in the absence of phenytoin. The duration, slope, and decline of single contractions remained largely unchanged. With respect to the time of effect onset after application of phenytoin, there was no obvious difference to the dynamics of effects on contraction frequency. In general, the recovery of the full height of contractions took longer than the recovery of frequency and was complete after 15 min in more than 80% of preparations. Especially

in six of nine antrum preparations, a transient increase in contraction height above control levels could be observed in the minutes after the washout of phenytoin. The high-frequency and low-amplitude component of colonic activity was reduced less (to  $87.7 \pm 32.6\%$  of control) than the giant contractions of the same tissue.

### Effects of phenytoin on high-potassium contractions

Elevations of  $[K^+]$  to 40 mM caused contractions with reproducible amplitude and shape under control conditions. Characteristic control responses of all tissues consisted of an increase in the force followed by a slow and incomplete relaxation. Phenytoin diminished the slope and amplitude of these contractions in all tissues (Fig. 2B). The amplitude reduction was significant at concentrations greater than or equal to 30  $\mu\text{M}$  in gastric fundus preparations and at a concentration of 100  $\mu\text{M}$  in preparations from gastric antrum, colon, and portal vein. In

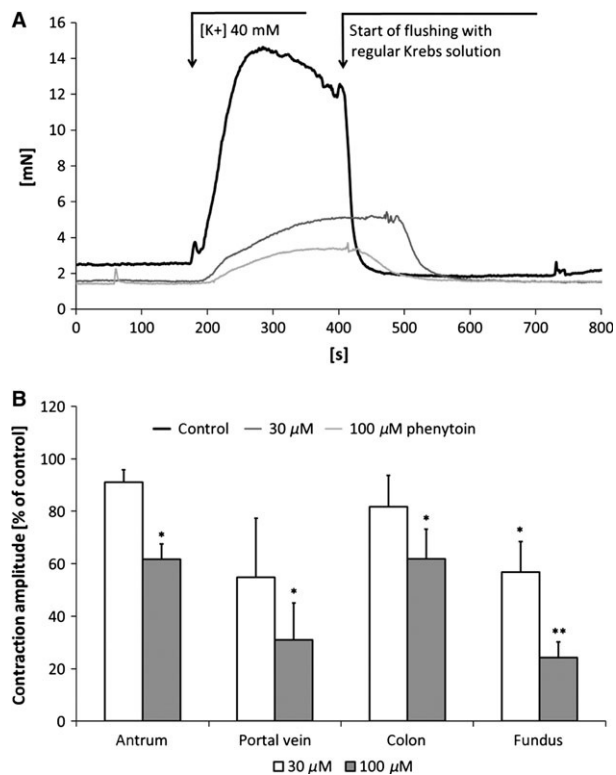


**Figure 2** Gastric fundus strips were contracted by stepping up the potassium concentration from control levels to 40 mM. After flushing with fresh Krebs solution, the preparations showed full relaxation. In (A), three evoked contractions have been overlaid and adapted to a common timescale to improve the comparability of the responses. The quantitative analysis of changes in contraction amplitudes is depicted in (B). All values are given as percentage of control values measured prior to adding phenytoin to the bathing solution. Error bars indicate SEM, \* $p < 0.05$ , \*\* $p < 0.01$ ;  $n = 8$ .

comparison to control, phenytoin 100  $\mu\text{M}$  reduced high- $[K^+]$  contraction on an average to  $61.7 \pm 15.5\%$  ( $p = 0.01$ ) in antrum preparations, to  $31.0 \pm 36.9\%$  ( $p = 0.03$ ) in portal vein preparations, to  $61.8 \pm 32.3\%$  ( $p = 0.012$ ) in colon preparations, and to  $24.3 \pm 17.7\%$  ( $p < 0.001$ ) in fundus preparations. Inhibitory force of phenytoin was fundus > portal vein > colon > antrum. Fig. 2A gives a representative recording of the inhibition phenytoin exerts on high- $[K^+]$  evoked contractions.

### Effects of phenytoin on contractions elicited by ACh

Contractions evoked by 10  $\mu\text{M}$  ACh were markedly reduced in the presence of phenytoin 100  $\mu\text{M}$  (Fig. 3B). Compared to the control conditions, maximum force was diminished on an average to  $59.4 \pm 33.9\%$  ( $p = 0.028$ ) (antrum), to  $24.5 \pm 17.1\%$  ( $p = 0.018$ ) (portal vein), to  $74.0 \pm 28.9\%$  ( $p = 0.008$ ) (colon), and to  $63.3 \pm 30.4\%$  ( $p = 0.011$ ) (fundus).

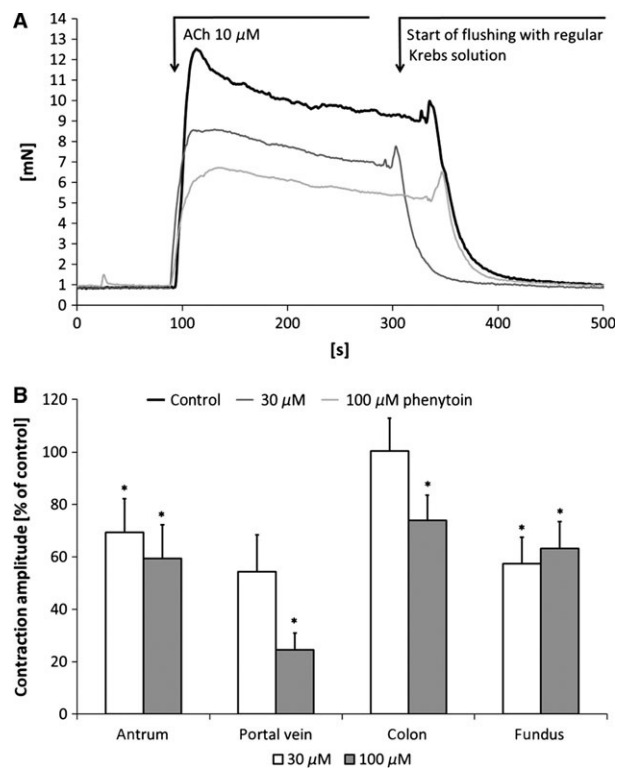


**Figure 3** Gastric fundus strips were contracted by adding ACh at a concentration of 10  $\mu\text{M}$ . After flushing with fresh Krebs solution, the preparations showed full relaxation. In (A), three evoked contractions have been overlaid and adapted to a common timescale to improve the comparability of the responses. The quantitative analysis of changes in contraction amplitudes is depicted in (B). All values are given as percentage of control values measured prior to adding phenytoin to the bathing solution. Error bars indicate SEM, \* $p < 0.05$ , \*\* $p < 0.01$ ;  $n = 8$  for all tissues.

Inhibitory force of phenytoin was strongest with portal vein whereas antrum, fundus, and colon were inhibited to an equal extent. Contractions evoked by KCl were stronger inhibited by phenytoin than those evoked by ACh. The temporal characteristics (slope, decline, phasic vs tonic response, time to onset) of ACh responses were largely unaltered by phenytoin. The inhibition of ACh evoked contractions by phenytoin is illustrated by a representative trace in Fig. 3A.

### Effects of phenytoin on enteric neuromuscular transmission

Electric field stimulation (EFS) produced rather small but reproducible contractions in smooth muscle preparations from gastric fundus. Increasing the number of stimuli applied during the fixed timeframe of stimulation led to more forceful contractions in return. Over the range of applied stimuli, mechanical responses were reduced by more than 90% when stimuli were applied in the presence of 1  $\mu$ M TTX.

In the presence of 30  $\mu$ M phenytoin, the response to 10 s of stimulation at 20 Hz was diminished to  $68.8 \pm 43.0\%$  of the response under control conditions, and was further reduced to  $30.3 \pm 20.1\%$  at 100  $\mu$ M phenytoin. Electric field stimulation-induced contractions reached 50% of their peak value after  $2.9 \pm 1.1$  s in the absence and after  $3.6 \pm 0.9$  s in the presence of 100  $\mu$ M phenytoin. An overlay of three contractions obtained by 10 s of stimulation with 20 Hz either under control conditions or in the presence of two concentrations of phenytoin is shown in the Fig. S1.

### Mechanism of action: voltage dependent sodium channels

Sodium channel blockade by 1  $\mu$ M TTX, a concentration which effectively blocked neuronal activity as shown during the EFS-experiments, had no effect on frequency or height of spontaneous contractions in any of the tissues. Lidocaine (10  $\mu$ M to 1 mM) failed to inhibit spontaneous activity as well. In the contrary, it even exerted excitatory effects on all preparations in the higher dose ranges tested both with respect to the spontaneous activity and to the contractions evoked by high  $[K^+]$  and ACh.

### Mechanism of action: calcium entry

The contractile response to increasing  $[Ca^{2+}]$  of fundic smooth muscle placed in an initially  $Ca^{2+}$ -free,  $K^+$ -rich

Krebs solution was significantly inhibited when phenytoin was added to the external solution. At the highest tested  $[Ca^{2+}]$  of 25 mM, the force generated in the presence of 10  $\mu$ M phenytoin was  $53.1 \pm 11.8\%$  ( $p = 0.003$ ) of control, whereas it was  $19.0 \pm 8.0\%$  ( $p = 0.007$ ) in the presence of 30  $\mu$ M phenytoin. Although  $[Ca^{2+}]$  was not increased up to the point where the force-response of preparations reached saturation, the effect of phenytoin in the tested concentration range can be designated as a rightward shift of the  $[Ca^{2+}]$ -force-response curve (Fig. 4). The amplitude of contractions produced in the presence of both phenytoin and suprphysiologic  $[Ca^{2+}]$  was comparable or even higher than that of the contractions elicited by increasing  $[K^+]$  transiently to 40 mM in normal Krebs solution.

Under control conditions, the L-type calcium channel agonist BAY K8644(-) increased the contraction amplitude in preparations from antrum, portal vein, and colon, whereas frequency was unaffected. When present in the bathing solution at a concentration of 0.3  $\mu$ M, BAY K8644(-) altered the effects of phenytoin both on the amplitude and on the frequency of the contractions for antrum, colon, and portal vein (Fig. 5). The dose dependent reduction in the amplitudes of spontaneous contractions produced by phenytoin was shifted to the right by BAY K8644(-), increasing the mean  $IC_{50}$  by a factor of 10.5, 4.3, and 3.7 in antrum, colon, and portal vein, respectively.

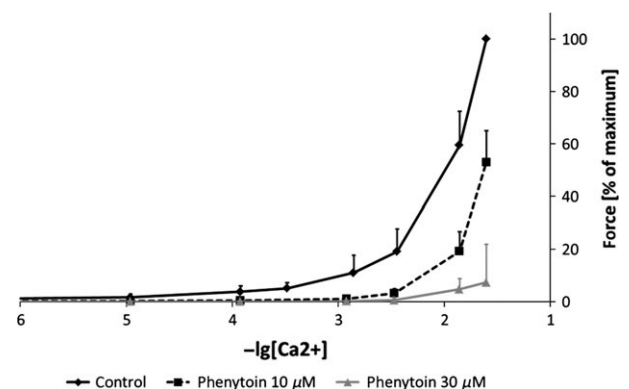


**Figure 4** Dependency of force development in depolarized fundic smooth muscle from  $[Ca^{2+}]$  in the bathing solution. When the bathing solution was changed with potassium-rich, calcium-free solution, the tissues showed full relaxation after remaining calcium was washed out. With  $Ca^{2+}$  added to the bathing solution, tonic contractions occurred. The data points shown here were measured under control conditions and in the presence of 10 or 30  $\mu$ M phenytoin. The x-axis represents the negative common logarithm of the tested calcium concentration in mol/L. All values are given as the percentage of the value measured with the highest  $[Ca^{2+}]$  tested under control conditions. Error bars indicate SEM;  $n = 6$ .

In the presence of 0.3  $\mu\text{M}$  BAY K8644(-), phenytoin decreased the frequency of spontaneous contractions in preparations from gastric antrum, but the concentration of phenytoin that was needed to achieve a 50% reduction in frequency was 5.8-fold higher than under the control conditions. In colon and portal vein, an inversion of the phenytoin effect was observed: Increasing concentrations of phenytoin led to increases in the contraction frequency to  $110 \pm 34\%$  (n.s.) ( $n = 7$ ) or

$143 \pm 13\%$  ( $p = 0.02$ ) ( $n = 5$ ) at 30  $\mu\text{M}$ , to  $208 \pm 52\%$  ( $p = 0.002$ ) or  $176 \pm 49\%$  ( $p = 0.025$ ) at 100  $\mu\text{M}$ , and to  $469 \pm 308\%$  ( $p = 0.007$ ) or  $258 \pm 36\%$  ( $p = 0.001$ ) at 1 mM in colon and portal vein, respectively.

A representative recording of this effect on a preparation from colon is shown in the Fig. S2.

To test the effects of phenytoin on calcium entry more directly, preparations from portal vein were studied using intravital fluorescence calcium micro-

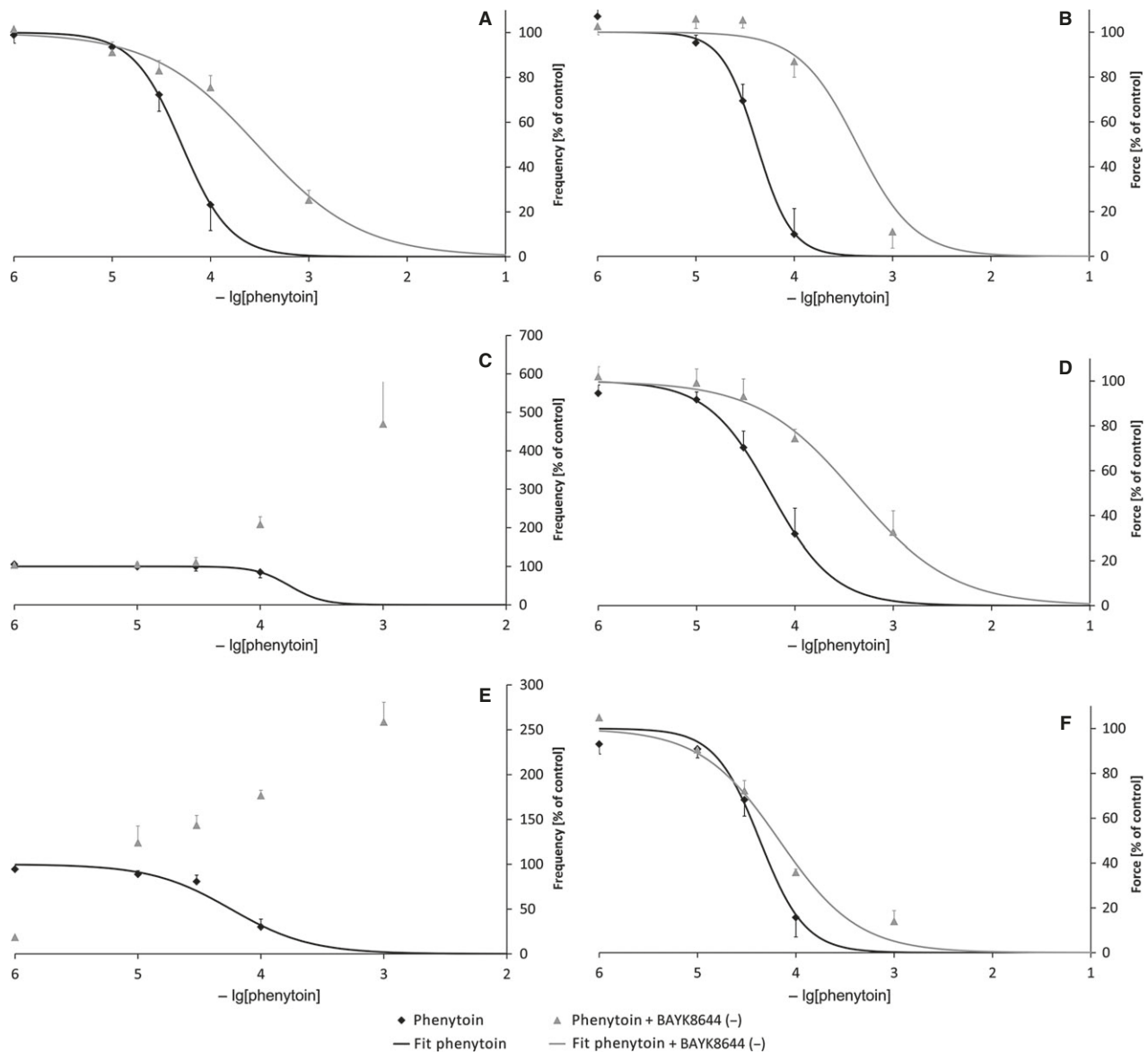


**Figure 5** Concentration-dependency of the action of phenytoin in the presence and absence of 0.3  $\mu\text{M}$  BAYK 8644(-). (A, C, and E) It shows changes frequency in gastric antrum, colon, and portal vein, respectively, whereas (B, D, and F) display effects on the amplitude of spontaneous contractions in the same order. The x-axis represents the negative common logarithm of the tested phenytoin concentration in mol/L. Effects are depicted as percentage of values measured under control conditions before any phenytoin was added to the bathing solution. Error bars indicate SEM. The continuous lines are calculated from Boltzmann equations of the type  $y = 100 - 100 / (1 + \text{EXP}[\ln[\text{IC}_{50}] - \ln[\text{phenytoin}]] / \text{slope})$  fitted automatically to the data points using a least square difference algorithm.

scopy. The change in the ratio of the 340/380 nm-triggered emission at 510 nm during a tissue activation by an increase in extracellular potassium to 75 mM was recorded, and the traces measured subsequently under control conditions and in the presence 100  $\mu$ M phenytoin were compared in seven experiments. Fig. 6 shows an example of such a recording with two subsequently acquired ratiotracings from one preparation that were rescaled and superimposed to illustrate the difference in calcium levels that were caused by the increased phenytoin concentrations. Over all experiments, phenytoin reduced the potassium-induced fluorescence-ratio change significantly by  $52.8 \pm 39.1\%$  ( $p = 0.012$ ).

### Mechanism of action: electromechanical coupling

Complex CAPs could be recorded in parallel with the spontaneous phasic contractions of the portal vein preparations in all experiments using the perfused capillary setup ( $n = 6$ ). Within the CAP, single spikes could be identified (Fig. 7). The maximum amplitude of CAP was not changed significantly in the presence of phenytoin ( $83.1 \pm 17.4\%$  of control with 30  $\mu$ M and  $87.3 \pm 12.4\%$  with 100  $\mu$ M in the perfusion solution). Time integrals of mechanical and electrical activity

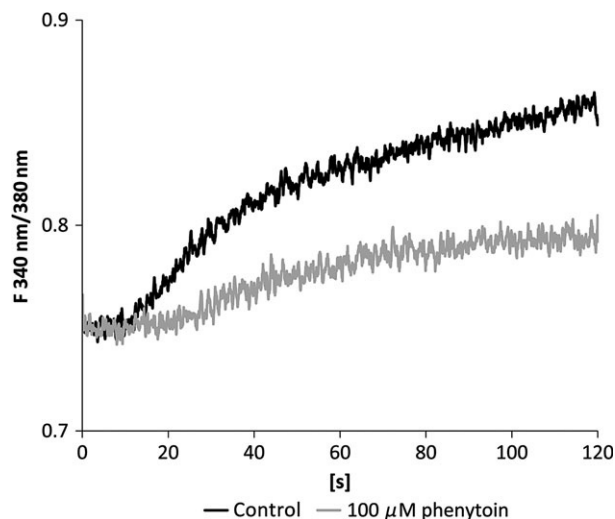


**Figure 6** Ratio of 510 nm-light emission triggered by alternating excitation with light of 340 and 380 nm wavelength over time. The recording was made from a portal vein loaded with the ratiometric dye Fura-2 and kept in an organ bath mounted on the fluorescence microscope. The external potassium concentration was increased to 75 mM once under control conditions and then, after flushing with regular Krebs solution and at least 15 min recovery time, in the presence of 100  $\mu$ M phenytoin added to the bathing solution.

during single spontaneous contractions were calculated numerically from the data. To compensate for the variance of both voltage and force amplitudes between preparations, a specific electromechanical coupling ratio (ECR) (force integral per voltage integral) was defined for each experiment. The effects of adding phenytoin or BAY K8644(-) were then calculated as relative changes in this ratio. Using this approach, it became evident that the ECR declines with rising concentrations of phenytoin (77.1% of control with 30  $\mu$ M and 48.1% with 100  $\mu$ M,  $n = 5$ ), indicating that its presence hinders the conversion of membrane potential depolarization to mechanical force (Fig. 8). With BAY K8644(-) in the perfusate, the integrated force of contractions increased more than the integrated electric activity, corresponding to an increase in ECR. The same effects were observed with increasing  $[Ca^{2+}]$  in the perfusate.

### DISCUSSION

Repetitive electrical excitation underlies both the pathological phenomenon of seizure activity of the cerebral cortex and the physiological phenomenon of spontaneous activity throughout the alimentary tract (for reviews, see Ref. [14–16]). Phenytoin is one of the most commonly used drugs in the treatment of epileptic seizures and status epilepticus.

This study demonstrates that phenytoin exerts strong inhibitory effects on the activity pattern of preparations from both upper and lower gastrointestinal tract. Furthermore, it shows that phenytoin suppresses the function of the portal vein, suggesting an

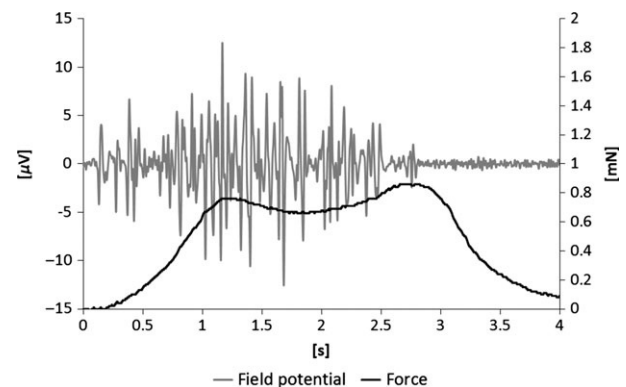


**Figure 7** Typical measurement of extracellular field potentials, plotted against the left ordinate, and simultaneously measured contractile force of a portal vein smooth muscle preparation, plotted against the right ordinate. Electrical discharges form a complex action potential which causes, and thus precedes the mechanical activation, whereas mechanical contraction lags behind.

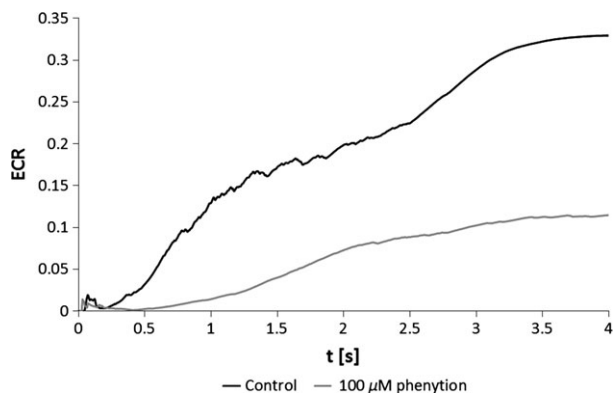


**Figure 8** Numerical integration of electrical and mechanical activity permits the calculation of an electromechanical coupling ratio (ECR) by dividing integrated force by integrated extracellular field potential, giving the ECR which reaches a plateau at the end of a spontaneous contraction. The ECR curve calculated during a contraction under control conditions lies far above that obtained in the presence of phenytoin 100  $\mu\text{M}$ , indicating decreased electromechanical coupling.

additional effect on blood drainage from the gastrointestinal tract. Neither the effects of anticonvulsants on the function of intestinal smooth muscle nor their physiological underlying mechanisms have been thoroughly studied by now.

The literature gives only sparse references: In a study on rabbit small intestine, phenytoin was reported to reduce tone, amplitude, and frequency of spontaneous contractions, leading to a complete cessation of activity at a concentration of 290  $\mu\text{M}$ .<sup>17</sup> Very similar concentrations have been reported to reduce spontaneous tone, ACh-induced contractions and electric activity in the smooth muscle from the guinea-pig ileum and tenia coli by another group.<sup>18</sup> These results are in accordance with our data from other parts of the gastrointestinal tract of rats, as we could demonstrate clear effects at concentrations of 30  $\mu\text{M}$  and a strong inhibition at 100  $\mu\text{M}$ .

Physiologically, gastrointestinal motility is based upon the specific endogenous motor patterns of the different parts of the alimentary canal, which are modulated by the enteric nervous system via different neurotransmitters that are released in the vicinity of interstitial cells of Cajal and smooth muscle cells or by circulating mediators. Drugs affecting gastrointestinal motility *in vivo* can do so by interfering with one or more components of this complex system.

To find out which components were affected by phenytoin, spontaneous and stimulated motor activity was studied. The following conclusions can be drawn from our experiments:

**1** As phenytoin led to a decrease in the frequency of spontaneous contractions, an interference with the

pacemaker function network can be stated. This may be due either to a direct inhibition of the pacemaker currents or due to an inhibition of the excitatory currents in the cells propagating the current that serve as amplifiers of the pacemaker current and only, thereby, enable the spread of excitation over the tissue and its mechanically effective involvement in contraction.<sup>15,19</sup> Both scenarios would, however, lead to different mechanical activity patterns: A mere reduction in pacemaker current would lead to a reduction in frequency and, by impaired recruitment of adjacent tissue, to a reduction in the amplitude of contractions. If inhibition reached a critical point, this would inevitably lead to a complete attenuation of spontaneous contractions. If only the amplification of pacemaker potentials was impaired, the rate of contractions would remain unchanged, even though the amplitude of contractions would be reduced. In both scenarios, at some point in between, it may happen that single contractions are canceled. The observed pattern allows the conclusion that the amplification of pacemaker potentials is hindered in all preparations, whereas pacemaker currents themselves are predominantly affected in gastric antrum and portal vein, but not in the colonic smooth muscle.

- The inhibition of contractions evoked by high  $[\text{K}^+]$  gives evidence that not only the pacemaking process or its propagation is impaired by phenytoin. In addition, the transformation from membrane potential depolarization of smooth muscle cells to force generation obviously is impaired, as the high  $[\text{K}^+]$  – mediated depolarization of membrane potential should give a depolarization that is sufficient to open voltage dependent L-type calcium channels. This is consistent with the finding that phenytoin produces a strong shift in the  $[\text{Ca}^{2+}]$ -response curve of permanently depolarized fundic smooth muscle.
- The amplitude of ACh-induced contractions is affected less than high  $[\text{K}^+]$ -induced contractions. As it is well-accepted that ACh mediates contractions in the investigated tissues not only by activating  $\text{Ca}^{2+}$ -influx from the extracellular space by opening voltage-dependent calcium channels, but also by promoting the release of stored  $\text{Ca}^{2+}$ , this finding gives further evidence that phenytoin inhibits calcium channel function.<sup>20</sup>
- The relative inhibition of fundic smooth muscle responses to EFS was more pronounced than the inhibition of ACh-induced contractions (ACh contractions reduced to 63% of control, EFS-contractions to 30%). As the responses were fully abolished by TTX, it can be stated that they were caused by enteric

nerve stimulation with subsequent neurotransmitter release. Thus, in the tested range of concentrations, phenytoin seems to affect enteric nerve function and ACh-release from postganglionic nerve terminals which may further contribute to the clinically observed changes in gastrointestinal motility. It is of interest that EFS-mediated contractions are inhibited by very low concentrations of phenytoin when compared to agonist-induced contractions. This may seem surprising, but fits well with the involvement of voltage-dependent sodium channels in EFS-mediated contractions demonstrated in the TTX-experiments. Phenytoin itself is, as stated above, classified as a substance with a high affinity to sodium channels, which is reflected by its historical categorization into the group of class I antiarrhythmics.

- 5 The effects of phenytoin are reduced or even inverted in the presence of the L-type calcium channel agonist BAY K8644(-). While a right-shift in the concentration-response curve and the  $IC_{50}$  can be expected from the discussed mechanisms, the increase in the frequency of the spontaneous contractions which can be observed in portal veins and colonic smooth muscle is surprising. This stimulatory effect is not observed with BAY K8644(-) alone, but only with increasing concentrations of phenytoin. A possible explanation may be that the inhibition of calcium currents directly impairs the amplificatory mechanism that is required to maintain homogeneous cell to cell coupling of slow wave depolarizations spreading throughout the tissue, whereas pacemaker cells are considered to be less dependent on L-type calcium channels. This may lead to an uncoupling of pace-making activity in the tissue, which may finally result in more frequent contractions of small amplitude arising from different areas of the preparation. Further experimental work is, however, necessary to test this hypothesis more directly.
- 6 In the presence of 100  $\mu$ M phenytoin, calcium signals as measured by Fura-2 are reduced when compared to control conditions. This fact itself does not necessarily depict on which level the transformation of the voltage signal into a calcium increase is disturbed by phenytoin, but when considered consistent with the results of the experiments with BAY K8644(-), it strongly supports an inhibition of the L-type calcium channels of the smooth muscle cell membrane as the central mechanism of action of phenytoin.

Data on the effects of phenytoin on lower colonic, gastric smooth muscle or the portal vein does not exist in the literature, and the same applies to systematic studies on possible mechanisms of action of phenytoin. Taken together, the observations stated above suggest

an interference of phenytoin with membrane excitation or electromechanical coupling as its mechanism of action in smooth muscle.

An alternative explanation for the inhibitory effects of phenytoin seen in our study would be an interaction with voltage-dependent sodium channels, because phenytoin is thought to inhibit seizure activity in epilepsy largely by inhibiting these. We thus tested whether voltage dependent sodium currents are involved in the spontaneous activity of the used tissue preparations by applying TTX and lidocaine to the preparations. As both substances failed to exhibit any inhibitory effect, it can be concluded that classic voltage-gated sodium channels are not involved in the spontaneous activity of the tested intestinal smooth muscles, a result which is in accordance with previous studies.<sup>21,22</sup>

Changes in intracellular  $[Ca^{2+}]$  are the central event in excitation contraction coupling of smooth muscle.<sup>23-25</sup> Published data on the interactions between phenytoin and high-voltage activated calcium channels from patch clamp studies in neurons is rather inconclusive, and studies in smooth muscle do not exist by now.<sup>26,27</sup> The partial rescue of the phenytoin-inhibited contractility and spontaneous activity that can be observed when increasing  $[Ca^{2+}]$  to supraphysiological levels supports the idea that phenytoin may interact with calcium entry, most likely via interference with the L-type calcium channel current ( $Ca_v1.2$ ). This conclusion is further supported by the finding that the agonist and activator of this channel, BAY K8644(-) antagonized the effect of phenytoin and lead to a rightward shift in concentration-response curves. As calcium ions, BAY K8644(-) itself, too had a stimulatory effect on the tissues, which is directly related to its channel activating properties.<sup>28</sup> In the experiments on the calcium dependency of the inhibitory actions of phenytoin using fundic smooth muscle strips continuously depolarized in a high-potassium solution, phenytoin interestingly exerted strong inhibitory effects at concentrations that were only modestly affecting contractions evoked by externally added agonists, as can be seen by comparing the Figs 2B and 3B with Fig. 4. The most likely explanation for this phenomenon is that phenytoin blocks calcium channels in a use-dependent manner, as it has been previously shown in other cell lines.<sup>29</sup> According to the Nernst equation,  $E_{K^+}$  shifts from -34 mV with 40 mM  $K^+$  to -5.7 mV with 117 mM  $K^+$ . The voltage-dependent calcium channels of fundic smooth muscle cells show a very steep increase in steady state activation over this potential range.<sup>30</sup> This results in an increased open probability and an increased sensi-

tivity to the use-dependent blocking by phenytoin, offering an attractive hypothesis to explain the increased inhibition of contractions at lower concentrations of phenytoin under conditions of sustained strong depolarization.

The simultaneous measurements of electrical and mechanical activity give further evidence that the inhibition of electromechanical coupling via an inhibition of the calcium system is the central mechanism of action of phenytoin in smooth muscle. The decrease in both the integrated contractile force and the integrated electrical activity can be fully explained by assuming that the conductivity of L-type calcium channels is diminished, but only to a degree at which channels would still be able to open upon depolarization and trigger the membrane depolarization. This would enable the propagation of the signal throughout the tissue, but it would nevertheless lead to a diminished cumulative  $\text{Ca}^{2+}$ -flux, and thus to a decrease in contractile force, which is exactly what is observed in these experiments.

The question arises whether the concentrations of phenytoin that have shown to exert relevant inhibitory effects on the tested smooth muscle tissues are of relevance in the context of clinical treatment. Because current recommendations have defined the therapeutic range of phenytoin plasma concentration to be between 10 and 20  $\mu\text{g}/\text{mL}$  (37–72  $\mu\text{M}$ ), this obviously seems to be the case.<sup>31</sup> It has to be considered, however, that phenytoin is protein bound to a variable extent of 60–90%, thus obviously reducing the pharmacologically active amount of the drug *in vivo*, whereas most of the phenytoin can be considered to be freely available *in vitro* as the organ bath medium is virtually void of protein. Therapeutic concentrations of free phenytoin have been reported to be 3.3–9.6  $\mu\text{M}$ ,<sup>32,33</sup> which may explain why severe disturbances in the gastrointestinal motility are not routinely associated with phenytoin treatment.

Nevertheless, there are at least three situations in which free phenytoin levels may easily cross the stated limit and may reach concentrations that may interfere with smooth muscle function: (i) Intravenous application for status epilepticus is an emergency intervention primarily guided on clinical grounds. Laboratory tests to measure free plasma concentrations of phenytoin still are not easily available even in developed countries, which is why supratherapeutic concentrations may be reached and kept for varying durations until either results from therapeutic drug monitoring analyzes are on hand or toxic effects are recognized. (ii) During critical illness and in the elderly, plasma

protein concentrations are significantly lowered, which can lead to dramatic increases in free phenytoin. The use of phenytoin in geriatric patients should thus be considered very carefully. Doses should be kept low and the time of treatment as short as possible. Therapeutic drug monitoring is of special importance in these patients. (iii) Many drugs and other substances interfere with the protein binding of phenytoin, e.g., alcohol, warfarin, tolbutamide, omeprazole, or salicylates. Considering these aspects, it seems likely that phenytoin concentrations may reach levels where smooth muscle function is inhibited in clinical practice. Besides, there are presumably patients whose gastrointestinal tract is susceptible to even lower concentrations of phenytoin than that found to be effective in this study, as many patients receive other drugs with inhibitory actions on motility at the same time, e.g., opioids or catecholamines.

Although the *in vitro* data from our study strongly suggest that phenytoin may cause clinically relevant reductions in the gastrointestinal motility, this hypothesis can only be proven by *in vivo* experiments and observational clinical studies. To our knowledge, such studies do not exist. In a small trial that had been designed to test effects of phenytoin on motion sickness found that phenytoin prevented increases in the frequency of gastric myoelectric activity as measured by electrogastrography ('gastric tachyarrhythmia').<sup>34</sup> Data addressing gastrointestinal complications of phenytoin use in the emergency medicine and intensive care setting are completely lacking by now. The mere fact that phenytoin is an old, approved substance may give a false feeling of safety, but it is important to note that the spectrum of patients receiving anticonvulsant drugs has changed dramatically over the last twenty years in the western world, with far more highly geriatric, severely diseased persons receiving that often develop highly refractory, often non-convulsive seizures on grounds of cerebrovascular and neurodegenerative alterations of the cerebral function. From this point, observational clinical studies on gastrointestinal complications associated with phenytoin applications in these groups are highly desirable. Furthermore, extended *in vitro* data are needed regarding the interactions of widely applied medications on smooth muscle function.

## ACKNOWLEDGMENTS

We thank K. Porat and T. Sellmann for their technical assistance during the experimental process and preparation of this manuscript.

## FUNDING

The resources used for this work were provided by the University of Rostock. No additional funding was used.

## DISCLOSURE

All authors declare that they have no conflicts of interest related to this work.

## AUTHOR CONTRIBUTION

RP and ACL performed the research, designed the research study, analyzed the data, and wrote the article; TN contributed essential reagents and tools and gave essential annotations during the development of manuscript.

## REFERENCES

- de Assis TM, Costa G, Bacellar A, Orsini M, Nascimento OJ. Status epilepticus in the elderly: epidemiology, clinical aspects and treatment. *Neurol Int* 2012; **4**: e17.
- Wu YW, Shek DW, Garcia PA, Zhao S, Johnston SC. Incidence and mortality of generalized convulsive status epilepticus in California. *Neurology* 2002; **58**: 1070–6.
- Knake S, Rosenow F, Vescovi M, Oertel WH, Mueller HH, Wirbatz A, Katsarou N, Hamer HM. Incidence of status epilepticus in adults in Germany: a prospective, population-based study. *Epilepsia* 2001; **42**: 714–8.
- Meierkord H, Boon P, Engelsens B, Gocke K, Shorvon S, Tinuper P, Holtkamp M. EFNS guideline on the management of status epilepticus in adults. *Eur J Neurol* 2010; **17**: 348–55.
- Cook AM, Castle A, Green A, Lesch C, Morrison C, Rhoney D *et al.* Practice variations in the management of status epilepticus. *Neurocrit Care* 2012; **17**: 24–30.
- Langer JE, Fountain NB. A retrospective observational study of current treatment for generalized convulsive status epilepticus. *Epilepsy Behav* 2014; **37**: 95–9.
- Tunnicliff G. Basis of the antiseizure action of phenytoin. *Gen Pharmacol* 1996; **27**: 1091–7.
- Jahromi SR, Togha M, Fesharaki SH, Najafi M, Moghadam NB, Kheradmand JA, Kazemi H, Gorji A. Gastrointestinal adverse effects of antiepileptic drugs in intractable epileptic patients. *Seizure* 2011; **20**: 343–6.
- Stupak DP, Abdelsayed GG, Soloway GN. Motility disorders of the upper gastrointestinal tract in the intensive care unit: pathophysiology and contemporary management. *J Clin Gastroenterol* 2012; **46**: 449–56.
- Nguyen NQ, Chapman MJ, Fraser RJ, Bryant LK, Burgstad C, Ching K, Bellon M, Holloway RH. The effects of sedation on gastric emptying and intra-gastric meal distribution in critical illness. *Intensive Care Med* 2008; **34**: 454–60.
- Gungabissoon U, Hacquoil K, Bains C, Irizarry M, Dukes G, Williamson R, Deane AM, Heyland DK. Prevalence, risk factors, clinical consequences, and treatment of enteral feed intolerance during critical illness. *JPEN J Parenter Enteral Nutr* 2015; **39**: 441–8.
- Nguyen T, Frenette A, Johanson C, Maclean RD, Patel R, Simpson A, Singh A, Balchin KS *et al.* Impaired gastrointestinal transit and its associated morbidity in the intensive care unit. *J Crit Care* 2013; **28**: 537.e11–7.
- Golenhofen K, von Loh D. Electrophysiology studies on normal spontaneous activity of the isolated guinea pig taenia coli. *Pflugers Arch* 1970; **314**: 312–28.
- Avoli M. Mechanisms of epileptiform synchronization in cortical neuronal networks. *Curr Med Chem* 2014; **21**: 653–62.
- Huizinga JD. Gastrointestinal peristalsis: joint action of enteric nerves, smooth muscle, and interstitial cells of Cajal. *Microsc Res Tech* 1999; **47**: 239–47.
- Bolton TB, Prestwich SA, Zholos AV, Gordienko DV. Excitation-contraction coupling in gastrointestinal and other smooth muscles. *Annu Rev Physiol* 1999; **61**: 85–115.
- Druckman R, Moore FJ. Effects of sodium diphenylhydantoinate upon isolated small intestine of the rabbit. *Proc Soc Exp Biol Med* 1955; **90**: 173–6.
- Ferrari M, Furlanut M. Effects of diphenylhydantoin on smooth muscle. *Arch Int Pharmacodyn Ther* 1973; **203**: 101–6.
- Patejdl R, Noack T. The propagation of excitation in portal vein smooth muscle - evidence for coupled "Hot Spots". *Trace Elem Electrolytes* 2010; **27**: 202–8.
- Zhou H, Kong D, Pan Q, Wang H. Sources of calcium in agonist-induced contraction of rat distal colon smooth muscle in vitro. *World J Gastroenterol* 2008; **14**: 1077–83.
- Kuriyama H, Osa T, Toida N. Effect of tetrodotoxin on smooth muscle cells of the guinea-pig taenia coli. *Br J Pharmacol Chemother* 1966; **27**: 366–76.
- Bulbring E, Tomita T. Properties of the inhibitory potential of smooth muscle as observed in the response to field stimulation of the guinea-pig taenia coli. *J Physiol* 1967; **189**: 299–315.
- Deitmer P, Golenhofen K, Noack T. Inhibitory effects of cicletanine on smooth muscle in comparison to those of nifedipine and sodium nitroprusside. *Naunyn Schmiedebergs Arch Pharmacol* 1993; **348**: 411–6.
- Bolton TB, Gordienko DV. Confocal imaging of calcium release events in single smooth muscle cells. *Acta Physiol Scand* 1998; **164**: 567–75.
- Patejdl R, Noack P, Hopp HH, Weston A, Noack T. The importance of the different ionic current components in action potential generation in vascular smooth muscle (portal vein). *Trace Elem Electrolytes* 2005; **22**: 248–53.
- Kito M, Maehara M, Watanabe K. Antiepileptic drugs–calcium current interaction in cultured human neuroblastoma cells. *Seizure* 1994; **3**: 141–9.
- Schumacher TB, Beck H, Steinhauser C, Schramm J, Elger CE. Effects of phenytoin, carbamazepine, and gabapentin on calcium channels in hippocampal granule cells from patients with temporal lobe epilepsy. *Epilepsia* 1998; **39**: 355–63.
- Noack T, Deitmer P. Effects of cicletanine on whole-cell currents of sin-

- gle smooth muscle cells from the guinea-pig portal vein. *Br J Pharmacol* 1993; **109**: 164–70.
- 29 Twombly DA, Yoshii M, Narahashi T. Mechanisms of calcium channel block by phenytoin. *J Pharmacol Exp Ther* 1988; **246**: 189–95.
- 30 Lammel E, Deitmer P, Noack T. Suppression of steady membrane currents by acetylcholine in single smooth muscle cells of the guinea-pig gastric fundus. *J Physiol* 1991; **432**: 259–82.
- 31 Patsalos PN, Berry DJ, Bourgeois BF, Cloyd JC, Glauser TA, Johannessen SI, Johannessen SI, Leppik IE *et al.* Antiepileptic drugs—best practice guidelines for therapeutic drug monitoring: a position paper by the sub-commission on therapeutic drug monitoring, ILAE Commission on Therapeutic Strategies. *Epilepsia* 2008; **49**: 1239–76.
- 32 Bryson SM, Al-Lanqawi Y, Kelman AW, Whiting B. Comparison of a Bayesian forecasting technique with a new method for estimating phenytoin dose requirements. *Ther Drug Monit* 1988; **10**: 80–4.
- 33 Levine M, Chang T. Therapeutic drug monitoring of phenytoin. Rationale and current status. *Clin Pharmacokinet* 1990; **19**: 341–58.
- 34 Stern RM, Uijtdehaage SH, Muth ER, Koch KL. Effects of phenytoin onvection-induced motion sickness and gastric myoelectric activity. *Aviat Space Environ Med* 1994; **65**: 518–21.

## SUPPORTING INFORMATION

Additional supporting information may be found in the online version of this article at the publisher's web site:

**Figure S1.** Representative traces depicting the spontaneous contractions of longitudinal smooth muscle preparations from gastric antrum (A), portal vein (B), and colon (C) under control conditions at higher temporal resolution. The preparations are the same as those shown in Fig. 1.

**Figure S2.** Overlay of three representative contractions of a gastric fundus smooth muscle preparation obtained at intervals of 10 min by 10 s of electric field stimulation under control conditions or in the presence of two concentrations of 30 and 100  $\mu$ M phenytoin. EFS with 20 Hz and 10 s duration was started as indicated by the upper bar. The other stimulus parameters were: stimulus voltage: 80 V; single pulse duration: 1 ms.



# Effects of ajmaline on contraction patterns of isolated rat gastric antrum and portal vein smooth muscle strips and on neurogenic relaxations of gastric fundus

Robert Patejdl<sup>1</sup> · Alina Gromann<sup>1</sup> · Dietmar Bänsch<sup>2</sup> · Thomas Noack<sup>1</sup>

Received: 19 February 2019 / Revised: 3 April 2019 / Accepted: 24 April 2019 / Published online: 2 May 2019  
© Springer-Verlag GmbH Germany, part of Springer Nature 2019

## Abstract

Class-I-antiarrhythmics like ajmaline are known to alter smooth muscle function, which may cause alterations in gastrointestinal motility. The effects of ajmaline on isolated gastric and portal vein smooth muscle and the underlying mechanisms are unknown. We studied the effects of ajmaline on the contractile patterns of isolated preparations of gastric antrum and portal vein from Wistar rats. The organ bath technique was used to measure spontaneous or pharmacologically induced isometric contractions. Changes in force observed after application of ajmaline or under control conditions are reported as % of the amplitude of an initial K<sup>+</sup>-induced contraction. Electric field stimulation was used to study neurogenic relaxations of gastric fundus smooth muscle. Ajmaline increased the amplitude of spontaneous contractions of muscle strips (portal vein: control 31.1 ± 15.2%, with 100 μM ajmaline 76.6 ± 32.3%, *n* = 9, *p* < 0.01; gastric antrum: control 9.5 ± 1.6%, with 100 μM ajmaline 63.9 ± 9.96%, *n* = 14, *p* < 0.01). The frequency of spontaneous activity was reduced in portal vein, but not in gastric antrum strips. The effects of ajmaline were not blocked by tetrodotoxin, L-nitroarginine methyl ester, or atropine. Ajmaline abolished coordinated neurogenic relaxations triggered by electric field stimulation and partly reversed the inhibition of GA spontaneous activity caused by the gap junction blocker carbenoxolone. Ajmaline enhances the amplitude of spontaneous contractions in rat gastric and portal vein smooth muscle. This effect may be accompanied, but not caused by an inhibition of enteric neurotransmission. Enhanced syncytial coupling as indicated by its ability to antagonize the effects of carbenoxolone is likely to underlie the enhancement of contractility.

**Keywords** Class-I-antiarrhythmics · Ajmaline · Gastrointestinal motility · Smooth muscle · Enteric nervous system

## Introduction

Antiarrhythmic drugs (AAD) are known to exert various side effects, the most prominent being their potential to induce clinically relevant cardiac arrhythmias by themselves [9, 31, 48]. Non-cardiac side effects are well known but have been considerably less thoroughly studied [13].

Class I AAD (e.g., flecainide or ajmaline) are used for the acute treatment of supraventricular tachycardia and the stabilization of sinus rhythm after cardioversion. Gastrointestinal symptoms, especially nausea (9%), abdominal pain (3%), and constipation (4%), are known side effects of both substances [13, 23, 29].

The physiological mechanisms underlying the gastrointestinal adverse effects of class I AAD are yet unknown. Theoretically, the substances could interact either with the intrinsic (“myogenic”) activation of smooth muscle and/or with the neurogenic modulation of the myogenic tone by the autonomic and enteric nervous systems. Both mechanisms are known to account for clinically relevant signs and symptoms of gastrointestinal dysfunction [1, 25, 27, 32, 36].

Use-dependent block of voltage-gated sodium channels (Na<sub>v</sub>) is considered to be the central mechanism of action for class I AAD in the heart [22, 31]. These channels are not considered to be essential for the generation of basic motor patterns of isolated intestinal smooth muscle. Na<sub>v</sub> channels are,

**Electronic supplementary material** The online version of this article (<https://doi.org/10.1007/s00424-019-02279-y>) contains supplementary material, which is available to authorized users.

✉ Robert Patejdl  
robert.patejdl@uni-rostock.de

<sup>1</sup> Oscar-Langendorff-Institut für Physiologie, Universitätsmedizin Rostock, Gertrudenstraße 9, 18057 Rostock, Germany

<sup>2</sup> Department of Cardiac Electrophysiology, KMG Hospital Güstrow, Güstrow, Germany

however, involved in neuronal modulation of myogenic tone, e.g., in the active process of adaptive gastric relaxation following the ingestion of food [42, 47]. Besides its affinity for  $\text{Na}_v$  channels of the heart, skeletal muscle, and neurons, ajmaline has been demonstrated to interact with voltage-dependent K channels ( $\text{K}_v$ ) and hERG-type K channels [2, 11, 18, 19, 24, 51]. Phenytoin, an anticonvulsive drug which has been used historically as a class  $\text{I}_A$  AAD, exerts inhibitory effects on the contractility of isolated intestinal and vascular smooth muscles from rats by inhibiting calcium entry [39]. Whereas stimulating effects on the contractile behavior of guinea pig ileum, taenia coli, and portal vein (PV) have been reported for ajmaline, the literature contains no information about its effects on neurotransmission in these tissues [4, 7, 10].

The present study investigates the effects of ajmaline on the spontaneous activity, on contractions induced by acetylcholine (ACh) and high- $\text{K}^+$ -depolarizations as well as neurogenic responses of isolated rat gastric and PV smooth muscle. These rat tissues were chosen because they are thoroughly characterized regarding their motor patterns and reflexes as well as their cellular mechanisms, i.e., ion channels and pharmacological properties. Both PV and gastric antrum (GA) are prototypical spontaneously active smooth muscles, but whereas spontaneous activity in isolated PV is not fully synchronized between different pacemaker sites, mechanical activations of the GA is considered to be fully coordinated [15, 16]. Therefore, under certain circumstances, differential responses of both tissues can be indicative for substance effects on intercellular coupling.

This study was designed to address three central questions:

1. Which effects does ajmaline have on the spontaneous tone and contractile patterns of isolated gastric and PV smooth muscle?
2. Are these effects related to actions of ajmaline on enteric neurotransmission?
3. Which mechanisms do account for effects of ajmaline on spontaneous activity?

## Materials and methods

### Preparation of tissues and organ bath experiments

The ARRIVE guidelines were followed as far as applicable for the experiments on isolated tissue strips performed in the context of this study [20]. All procedures performed were in accordance with the ethical standards of the University of Rostock as well as German national law (Tierschutzgesetz, §7) and the regulations of the state of Mecklenburg-West Pomerania. Following these regulations, a formal notification was made for housing and breeding the animals to the federal state authority (internal code: A4214/74KL), whereas an ethics statement

or other institutional approval was not necessary since no interventions were made on the animals while alive. Animals were kept in 800 cm<sup>2</sup> cages (Zoonlab, Castrop-Rauxel, Germany) on wood shavings (Abedd, Vienna, Austria), had free access to tap water and pellet food (1534-000, Sniff Spezialdiäten, Soest, Germany), and were kept at a 12-h dark-light cycle. Thirty-eight Wistar rats of both sexes bred at our institution (mean  $\pm$  standard deviation: weight, 261  $\pm$  37 g; age, 168  $\pm$  41 days) were anesthetized with ether, and killed by decapitation. After opening the abdomen, the stomach and the PV were excised and stored in preparation buffer (PB) at 4 °C. Connective tissue and fat were removed by sharp dissection under the preparation microscope (Olympus SZ40, Olympus, Shinjuku, Japan) in Sylgard dishes filled with PB at a magnification of 0.8–2 for stomach and 3–5 for PV. From the stomach, longitudinal smooth muscle strips of an in situ length of 5–10 mm and 2 mm width were excised from the antrum in lines running parallel to the greater curvature without lesioning the mucosa. Strips of identical dimensions were taken from the fundus in a similar manner, but by cutting in a rectangular angle to the greater curvature following the visible direction of circular muscle bundles. After cleaning, portal veins were split longitudinally and cut to a length of 10 mm. Preparations of PV and GA were tethered to glass holders, whereas fundus strips were tethered to plastic holders with integrated platinum wires for field stimulation. The holders were then mounted vertically in organ baths with volume capacities of either 20 or 30 ml. Each bath was filled with Krebs solution and bubbled with 95%  $\text{O}_2$  and 5%  $\text{CO}_2$  at a temperature of 36 °C and a pH of 7.4. The amounts of added drugs were always adapted to the organ bath size to give equivalent concentrations. The tissue strips were connected to mechanoelectrical transducers with a force resolution of 0.01 mN coupled to a bridge amplifier operating in differential (full bridge) mode (FORT10g/Transbridge TBM4M, both World Precision Instruments, Sarasota, FL, USA). The obtained signal was sampled at a rate of 100/s and low-pass filtered with 2 Hz using PowerLab8/32 (ADInstruments, Bella Vista, Australia), and then stored for further processing with LabChart (LabchartPro edition, Version 7.3.1, ADInstruments, Bella Vista, Australia) and MS Excel 2010 (Microsoft, Redmond, WA, USA). After placing the preparations in the organ bath, they were adjusted to a pre-strain of 2–3 mN to bring them to their in situ length. Before first substance applications were made, they were then allowed to equilibrate over 1 h. Then, before any other maneuver, a reference contraction was induced by increasing the potassium concentration to 60 mM by changing the organ bath solution with a modified Krebs buffer in which  $\text{Na}^+$  had been substituted with equimolar amounts of  $\text{K}^+$ . To compensate for differences in thickness of muscle strips, all tension values reported are given as % of the maximum of this contraction except when stated differently. After flushing with regular Krebs solution, preparations were allowed to equilibrate again

for 20 min before any other substance testing. In experiments testing ajmaline effects on spontaneous activity, ajmaline concentration was increased at intervals of 10 min. At the end of each experiment, a second high-K<sup>+</sup>-contraction was induced in the same manner as the initial reference contraction. To test for a contribution of constitutive neurotransmission in mediating the effects of ajmaline in GA, tetrodotoxin (TTX, 1 μM), atropine (10 μM), and L-nitroarginine methyl ester (L-NAME, 10 μM) were added to the organ bath prior to the first application of ajmaline. Two series of experiments on interactions of ajmaline with carbenoxolone and tetraethylammonium (TEA) in the setting of spontaneously active GA are described in detail in the respective paragraph of the results.

### Spectral analysis of spontaneous activity

The spectral analysis function of the LabChart software was used to calculate fast Fourier transforms (FFT) of 3-min intervals of tension recordings from PV and GA under control conditions and in the presence of 100 μM ajmaline. For calculating the FFT, a size of 8 k and the Hann-Data window were applied with an overlap set to 50%. Spectrum values display signal amplitude in microvolts at a particular given frequency. Only preparations with a fully continuous regular spontaneous activity were selected. Amplitude spectra from five PV and five GA preparations were calculated, exported to MS Excel 2010 and normalized to the amplitude of the high-K<sup>+</sup>-contraction obtained in the respective preparation. Finally, the mean spectra for PV and GA were calculated from the single measurements.

### Responses evoked by electric field stimulation

Fundus muscle strips were tethered to holders with inserted platinum wires in the same organ baths as described above. The distance between platinum wires and smooth muscle tissue was adjusted to values between 1 and 2 mm. Pulses were generated by a Grass S-8 stimulator (Grass Technologies, Warwick, RI, USA) that was connected to the electrodes. The protocol used was adapted from D'Amato et al. [8]. Briefly, serotonin was added at a concentration of 0.3 μM and equilibrated for 20 min to establish a plateau from which dilatations and contractions could be studied. Over the whole experiment, the Krebs buffer contained guanethidine (4 μM) and atropine (1 μM) to establish non-cholinergic, non-adrenergic (NANC) conditions for stimulation. Electric stimuli were applied subsequently with a frequency of 20 Hz and a train duration of 5 s at intervals of 100 s. Single pulse voltage amplitude was 60 V and square pulse duration was 0.5 ms to selectively stimulate nerve varicosities and not smooth muscle cells. The effects of ajmaline on the resulting dilatations were measured by normalizing them to the dilatation amplitude measured prior to the addition of ajmaline in the respective preparation.

### Contractions evoked by high potassium

To estimate the influx of Ca<sup>2+</sup> via voltage-dependent calcium channels (VDCC), contractions were evoked by depolarizing the tissue with potassium (60 mM). As a measure of ajmaline effects on membrane-potential dependent calcium entry, the contractions evoked by high K<sup>+</sup> in the presence of ajmaline were normalized to those evoked under control conditions. This was done separately for the early and the late K<sup>+</sup>-induced contraction by comparing the arithmetic means of tension values from the first 30 s after increasing K<sup>+</sup> or from the last 30 s of the K<sup>+</sup> elevation period.

### Acetylcholine induced contractions

Responses to ACh (10 μM) were tested to measure effects of ajmaline on intracellular signaling cascades and release of Ca<sup>2+</sup> from intracellular stores. Ratios of early and late contractions with and without ajmaline in the organ bath were calculated in the same manner as described above for high-K<sup>+</sup>-contractions.

### Simultaneous registration of electrical and mechanical activity

The setup used for recording electrical activity has been described previously [14, 38, 39]. Briefly, PV preparations were placed in a plastic tube of 2.5 mm width and were tethered to a force transducer. The tube was continuously perfused with fresh Krebs solution. The extracellular electric potentials preceding and accompanying contractions were recorded using ring-shaped platinum electrodes fixed on the inside of a small tube. One end of the PV was placed at a fixed position within the tube and the other was tethered to an isometric force transducer of the same type that was used for the conventional organ bath experiments. The preparation was moved along the longitudinal axis of the tube up to a position where the amplitude of spike complexes reached a maximum. Electrical signals were recorded using an AnimalBioAmp connected to a PowerLab8/32 (both ADInstruments, Bella Vista, Australia) set to a 10–65-Hz bandpass at a sampling rate of 2 kHz. Simultaneously, tension was recorded using the above-mentioned equipment, low-pass filtered at 1 Hz, and then stored. For distinct spontaneous contractions, the mean amplitudes of field potentials were measured and compared between control conditions and in the presence of ajmaline 100 μM.

### Calcium sensitivity of depolarized smooth muscle

Strips of gastric fundus were equilibrated for 45 min in regular Krebs solution. Then, the bathing solution was exchanged three times with potassium-rich, calcium-free solution in which Ca<sup>2+</sup> was substituted with Mg<sup>2+</sup>. After that, the

preparations were equilibrated for another 30 min. Then,  $\text{Ca}^{2+}$  was added stepwise to the bathing solution. When a concentration of 30 mM was reached, the organ bath was flushed again with regular Krebs solution, again equilibrated, and the change to  $\text{Ca}^{2+}$ -free solution and the  $\text{Ca}^{2+}$  titration were repeated as before, but ajmaline was added to the organ bath after the final exchange of  $\text{Ca}^{2+}$ -free solution. The concentration dependency of force generation associated with increasing concentrations of  $\text{Ca}^{2+}$  was measured under control conditions and compared to that estimated in the presence of 100  $\mu\text{M}$  ajmaline. The responses were normalized to the maximum value obtained under control conditions.

## Drugs and solutions

The solutions used were composed as follows: PB: NaCl 145 mM, KCl 4.5 mM,  $\text{NaH}_2\text{PO}_4$  1.2 mM,  $\text{MgSO}_4$  1.2 mM,  $\text{CaCl}_2$  1 mM, EDTA 0.025 mM, HEPES 5 mM. Krebs solution: NaCl 112 mM,  $\text{NaHCO}_3$  25 mM,  $\text{KH}_2\text{PO}_4$  1.2 mM, KCl 4.7 mM,  $\text{MgCl}_2$  1.2 mM,  $\text{CaCl}_2$  2.5 mM, glucose 11.5 mM. Potassium-rich Krebs solution: NaCl 57.7 mM, KCl 58.8 mM,  $\text{NaHCO}_3$  25 mM,  $\text{KH}_2\text{PO}_4$  1.2 mM,  $\text{MgCl}_2$  1.2 mM,  $\text{CaCl}_2$  2.5 mM, glucose 11.5 mM. Potassium-rich, calcium-free Krebs solution: KCl 116.7 mM,  $\text{NaHCO}_3$  25 mM,  $\text{KH}_2\text{PO}_4$  1.2 mM,  $\text{MgCl}_2$  3.7 mM, glucose 11.5 mM. Calcium solution for titrating [ $\text{Ca}^{2+}$ ] in potassium-rich, calcium-free Krebs solution:  $\text{CaCl}_2$  110 mM. The pH was 7.4 at 36.6 °C with continuous carbogen gas bubbling during all experiments (95%  $\text{O}_2$ , 5%  $\text{CO}_2$ ). Atropine, carbenoxolone, serotonin, sodium nitroprusside (SNP), TEA, and all above-mentioned salts were purchased from Sigma-Aldrich (St. Louis, MO, USA). Ajmaline (Gilurytmal®) was purchased from Carinopharm (Elze, Germany). Other substances used in this study were acetylcholine (Michol-E®, Ciba Vision, Germany) and guanethidine (Santa Cruz Biotechnology). All substances were dissolved in double distilled water and stored according to the distributor's recommendations.

## Data presentation and statistics

Values are given as mean values  $\pm$  standard deviation of mean (SDM). Error bars indicate standard error of mean (SEM). The legend for box plots given in Fig. 5 (b4) applies for all box plots. Sample size was calculated using G\*Power 3.1 (F. Faul, Kiel University, Kiel, Germany) in a pre-test-approach to assure detection of significance for changes of mean values larger than 20% with a power of 0.8 on the basis of an estimated SDM of 30%. The data were analyzed using MS Excel 2010 (Microsoft, Redmond, WA, USA), SPSS 22 (IBM, Armonk, NY, USA), and OriginLab 2018b (Northampton, MA, USA). For statistical testing, the Wilcoxon test for dependent samples and the Mann–Whitney test for independent samples were applied. All tests of significance were performed at  $\alpha = 0.05$ .

## Results

### Contraction patterns under control conditions

After equilibration in Krebs solution, tissue preparations from PV and GA showed characteristic motor patterns which resemble that seen in the very beginning of the recordings shown in Fig. 1 (a1 and b1) prior to adding ajmaline. Portal veins developed contractions with amplitudes of  $1.6 \pm 0.8$  mN or  $31.1 \pm 6.8\%$  of an initial test contraction evoked by stepping  $[\text{K}^+]$  up to 60 mM. The mean frequency of PV was  $4.7 \pm 2.1$   $\text{min}^{-1}$ , baseline tension under control conditions was  $2.2 \pm 1.4$  mN,  $n = 9$ . GA strips exhibited regular phasic contractions at a mean frequency of  $3 \pm 0.8$   $\text{min}^{-1}$  and with a mean amplitude of  $0.8 \pm 0.2$  mN or  $9.5 \pm 1.6\%$  of a respective high- $\text{K}^+$ -contraction ( $n = 14$ ). Baseline tension of GA under control conditions was  $1.4 \pm 0.5$  mN,  $n = 14$ .

The mean frequency spectra of spontaneous activity depict the temporal variance in the rhythmicity of the endogenously paced activations of the tissue under control conditions for PV (Fig. 1, a2) and GA (Fig. 1, a2). Whereas the frequency spectrum of PV shows three small peaks, there is one clear dominant frequency in GA, indicating a higher degree of intrinsic oscillator coupling.

### Effects of ajmaline on spontaneous activity

The amplitude of spontaneous contractions grew in both tissues when ajmaline was added to the Krebs solution. In PV preparations, the increase was significant from concentrations of 10  $\mu\text{M}$  onwards, strengthened remarkably up to 30  $\mu\text{M}$  whereas 100  $\mu\text{M}$  did not produce further increase (Fig. 1, a1, c). The ajmaline-induced increase in force of spontaneous contractions of GA was very similar to that observed in muscle strips from PV, but reached significance already from concentrations of 1  $\mu\text{M}$  onwards and failed to saturate up to 100  $\mu\text{M}$  (Fig. 1, b1, c).

Despite the remarkably large effects on spontaneous contractions, the full relaxation to baseline in between spontaneous contractions, which is a characteristic for both PV and GA, was fully maintained (seen also in Fig. 1, a1 and b1; data for GA: mean change from tension under control conditions:  $-0.03 \pm 0.13$  mN at 1  $\mu\text{M}$ ;  $-0.04 \pm 0.15$  mN at 10  $\mu\text{M}$ ;  $-0.13 \pm 0.29$  mN at 100  $\mu\text{M}$  ajmaline;  $p > 0.05$  for all;  $n = 14$ ; data for PV: mean change from tension under control conditions:  $0.02 \pm 0.08$  mN at 1  $\mu\text{M}$ ;  $-0.03 \pm 0.15$  mN at 10  $\mu\text{M}$ ;  $-0.01 \pm 0.12$  mN at 100  $\mu\text{M}$  ajmaline;  $p > 0.05$  for all;  $n = 9$ ).

Effects of ajmaline on frequency were measured using spectra calculated by FFT of tension recordings. In comparison with spectra obtained under control conditions, it became evident that ajmaline causes a clear shift to lower frequencies in PV (Fig. 1, a2). When ajmaline was added, intervals between spontaneous contractions of PV became longer and the

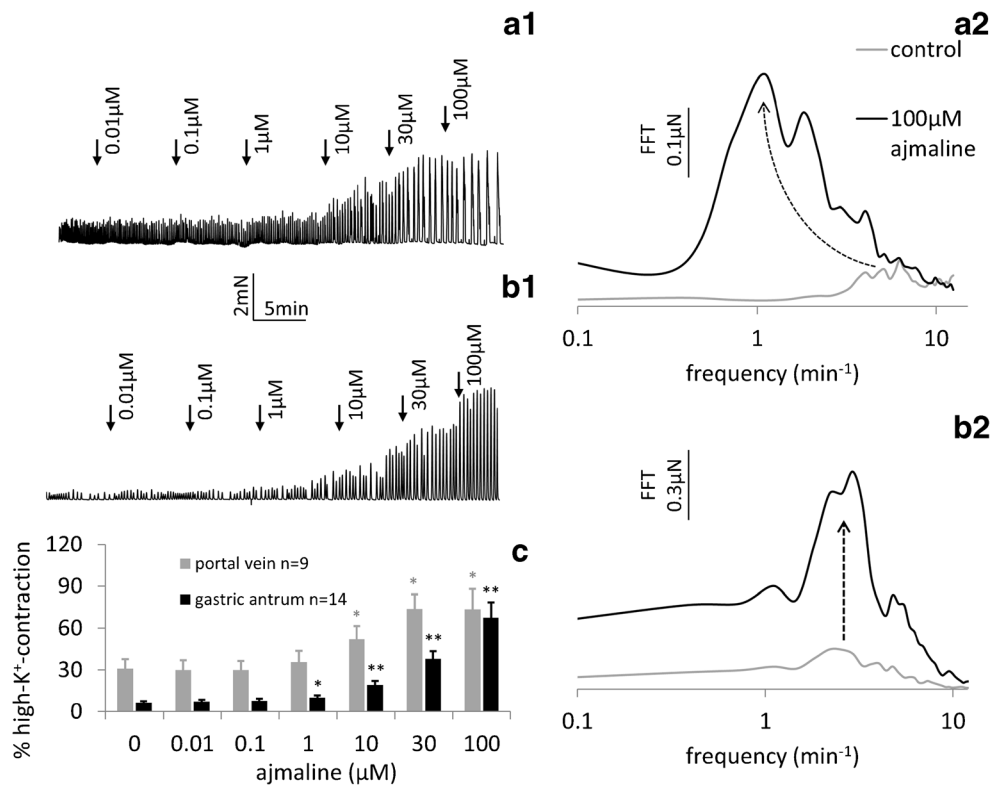


**Fig. 1** Representative recordings of tension generated spontaneously by isolated longitudinal strips from PV (a1) and GA (b1) under control conditions and in the presence of increasing concentrations of ajmaline. Frequency spectra of 5-min samples from PV (a2) and GA strips (b2). The ordinate alignment is given separately for both graphs. Zero values of force correspond to the intersection level with the logarithmically scaled abscissa which displays frequency. Spectra were calculated using a fast Fourier transform (FFT), values display signal amplitude in millivolts at a given frequency. Lines in both a2 and b2 are means from five preparations. Gray lines show spectra obtained under control

conditions, black lines obtained with ajmaline 100 μM in the organ bath. Mean amplitude of spontaneous portal vein and antrum contractions estimated over 2 min before stepping to the next concentration of ajmaline (c). Tension is expressed as percentage of an initial high-K<sup>+</sup>-contraction. Calculated mean values and SD for PV: 31.1 ± 15.2% under control conditions; 1 μM: 35.8 ± 18.8%,  $p > 0.05$ ; 10 μM: 52.1 ± 20.9%,  $p < 0.01$ ; 100 μM: 73.6 ± 32.3%,  $n = 6$ ,  $p < 0.01$ . Data for GA: 1 μM: 9.5 ± 1.6%, 10 μM: 17.2 ± 2.8%, 30 μM: 34.3 ± 4.9%, 100 μM: 63.9 ± 9.96%,  $n = 14$ ,  $p < 0.05$  for 1 μM and  $p < 0.01$  for 10, 30, and 100 μM. Error bars show SEM. \* $p < 0.05$ , \*\* $p < 0.01$

contractions themselves became larger and broader. In contrast to that, the FFT of GA activity did not show any relevant shift in the dominant frequency (Fig. 1, b2).

### Constitutive endogenous neurotransmission

The ajmaline-induced increase in the amplitude of spontaneous contractions was neither forestalled nor blocked by adding TTX (Fig. 2a), L-NAME (Fig. 2b), or atropine (Fig. 2c) to the bathing solution 15 min before starting ajmaline application (contraction amplitude with 100 μM ajmaline: 74 ± 15.8% for TTX, 63 ± 13.1% for L-NAME, 72 ± 19.0% for atropine, for all  $n = 5$ ,  $p > 0.05$  when compared to the amplitude obtained with 100 μM ajmaline added to control conditions).

### Spontaneous electrical activity

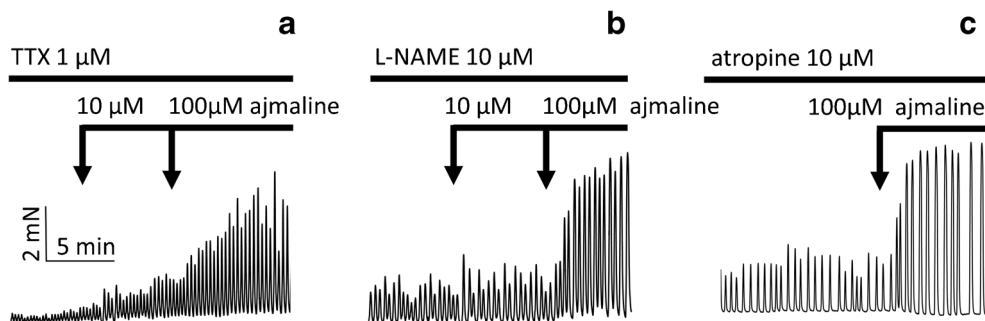
Ajmaline increased the coordinated spontaneous electrical activity that triggers and maintains phasic contractions. Although the absolute value of the recorded field potentials

varied between preparations (2–50 μV for GA, Fig. 3a, 5–25 μV for PV, Fig. 3b), the mean ratio between field potentials recorded in the presence of 100 μM ajmaline and under control conditions was significantly greater than 1. For PV, it was 1.4 ± 0.07,  $p < 0.05$ ,  $n = 5$ , whereas it was 2.1 ± 0.4 ( $p < 0.05$ ,  $n = 5$ ) for GA.

### Effects of ajmaline on neuronally mediated responses

Strips from gastric fundus developed a stable basal tone of 6.6 ± 1.6 mN ( $n = 7$ ) without phasic contractions after equilibration as can be seen in the very left part of Fig. 4. Serotonin (0.3 μM) produced a contraction with an initial peak followed by a slow and steady decline over several minutes that stabilizes as a plateau-like tension which was still above the initial level. When electric field stimulation was applied during the plateau phase of the serotonin contraction under control conditions, relaxations of uniform shape and amplitude followed each electric field stimulation (EFS) pulse train

**Fig. 2** **a** Effects of ajmaline on spontaneous activity of GA strips pretreated with 1  $\mu\text{M}$  TTX for 15 min. **b** Effects of ajmaline on spontaneous activity of GA strips pretreated with 10  $\mu\text{M}$  L-NAME for 15 min. **c** Effects of atropine on spontaneous activity of GA strips pretreated with 10  $\mu\text{M}$  L-NAME for 15 min



(middle part of Fig. 4). After application of ajmaline, baseline tension increased and irregular oscillations became obvious (100  $\mu\text{M}$ , right part of Fig. 4). In this situation, EFS trains failed to produce clearly identifiable relaxations in all of the tested preparations ( $n = 5$ ). Nominally, the mean amplitude of EFS-induced relaxations obtained in the presence of 100  $\mu\text{M}$  ajmaline was reduced to  $3.2 \pm 2.8\%$  of the mean relaxation obtained under control conditions ( $p < 0.01$ ,  $n = 5$ ).

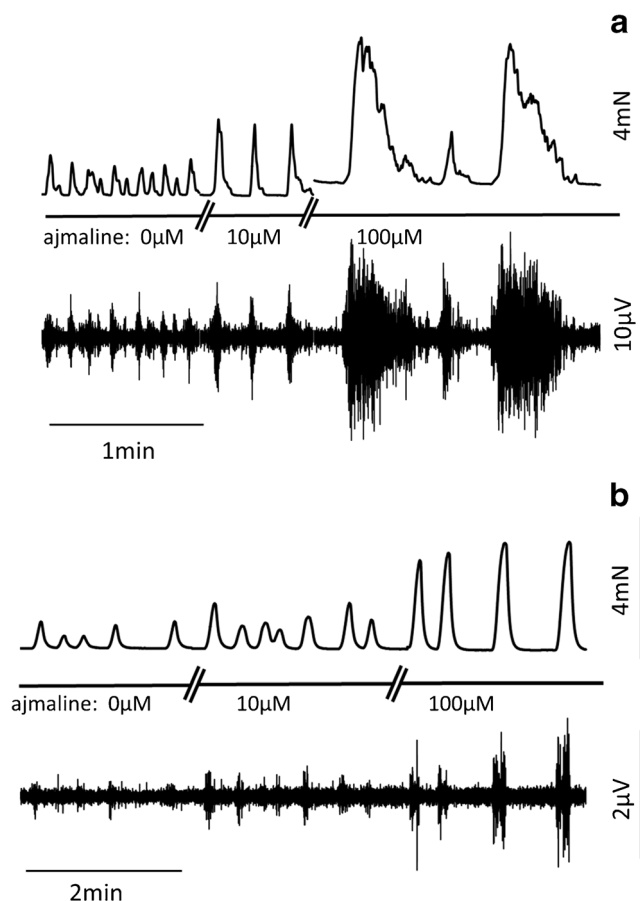


**Fig. 3** Representative measurement of extracellular field potentials (EFP, upper traces) and simultaneously measured contractile force (lower traces) of a PV (**a**) and GA (**b**) smooth muscle preparation. Concentration of ajmaline is given in the middle horizontal line, at intermissions 15 min of recorded data are skipped

### Effects on evoked contractions: high- $\text{K}^+$ -depolarization and acetylcholine

When the potassium concentration of the Krebs solution was stepped up to 60 mM, PV and GA strips contracted with a characteristic shape and time course. An early peak of contractions was regularly observed within the first minute of high- $\text{K}^+$ -exposure which was then followed by a slow increase under control conditions or a decline in the presence of ajmaline (Fig. 5, a1, b1). In PV, already the early contraction induced by high  $\text{K}^+$  in the presence of ajmaline was reduced when compared to control conditions. After 2 min of high- $\text{K}^+$ -activation, there was a further significant drop in the presence of ajmaline (Fig. 5, a2). In GA, the amplitude of the early phase of high- $\text{K}^+$ -contractions of GA was not different in the presence of 100  $\mu\text{M}$  ajmaline when compared to control conditions, the contraction after 2 min exposure to high  $\text{K}^+$  was significantly lower with ajmaline (Fig. 5, b2).

Acetylcholine (10  $\mu\text{M}$ ) was added in the presence and absence of 100  $\mu\text{M}$  ajmaline. Acetylcholine responses of PV were unaltered by ajmaline (Fig. 5, a3, a4), whereas ajmaline caused a significant increase of the early and late ACh response of GA (Fig. 5, b3, b4).

### Calcium sensitivity of depolarized smooth muscle

Gastric fundus strips incubated in calcium-free high-potassium solution developed stable contractions when calcium was added to the solution. The concentration dependency of force generation was measured under control conditions and compared to that measured in the presence of 100  $\mu\text{M}$  ajmaline. The responses were normalized to the maximum value obtained under control conditions (Fig. 6). At calcium concentrations of 3 mM and above, the resulting force was significantly reduced in the presence of ajmaline compared to control conditions ( $n = 9$ ,  $p < 0.01$  for 3, 10, and 20 mM  $\text{Ca}^{2+}$ ).

### Modification of carbenoxolone effects by ajmaline in GA

The gap junction blocker carbenoxolone was used to alter intercellular electric current propagation and thus intercellular

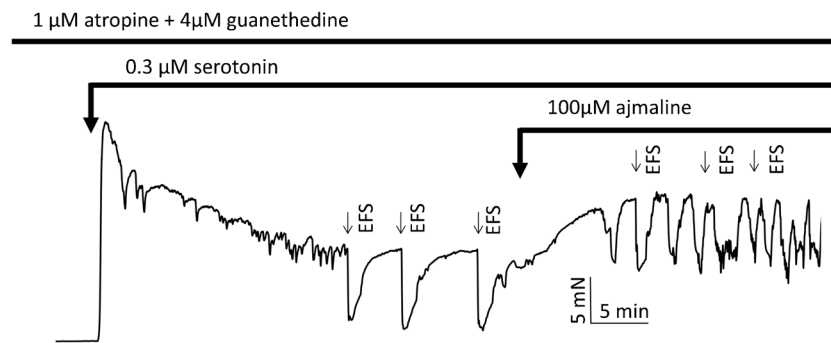


**Fig. 4** Interactions of ajmaline with electric field stimulation: Tension recording from a gastric fundus strip precontracted with 0.3  $\mu\text{M}$  serotonin. At the indicated time points, electric field stimulation ( $\downarrow\text{EFS}$ ) was applied for 10 s with 1 ms pulses at a frequency of  $10\text{ s}^{-1}$  and 80 mA.

Whereas after first EFS train after 9 min of ajmaline incubation, a dilatation similar to those observed under control conditions occurs, subsequent EFS trains only evoke very barely recognizable, transient responses

coupling [6, 37]. After preparations of GA had been equilibrated and a reference contraction measured as described in the section on spontaneous activity, carbenoxolone (20  $\mu\text{M}$ ) was added. Over the following 5 min, the amplitude of contractions declined significantly from  $20.0 \pm 14.4$  to  $3.5 \pm 4.1\%$  of the high- $\text{K}^+$ -contraction amplitude ( $p < 0.05$ ,  $n = 5$ ). After adding ajmaline (100  $\mu\text{M}$ ), the amplitude increased again up to  $13.0 \pm 6.4\%$  ( $p < 0.05$ ,  $n = 5$ , Fig. 7a).

### Effects of TEA on GA in the presence of ajmaline

After the same pretreatment as described in the section on carbenoxolone, adding TEA to concentrations of 1 and 10 mM led to a dose-dependent increase in the high- $\text{K}^+$ -normalized amplitude of phasic contractions. Compared to basal conditions, mean amplitudes of spontaneous phasic contractions were increased equally by 1 mM TEA in the presence or absence of ajmaline (% of high- $\text{K}^+$ -contraction:  $64 \pm 28\%$  without ajmaline,  $60 \pm 24\%$  with 100  $\mu\text{M}$  ajmaline,  $n = 7$ ,  $p > 0.05$ , Fig. 7b). Increasing TEA from 1 to 10 mM evoked a further tension increase which again was not different between ajmaline-pretreated and control muscle strips (% of high- $\text{K}^+$ -contraction:  $132 \pm 56\%$  without,  $112 \pm 73\%$  with 100  $\mu\text{M}$  ajmaline,  $n = 8$ ,  $p > 0.05$ , Fig. 7c).

## Discussion

### Main findings

In this study, it is shown that the class-I-antiarrhythmic agent ajmaline exerts three major effects in the isolated rat PV, GA, and gastric fundus smooth muscle.

Ajmaline increases the amplitude of per se spontaneously occurring phasic contractions in smooth muscle strips of PV and GA in a concentration-dependent manner.

In PV, but not in GA, ajmaline changes the frequency of the rhythmical activity and increases the contraction phases as well as the inter-contraction intervals.

A third finding is that ajmaline virtually abrogates coordinated neurogenic dilatatory responses in gastric fundus strips.

### Underlying mechanisms

The loss of effective neurogenic relaxations might be explained on the presynaptic level by the  $\text{Na}_v$ -blocking properties of ajmaline [18, 51]. Alternatively, it is possible that ajmaline switches the smooth muscle to an oscillatory, unstable state by inhibiting stabilizing mechanisms, e.g., by blocking ion channels carrying voltage-activated outward currents. Both mechanisms would offer an explanation for the observed increase in the amplitude of phasic contractions. An abrogation of constitutive inhibitory neurotransmission by ajmaline via presynaptic inhibition of transmitter release is, however, unlikely to account for the observed increase in phasic contractions since neither a specific block of  $\text{Na}_v$  by TTX nor a global inhibition of nitric oxide synthesis with L-NAME caused increases in phasic contractions under the basal experimental conditions tested.

Furthermore, it could be speculated that ajmaline acts via an increased release of the major excitatory neurotransmitter ACh due to an ajmaline-induced “leaky” release from varicosities that has been described for other  $\text{Na}_v$ -blocking drugs as a result of collateral  $\text{K}^+$  channel inhibition [44]. Since it was observed that atropine did not counteract the ajmaline-induced increase in contractions, this mechanism is also unlikely.

To further clarify the mechanism of action of ajmaline, we compared its effects on two different types of contractions of smooth muscle:

On the one hand, adding acetylcholine or potassium to the bathing solution elicits contractions which are carried by the full number of smooth muscle cells present in the preparation, since all regions of the tissue are exposed to the chemical (ACh) or electrical (high  $[\text{K}^+]$ ) stimulus. The same applies to the addition of  $\text{Ca}^{2+}$  to depolarized smooth muscle strips.

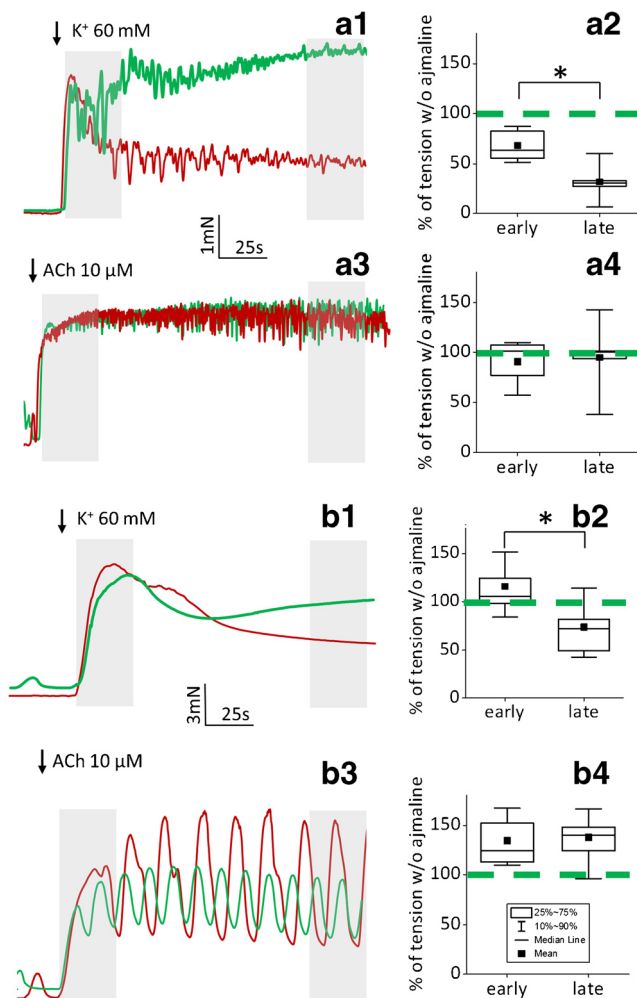


**Fig. 5** Contractions evoked by a single step application of  $K^+$  to 60 mM or ACh to 10  $\mu$ M. Representative traces obtained under control conditions are given in green, traces obtained in the presence of 100  $\mu$ M ajmaline in red. a1,  $K^+$  induced contraction of PV; a3, ACh induced contraction of PV; b1,  $K^+$  induced contraction of GA; b3, ACh induced contraction of GA. Mean values of tension were calculated over a 30-s period (shaded period on the left in a1, a3, b1, b3) immediately after application of  $K^+$  or ACh and for a 30-s period before flushing with regular Krebs buffer (shaded period on the right in a1, a3, b1, b3). Ratios were calculated between the respective means obtained in the presence of 100  $\mu$ M ajmaline and under control conditions in the same tissue sample. The distribution of the obtained early and late ratios is represented by the box plots shown next to the recording traces: a2,  $K^+$  induced contraction of PV; a4, ACh induced contraction of PV; b2,  $K^+$  induced contraction of GA; b4, ACh induced contraction of GA. Box plot designations for all are given in the legend in b4. For both  $K^+$  and ACh,  $n = 17$  for GA,  $n = 6$  for PV

Increases of contractions evoked in this “extrinsic” manner would reflect changes in force produced on the single cell level, e.g., by enhanced excitation-contraction-coupling or calcium sensitization. Our findings suggest that such changes occur only very moderately: Only ACh-induced contractions of GA were slightly increased, whereas  $K^+$ -induced contractions and  $Ca^{2+}$  sensitivity of GA and PV preparations were unchanged or even decreased.

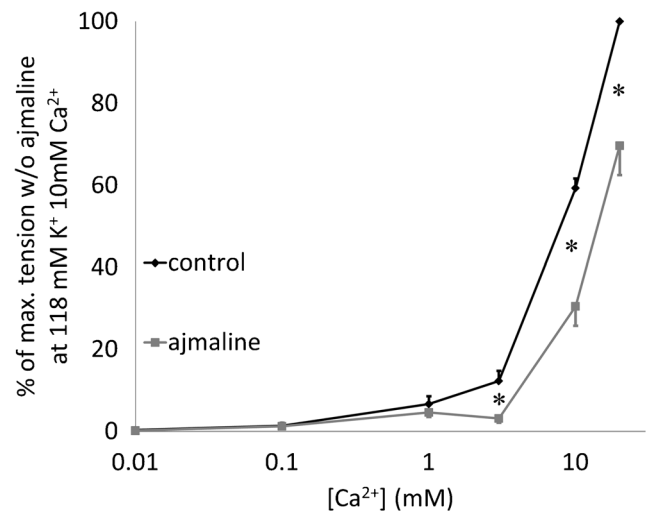


**Fig. 6** Tension development of depolarized fundus smooth muscle depends on  $[Ca^{2+}]$  in the bathing solution. The data points shown were measured under control conditions and in the presence of 100  $\mu$ M ajmaline. All values are given as the percentage of the value measured with the highest  $[Ca^{2+}]$  tested under control conditions;  $n = 9$

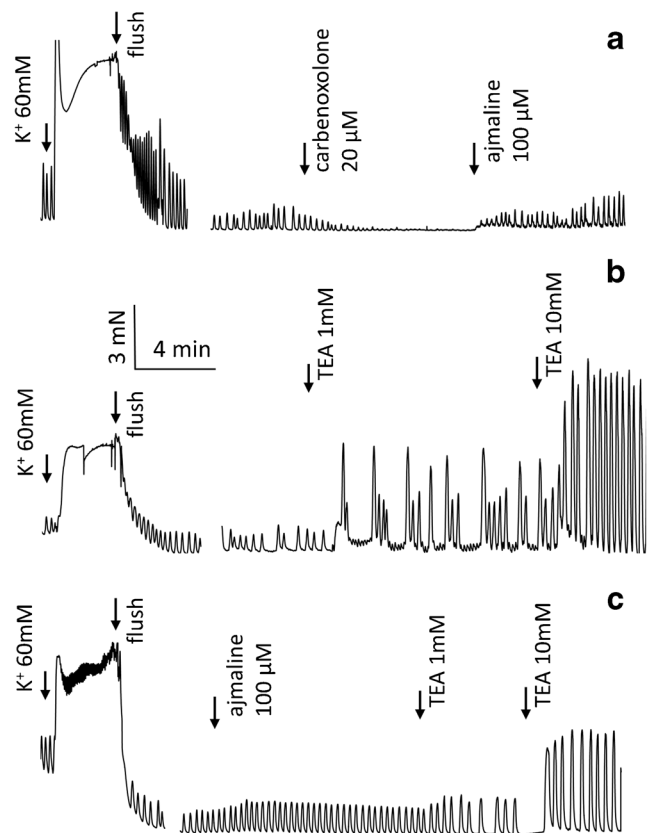


**Fig. 7** a Carbenoxolone was added at the indicated time point after equilibration and reference contraction had been obtained as for regular experiments on spontaneous activity in GA. By cumulatively adding ajmaline, this effect was counteracted. b TEA at 1 and 10 mM were added at the indicated time points. c Ajmaline (100  $\mu$ M) added prior to the application of TEA

On the other hand, the spontaneous phasic contractions of longitudinal strips of PV and GA were markedly increased. They might be considered to result from the spread of pacemaker potentials generated by Interstitial Cells of Cajal (ICC) [5, 49]. However, the direct reduction of  $K^+$  currents by  $K^+$  channel blockers can also hold for stronger rhythmical contractions. Tetraethylammonium used at 1 mM inhibits  $K^+$  channels of high conductance ( $BK_{(Ca)}$ ) more or less selectively [3]. At higher concentrations, its action is also present on  $K_v$  channels in PV and GA smooth muscle [26, 33, 34]. Remarkably, the effects of TEA and ajmaline were non-additive, as would be expected if both act at common targets, i.e.,  $K^+$  channels.

Different studies in man, guinea pig, rat, and mice have shown the intercellular coupling within the longitudinal layer of gastric smooth muscle to be relatively poor, which is reflected by the slow propagation of excitation in the longitudinal in comparison to the rather fast propagation within the circular muscle layer [17, 45, 49]. The difference in velocities resulting from the different degree of coupling is the basis for the effective propagation of circular contractions from gastric corpus towards the pyloric region via the antrum. Due to the weak electrical coupling in the longitudinal direction, slow wave potentials generated by ICC under the basal conditions that are present during organ bath experiments in standard Krebs buffer may spread incompletely within the excised muscle strip and may fail to reach the threshold for smooth muscle cell excitation at some point along the longitudinal axis of the strip. The amount of force generated would then be smaller than the force developed by the very same muscle strip when all of its smooth muscle cells are activated by exogenous agonists of high  $K^+$ .

The fact that ajmaline strongly increases the amplitude of endogenously generated spontaneous contractions, whereas it has far less pronounced effects on exogenously evoked ones, may indicate that ajmaline acts by enhancing intercellular coupling. This hypothesis would be supported by the finding that it antagonizes the effects of the gap junction blocker carbenoxolone. Data from the literature and our own experiments on  $Ca^{2+}$  sensitivity make it unlikely that improved spread of excitation within the tissue is due to increased calcium currents. Instead, inhibition of voltage-activated  $K^+$  currents by ajmaline can be considered to improve intercellular coupling: In analogy to nerve and cardiac muscle, inhibiting  $K^+$  currents would increase membrane resistance and thus increase length constant. Furthermore, it would cause an increase in action potential amplitude and duration and thus an increase in the duration and amplitude of electrotonic current spread from active to yet undepolarized cells, as it is supported by our finding that ajmaline increases the amplitude of field potentials from PV and GA. The observed interaction with carbenoxolone would thus reflect a functional antagonism on the level of electric tissue properties rather than a competitive antagonism, e.g., at the level of connexins. The

synchronizing action of ajmaline reduced frequencies of spontaneous activity in PV, but not in GA might well be explained by the fact that only the PV exhibits asynchronously working pacemaker sites under the basal conditions [15, 16].

Although  $K^+$  channel block is not considered as a leading mechanism of action for class I AAD, the literature reports  $K^+$  channel blocking properties for some local anesthetics which are also classified as class I AAD [19, 43, 50]. Ajmaline has been reported to inhibit several types of  $Na_v$  and  $K_v$  channels already at low micromolar concentrations [2, 11, 12, 24]. Therefore, it is likely that it will also inhibit other voltage-dependent ion channels, especially potassium and calcium channels—but with a higher  $IC_{50}$ . Since decreasing target specificity with increasing concentration is known for several drugs like nifedipine, verapamil, mibefradil, ciclazindol, phenytoin, and others and could well explain the effects of ajmaline observed on tissue level in the concentration range used in this study [28, 30, 35, 39, 52].

### Clinical implications

From the clinical point of view, the relation between the concentrations tested and those occurring in vivo over the course of treatment is relevant. Ajmaline is almost exclusively administered by the intravenous route. According to the literature, plasma concentrations of 2.4 to 5.0 mg/l (7.3 to 15.3  $\mu$ M) occur in the first minutes after injection and decline to less than 1% of their maximum value within the next hour [21]. Concentrations of 1  $\mu$ M led to significant effects in preparations from GA in this ex vivo study and are therefore likely to cause effects in vivo, too. Stomach cramps may be attributed to augmented spontaneous contractions caused by potassium channel inhibition, whereas abdominal discomfort and dyspeptic symptoms after food ingestion could reflect an impaired gastric accommodation reflex due to ineffective neurogenic relaxation. In sum, both pathways may contribute to key symptoms of dyspepsia.

Besides the potential adverse effects that may occur in patients without preexisting gastrointestinal dysmotility, the stimulatory effects of ajmaline should raise interest in the potential of group I AAD for treating hypomotile conditions as chronic gastroparesis, for which existing medical treatments fail to give sufficient relief [36, 40]. This applies especially to the group of patients with neuropathic (e.g., diabetic) gastroparesis since the potentially harmful inhibitory effects of ajmaline on neurotransmission can be expected to be negligible when there is already no effective organ innervation at the onset of treatment. Despite the potential side effects in terms of cardiac arrhythmias and impaired gastric accommodation, a potential of class I AAR in this field is supported by the fact that the local anesthetic procaine has been reported to be effective in the treatment of gastrointestinal hypomotility following gastrointestinal tract surgery [41, 46].

## Limitations

This study has some limitations: Although it gives strong support to the hypothesis of increased coupling as the reason for the observed increase in force, the methodology is not suited to detect the specific type of ion channels involved and to characterize the changes in the spatial pattern of tissue excitation. For the further clarification of the underlying mechanisms, follow-up studies using single cell patch clamp studies, supravital fluorescence microscopy, and pressure measurements on whole isolated organs will be necessary and are currently in preparation.

**Authorship contribution** Robert Patejdl, Dietmar Bänsch, and Thomas Noack designed research; Alina Gromann and Robert Patejdl performed research and analyzed data; Robert Patejdl wrote the paper. All authors reviewed the manuscript.

**Funding** The resources used for this work were provided by the University of Rostock. No additional funding was used.

## Compliance with ethical standards

**Conflict of interest** Robert Patejdl, Alina Gromann, Dietmar Bänsch, and Thomas Noack declare that they have no conflicts of interest or competing interests related to this work.

Dietmar Bänsch received research grants from Biosense, Biotronik, Medtronic, National Heart Foundation Mayo Clinic, and Zoll Medical.

Dietmar Bänsch received honoraria for lectures and consultancy from Biotronik, Bayer Medical, and Zoll Medical.

## References

- Bashashati M, McCallum RW (2015) Is interstitial cells of cajalopathy present in gastroparesis? *J Neurogastroenterol Motil* 21(4):486–493. <https://doi.org/10.5056/jnm15075>
- Bebarova M, Matejovic P, Pasek M et al (2005) Effect of ajmaline on action potential and ionic currents in rat ventricular myocytes. *Gen Physiol Biophys* 24(3):311–325
- Benham CD, Bolton TB, Lang RJ, Takewaki T (1986) Calcium-activated potassium channels in single smooth muscle cells of rabbit jejunum and guinea-pig mesenteric artery. *J Physiol* 371:45–67
- Biamino G, Wessel HJ, Noring J (1975) Ajmaline-induced changes in mechanical and electrical activity of vascular smooth muscle. *Blood Vessels* 12(1):68–80
- Bolton TB, Gordienko DV, Povstyan OV, Harhun MI, Pucovsky V (2004) Smooth muscle cells and interstitial cells of blood vessels. *Cell Calcium* 35(6):643–657. <https://doi.org/10.1016/j.ceca.2004.01.018>
- Breyne J, Vanheel BJ (2004) Role of Ba<sup>2+</sup>-resistant K<sup>+</sup> channels in endothelium-dependent hyperpolarization of rat small mesenteric arteries. *Can J Physiol Pharmacol* 82(1):65–71. <https://doi.org/10.1139/y03-132>
- Chatterjee ML, De MS (1963) Pharmacological action of ajmaline, the possible mechanism of its antiarrhythmic action, and its therapeutic possibilities. *Nature* 200:1067–1068
- D'Amato M, Curro D, Ciabattoni G et al (1990) Is peptide histidine isoleucine an inhibitory nonadrenergic noncholinergic neurotransmitter in the rat gastric fundus? *Arch Int Pharmacodyn Ther* 303:216–231
- Echt DS, Liebson PR, Mitchell LB et al (1991) Mortality and morbidity in patients receiving encainide, flecainide, or placebo. *N Engl J Med* 324(12):781–788. <https://doi.org/10.1056/NEJM199103213241201>
- Ferrari M, Furlanut M, Maragno I (1972) Effects of quinidine and ajmaline on the mechanical and electrical activity of smooth muscle. *Arch Int Pharmacodyn Ther* 200(1):64–69
- Fischer F, Vonderlin N, Zitron E et al (2013) Inhibition of cardiac Kv1.5 and Kv4.3 potassium channels by the class Ia antiarrhythmic ajmaline: mode of action. *Naunyn Schmiedeberg's Arch Pharmacol* 386(11):991–999. <https://doi.org/10.1007/s00210-013-0901-0>
- Friedrich O, Wegner F, Wink M et al (2007) Na<sup>+</sup>- and K<sup>+</sup>-channels as molecular targets of the alkaloid ajmaline in skeletal muscle fibres. *Br J Pharmacol* 151(1):82–93. <https://doi.org/10.1038/sj.bjp.0707194>
- Gentzkow GD, Sullivan JY (1984) Extracardiac adverse effects of flecainide. *Am J Cardiol* 53(5):101B–105B
- Golenhofen K, von Loh D (1970) Electrophysiology studies on normal spontaneous activity of the isolated guinea pig taenia coli (Elektrophysiologische Untersuchungen zur normalen Spontanaktivität der isolierten Taenia coli des Meerschweinchens). *Pflügers Arch* 314(4):312–328
- Hermesmeyer K (1973) Multiple pacemaker sites in spontaneously active vascular muscle. *Circ Res* 33(2):244–251
- Hirst GDS, Garcia-Londono AP, Edwards FR (2006) Propagation of slow waves in the guinea-pig gastric antrum. *J Physiol* 571(Pt 1):165–177. <https://doi.org/10.1113/jphysiol.2005.100735>
- Huizinga JD, Liu LW, Blennerhassett MG et al (1992) Intercellular communication in smooth muscle. *Experientia* 48(10):932–941
- Khodorov BI, Zaborovskaya LD (1986) Use-dependent blockade of sodium channels by local anaesthetics and antiarrhythmic drugs. Effects of chloramine-T and calcium ions. *Drugs Exp Clin Res* 12(9–10):743–752
- Kiesecker C, Zitron E, Lück S et al (2004) Class Ia antiarrhythmic drug ajmaline blocks HERG potassium channels: mode of action. *Naunyn Schmiedeberg's Arch Pharmacol* 370(6):423–435. <https://doi.org/10.1007/s00210-004-0976-8>
- Kilkenny C, Browne WJ, Cuthill IC, Emerson M, Altman DG (2010) Improving bioscience research reporting: the ARRIVE guidelines for reporting animal research. *PLoS Biol* 8(6):e1000412. <https://doi.org/10.1371/journal.pbio.1000412>
- Kleinsorge H, Gaida P (1962) Behavior of the serum level after intravenous injections of ajmaline. *Klin Wochenschr* 40:149–151
- Kohlhardt M (1984) Block of sodium currents by antiarrhythmic agents: analysis of the electrophysiologic effects of propafenone in heart muscle. *Am J Cardiol* 54(9):13D–19D
- Koppel C, Oberdisse U, Heinemeyer G (1990) Clinical course and outcome in class IC antiarrhythmic overdose. *J Toxicol Clin Toxicol* 28(4):433–444
- Körper S, Wink M, Fink RH (1998) Differential effects of alkaloids on sodium currents of isolated single skeletal muscle fibers. *FEBS Lett* 436(2):251–255
- Ladabaum U, Hasler WL (1999) Motility of the small intestine. *Curr Opin Gastroenterol* 15(2):125–131
- Lammell E, Deitmer P, Noack T (1991) Suppression of steady membrane currents by acetylcholine in single smooth muscle cells of the guinea-pig gastric fundus. *J Physiol* 432:259–282
- Lang IM (2016) The role of central and enteric nervous systems in the control of the retrograde giant contraction. *J Neurogastroenterol Motil* 22(2):321–332. <https://doi.org/10.5056/jnm15141>
- Li X-T, Li X-Q, Hu X-M, Qiu XY (2015) The inhibitory effects of Ca<sup>2+</sup> channel blocker nifedipine on rat Kv2.1 potassium channels. *PLoS One* 10(4):e0124602. <https://doi.org/10.1371/journal.pone.0124602>

29. Meinertz T, Zehender MK, Geibel A et al (1984) Long-term antiarrhythmic therapy with flecainide. *Am J Cardiol* 54(1):91–96
30. Meissner A, Noack T (2008) Proliferation of human lens epithelial cells (HLE-B3) is inhibited by blocking of voltage-gated calcium channels. *Pflugers Arch* 457(1):47–59. <https://doi.org/10.1007/s00424-008-0514-5>
31. Naccarelli GV, Wolbrette DL, Khan M et al (2003) Old and new antiarrhythmic drugs for converting and maintaining sinus rhythm in atrial fibrillation: comparative efficacy and results of trials. *Am J Cardiol* 91(6A):15D–26D
32. Nguyen LA, Snape WJ Jr (2015) Clinical presentation and pathophysiology of gastroparesis. *Gastroenterol Clin N Am* 44(1):21–30. <https://doi.org/10.1016/j.gtc.2014.11.003>
33. Noack T, Deitmer P, Golenhofen K (1990) Features of a calcium independent, caffeine sensitive outward current in single smooth muscle cells from guinea pig portal vein. *Pflugers Arch* 416(4):467–469
34. Noack T, Deitmer P, Lammel E (1992) Characterization of membrane currents in single smooth muscle cells from the guinea-pig gastric antrum. *J Physiol* 451:387–417
35. Noack T, Edwards G, Deitmer P, Greengrass P, Morita T, Andersson PO, Criddle D, Wyllie MG, Weston AH (1992) The involvement of potassium channels in the action of cizolindol in rat portal vein. *Br J Pharmacol* 106(1):17–24
36. Oh JH, Pasricha PJ (2013) Recent advances in the pathophysiology and treatment of gastroparesis. *J Neurogastroenterol Motil* 19(1):18–24. <https://doi.org/10.5056/jnm.2013.19.1.18>
37. Palani D, Ghildyal P, Manchanda R (2006) Effects of carbenoxolone on syncytial electrical properties and junction potentials of guinea-pig vas deferens. *Naunyn Schmiedeberg's Arch Pharmacol* 374(3):207–214. <https://doi.org/10.1007/s00210-006-0109-7>
38. Patejdl R, Noack T (2010) The propagation of excitation in portal vein smooth muscle—evidence for coupled “hot spots”. *Trace Elem Electrolytes* 27(4):202–208
39. Patejdl R, Leroux A-C, Noack T (2015) Phenytoin inhibits contractions of rat gastrointestinal and portal vein smooth muscle by inhibiting calcium entry. *Neurogastroenterol Motil* 27(10):1453–1465. <https://doi.org/10.1111/nmo.12645>
40. Rey E, Choung RS, Schleck CD et al (2012) Prevalence of hidden gastroparesis in the community: the gastroparesis “iceberg”. *J Neurogastroenterol Motil* 18(1):34–42. <https://doi.org/10.5056/jnm.2012.18.1.34>
41. Rimbäck G, Cassuto J, Faxén A et al (1986) Effect of intra-abdominal bupivacaine instillation on postoperative colonic motility. *Gut* 27(2):170–175
42. Sage D, Salin P, Alcaraz G, Castets F, Giraud P, Crest M, Mazet B, Clerc N (2007) Na(v)1.7 and Na(v)1.3 are the only tetrodotoxin-sensitive sodium channels expressed by the adult guinea pig enteric nervous system. *J Comp Neurol* 504(4):363–378. <https://doi.org/10.1002/cne.21450>
43. Scholz A (2002) Mechanisms of (local) anaesthetics on voltage-gated sodium and other ion channels. *Br J Anaesth* 89(1):52–61. <https://doi.org/10.1093/bja/ae163>
44. Sircuta C, Lazar A, Azamfirei L et al (2016) Correlation between the increased release of catecholamines evoked by local anesthetics and their analgesic and adverse effects: role of K(+) channel inhibition. *Brain Res Bull* 124:21–26. <https://doi.org/10.1016/j.brainresbull.2016.03.009>
45. Stevens RJ, Weinert JS, Publicover NG (1999) Visualization of origins and propagation of excitation in canine gastric smooth muscle. *Am J Phys* 277(3 Pt 1):C448–C460
46. Syrbu IF, Sokolov IS, Ozerov VN (1979) Profilaktika posleoperatsionnogo pareza zheludka i kishhechnika (Prevention of postoperative gastric and intestinal paresis). *Khirurgiia (Mosk)* 10:107–108
47. Takahashi T, Owyang C (1997) Characterization of vagal pathways mediating gastric accommodation reflex in rats. *J Physiol* 504(Pt 2):479–488
48. Teo KK, Yusuf S, Furberg CD (1993) Effects of prophylactic antiarrhythmic drug therapy in acute myocardial infarction. An overview of results from randomized controlled trials. *JAMA* 270(13):1589–1595
49. van Helden DF, Laver DR, Holdsworth J, Imtiaz MS (2010) Generation and propagation of gastric slow waves. *Clin Exp Pharmacol Physiol* 37(4):516–524. <https://doi.org/10.1111/j.1440-1681.2009.05331.x>
50. Wolff M, Schnöbel-Ehehalt R, Mühling J et al (2014) Mechanisms of lidocaine's action on subtypes of spinal dorsal horn neurons subject to the diverse roles of Na(+) and K(+) channels in action potential generation. *Anesth Analg* 119(2):463–470. <https://doi.org/10.1213/ANE.0000000000000280>
51. Zaborovskaia LD, Khodorov BI (1982) Razlichie v blokiruišem deistvii benzokaina i aminnykh soedinenii na modifitsirovannye batrakhotosinom natrievye kanaly perekhvata Ranv'e (Differences in the blocking action of benzocaine and amino compounds on batrachotoxin-modified node of Ranvier sodium channels). *Neirofiziologiia* 14(6):636–643
52. Zhang S, Zhou Z, Gong Q et al (1999) Mechanism of block and identification of the verapamil binding domain to HERG potassium channels. *Circ Res* 84(9):989–998

**Publisher's note** Springer Nature remains neutral with regard to jurisdictional claims in published maps and institutional affiliations.

# The sphingosine analog fingolimod (FTY720) enhances tone and contractility of rat gastric fundus smooth muscle

M. Kraft<sup>1</sup> | U. K. Zettl<sup>2</sup> | T. Noack<sup>1</sup> | R. Patejdl<sup>1</sup> 

<sup>1</sup>Oscar Langendorff Institut für Physiologie, Universität Rostock, Rostock, Germany

<sup>2</sup>Klinik und Poliklinik für Neurologie Sektion Neuroimmunologie, Universität Rostock, Rostock, Germany

## Correspondence

Robert Patejdl, Oscar Langendorff Institut für Physiologie, Universitätsmedizin Rostock, Rostock, Germany.  
Email: robert.patejdl@uni-rostock.de

## Funding information

The resources used for this work were provided by the University of Rostock. No additional funding was used.

## Abstract

**Background:** Sphingosine and its metabolite sphingosine phosphate (S1P) regulate a multitude of biological functions, including the contractile state of smooth. Gastrointestinal side effects have been reported in patients treated with FTY720, a sphingosine analog that is approved for the treatment of multiple sclerosis. The aim of this study was to characterize the effects of FTY720 on rat gastric fundus smooth muscle under basal conditions and during activation induced by high-K<sup>+</sup> solution.

**Methods:** Isometric contractions of isolated circular strips of gastric fundus smooth muscle were recorded using the organ bath method. The effects of FTY720 or vehicle were recorded under control conditions and in the presence of indomethacin, L-NAME, HA-1100, nifedipine, JTE-013, and suramin. Tone and contractions recorded in the presence of FTY720 or vehicle are reported as % of the amplitude of an initial high-K<sup>+</sup> contraction obtained under control conditions.

**Key Results:** From a concentration of 10 μmol L<sup>-1</sup> onwards, FTY720 increased the tone, reaching 8.9% ± 7.5% at 100 μmol L<sup>-1</sup> (*P* < .05). With indomethacin in the solution, the effects of FTY720 were enhanced (32.1% ± 7.7%; *P* < .001). The FTY720-induced increase in tone was abolished in the absence of extracellular Ca<sup>2+</sup> and reduced by nifedipine, HA-1100, JTE-013, and suramin. Furthermore, FTY720 increased high-K<sup>+</sup> contractions in the presence of indomethacin.

**Conclusions & Inferences:** FTY720 increases tone and contractile responses to depolarization in gastric fundus smooth muscle by triggering calcium entry and calcium sensitization in a S1P receptor-dependent manner. Taken together, the experimental results presented in this work suggest that FTY720 may increase gastric tone and contractility in patients.

## KEYWORDS

FTY720, gastric fundus, smooth muscle, sphingosine, sphingosine receptors

## 1 | INTRODUCTION

Sphingosine-1-phosphate (S1P) signaling via S1P receptors (S1PR) has been shown to modulate cardiovascular homeostasis, inflammation,

and other important physiological functions.<sup>1-5</sup> The sphingosine analog FTY720 (fingolimod) has been approved for the immunomodulatory treatment of multiple sclerosis. In a phase III trial (FREDOMS II), patients treated with FTY720 experienced gastrointestinal

**Abbreviations:** COX, cyclooxygenase; ddH<sub>2</sub>O, double-distilled water; DMSO, dimethylsulfoxid; EC<sub>50</sub>, half maximal effective concentration; FTY720, Fingolimod (trade name Gilenya); FTY720-P, FTY720-Phosphate; HA-1100, hydroxyfasudil; ICC, interstitial cells of Cajal; KCl, potassium chloride; Km, Michaelis-Menten constant; L-NAME, N<sup>ω</sup>-Nitro-L-arginine Methyl Ester hydrochloride; MS, multiple sclerosis; NO, nitric oxide; NOS, nitric oxide synthase; NSAID, non-steroidal anti-inflammatory drug; RhoA, ras homolog gene family, member A; ROK, rho-kinase; S1PR, sphingosine phosphate receptor; S1P, sphingosine phosphate; Sbt, stabilized basal tone; SEM, standard error of the mean; SPK2, sphingosine kinase 2; VOCC, voltage operated L-type Ca<sup>2+</sup> channels.

complications more frequently than patients on placebo. Whereas 40% of participants on placebo reported any kind of gastrointestinal disorder (nausea, diarrhea, vomiting, or dyspepsia), it were 43% of the patients receiving 0.5 mg fingolimod per day and 49% in those on 1.25 mg fingolimod per day.<sup>6</sup> The pharmacodynamic basis of these treatment related events has not yet been elucidated.

The mechanism of action on the immune system and other organ systems is complex since FTY720 can either be phosphorylated to FTY720-P which acts as an agonist on S1PR, or it can act as a functional antagonist to endogenous S1P by leading to internalization of S1PR or by inhibiting sphingosine kinase 1 (SPK1).<sup>7</sup> Furthermore, FTY720 inhibits phospholipase A2 in an S1PR-independent pathway and acts as an antagonist on cannabinoid receptors.<sup>8,9</sup> Five different S1PR subtypes exist, of which S1PR 1, 3, 4, and 5 have been unequivocally reported to be activated by FTY720-P.<sup>10</sup> The downstream signaling of both S1PR-dependent and S1PR-independent pathways affects various elements that contribute to the control of smooth muscle function, among them L-type calcium channels, rho-kinase (ROK), and nitric oxide synthase (NOS) (for a review, see<sup>11</sup>).

Different groups have studied the effects of S1P and FTY720 on the contractility of vascular smooth muscle.<sup>12-16</sup> According to Spijkers et al., FTY720 causes contractions of carotid arteries in spontaneously hypertensive rats that were abolished by endothelium denudation and cyclooxygenase (COX) inhibition.<sup>12</sup> Very little is known about the effects of FTY720 on gastrointestinal smooth muscle.

A study on isolated cells from the circular portion layer of rabbit gastric antrum demonstrated that S1P led to a biphasic contractile response that was mediated by S1PR<sub>1</sub> and S1PR<sub>2</sub>.<sup>17</sup> Another study on dispersed cells from cat esophagus reported that S1P caused an S1PR<sub>2</sub> mediated contraction.<sup>18</sup> Two studies reported modulatory effects of S1P and its analogs on spontaneous activity of cultured interstitial cells of Cajal (ICC).<sup>19,20</sup>

This study investigates the effects of FTY720 on gastrointestinal smooth muscle force. An *ex vivo* model of smooth muscle preparation from rats was used under basal conditions and with a depolarization activating L-type Ca<sup>2+</sup> channels. To our knowledge, the actions of FTY720 on native isolated tissue preparations of gastric smooth muscle have not yet been studied. Gastrointestinal motility has been recognized over recent decades not to be a function of a single cell type but rather the result of a complex interaction between neurons, ICC, and myocytes.<sup>21</sup> Thus, studies on intact tissue specimen are essential to predict and analyze the *in vivo* responses of drugs and mediators acting on gastrointestinal function.

## 2 | MATERIALS AND METHODS

### 2.1 | Tissue preparation

Wistar albino rats of 200- to 300-day-old (20 males, 16 females) were killed by decapitation after anesthesia according to German national law and the regulations and ethical standards of the

### Key Points

- It is not known how FTY720, a drug approved for multiple sclerosis, modulates native gastric smooth muscle function.
- FTY720 increases tone and contractions of fundus smooth muscle. Inhibiting prostaglandin or NO synthesis enhances these effects. The effects of FTY720 depend on Ca<sup>2+</sup> entry and Ca<sup>2+</sup> sensitization and on the activation sphingosine receptors.
- The results of this study raise the possibility that gastrointestinal complications in multiple sclerosis patients treated with FTY720 may be due to direct drug effects on gastrointestinal muscle.

University of Rostock. The whole stomach was excised and placed in a cold physiological salt solution containing 145 mmol L<sup>-1</sup> NaCl, 4.5 mmol L<sup>-1</sup> KCl, 0.1 mmol L<sup>-1</sup> CaCl<sub>2</sub>, 1.1 mmol L<sup>-1</sup> NaH<sub>2</sub>PO<sub>4</sub>, 1 mmol L<sup>-1</sup> MgSO<sub>4</sub>, 0.025 mmol L<sup>-1</sup> ethylenediaminetetraacetic acid (EDTA), 5 mmol L<sup>-1</sup> 4-(2-hydroxyethyl)-1-piperazineethanesulfonic acid (HEPES) (pH 7.4), stored at 4°C. The stomach was pinned to a Sylgard dish at the esophageal and duodenal endings. Fat and adhering tissue were removed.

Muscle strips of 1 mm thickness were cut from the fundus in a circular direction, cutting perpendicular to the proximal part of the greater curvature without opening the stomach. Afterward, the strips were suspended in cold physiological salt solution, tethered to glass holders with one ending transferred into a vertical organ bath and finally tethered to a force transducer with the other ending.

The organ baths were filled with modified Krebs-Henseleit buffer (112 mmol L<sup>-1</sup> NaCl, 4.7 mmol L<sup>-1</sup> KCl, 2.5 mmol L<sup>-1</sup> CaCl<sub>2</sub>, 1.2 mmol L<sup>-1</sup> MgCl<sub>2</sub>, 25 mmol L<sup>-1</sup> NaHCO<sub>3</sub>, 1.2 mmol L<sup>-1</sup> KH<sub>2</sub>PO<sub>4</sub>, 11.5 mmol L<sup>-1</sup> glucose) and equilibrated with 95% O<sub>2</sub> and 5% CO<sub>2</sub> at a temperature of 36°C and a pH of 7.4. Isometric force was recorded using mechano-electrical transducers coupled to a bridge amplifier (both World Precision Instruments, Sarasota, FL, USA), low-pass filtered at 1 Hz, and digitized by a PowerLab 8/32 at 100/s (ADInstruments, Bella Vista, Australia). LabChart7 (ADInstruments) and MSEXcel (Microsoft, Redmond, WA, USA) were used for the further processing of the data.

### 2.2 | Procedure

The circular smooth muscle strips were tested for tone increases induced by FTY720 and for FTY720 induced changes in high-K<sup>+</sup>-induced contractions. Strips were placed in Krebs-Henseleit buffer (Krebs solution) or in COX inhibitor (indomethacin 10 μmol L<sup>-1</sup>) containing Krebs solution. A prestrain of 3 mN was set and strips were then left for least 1 hour to ensure sufficient equilibration

time for developing their specific motor pattern. Afterward, a reference contraction was induced by increasing potassium concentration in the Krebs solution by 50 mmol L<sup>-1</sup> (total concentration of K<sup>+</sup>: 54.7 mmol L<sup>-1</sup>). All force changes observed during further measurements of contraction and tone refer to the amplitude of this first K<sup>+</sup>-induced contraction. After the maximum of contraction was reached, the organ bath solution was replaced by either fresh Krebs-Henseleit buffer or another modified solution, depending on the experiment. A Ca<sup>2+</sup>-free solution (112 mmol L<sup>-1</sup> NaCl, 4.7 mmol L<sup>-1</sup> KCl, 3.7 mmol L<sup>-1</sup> MgCl<sub>2</sub>, 25 mmol L<sup>-1</sup> NaHCO<sub>3</sub>, 1.2 mmol L<sup>-1</sup> KH<sub>2</sub>PO<sub>4</sub>, 11.5 glucose, 1 mmol L<sup>-1</sup> EGTA) and an indomethacin-containing solution supplemented with the NOS inhibitor L-NAME were used.

When the tone had stabilized following the initial high-K<sup>+</sup> contraction and the successive washout step, either a first dose of FTY720 was added or the strips were pretreated with HA-1100/JTE-013/nifedipine followed by FTY720. In time control experiments, double-distilled water (ddH<sub>2</sub>O) was added at time points and volumes identical to those added in experiments with using FTY720.

### 2.3 | Reagents

FTY720, indomethacin, N $\omega$ -Nitro-L-arginine Methyl Ester hydrochloride (L-NAME), nifedipine, and JTE-013 were from Sigma Aldrich (St. Louis, MO, USA). HA-1100 hydrochloride (hydroxyfasudil) and suramin were purchased from Tocris Bioscience (Ellisville, MO, USA).

Indomethacin was dissolved in DMSO, all other substances in ddH<sub>2</sub>O. Since nifedipine is highly photosensitive, all work steps and the measurements were performed under darkroom conditions using a sodium lamp for illumination.

### 2.4 | Data presentation and statistics

Changes in tone and contraction amplitudes were normalized to the first K<sup>+</sup>-induced contraction of the sample to account for variability in total strength between individual strips (Figure 1). As a reference value for the estimation of changes in tone, the mean force of the last 2 minutes prior to the first FTY720/ddH<sub>2</sub>O-application was determined. It was subtracted from the subsequent force data to give the changes in tone after the application of the substances. At the end of each experiment, a second reference contraction was induced by adding KCl as described above. The percentage of force observed during this second K<sup>+</sup> application in relation to the first is designated as FTY720<sub>K50</sub> or ddH<sub>2</sub>O<sub>K50</sub>, depending on whether it was evoked in the presence of FTY720 or vehicle.

Values are given as mean  $\pm$  SEM of mean. For statistical testing, the Shapiro-Wilk test and the equal variance test were applied by using SigmaPlot 13.0 (Systat Software, San Jose, California, USA). For normally distributed values, the *t* test for independent samples was applied; otherwise, the Mann-Whitney *U* test for independent samples was used.

## 3 | RESULTS

### 3.1 | Effects of FTY720 on tone and high-K<sup>+</sup> contractions under control conditions

When added to the organ bath after a defined period of equilibration and in the absence of any exogenous drugs, FTY720 increased the tone of fundus strips significantly from a concentration of 10  $\mu$ mol L<sup>-1</sup> onwards (2.9%  $\pm$  2.1%, *n* = 11, *P* < .05). The

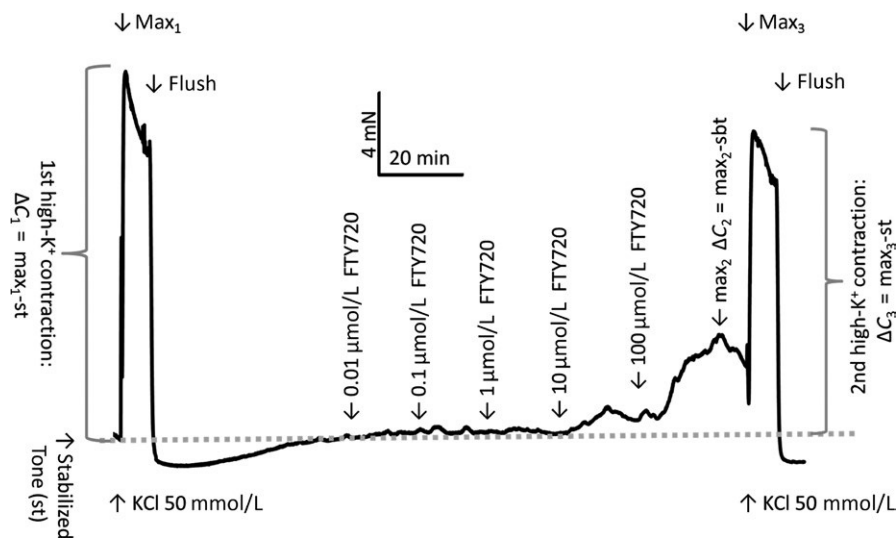


**FIGURE 1** Extraction of numerical data from time-based isometric force measurements. The equations given next to the trace were used to calculate the readout parameters used in this study. The maximal isometric force for both high-K<sup>+</sup> contractions and for the FTY720 effect was determined ( $max_{1,3}$ ). The stabilized tone (sbt) was taken after equilibration following the first high-K<sup>+</sup> contraction. The sbt was then subtracted from all  $max$ -values. The subsequent FTY720 induced changes in tone and the second high-K<sup>+</sup> contraction were normalized on the first high-K<sup>+</sup> contraction and are given as respective %-values, ie, effect of 100  $\mu$ mol L<sup>-1</sup> FTY =  $100 \cdot \Delta C_2 / \Delta C_1$ ; size of second K<sup>+</sup> contraction =  $100 \cdot \Delta C_3 / \Delta C_1$

increase was even more pronounced at  $100 \mu\text{mol L}^{-1}$  ( $8.9\% \pm 2.4\%$ ,  $n = 11$ ,  $P < .05$ ). The effects of cumulatively increasing [FTY720] in the bathing solution are depicted in the representative trace of Figure 2A. The increase in tone occurred with a delay of several minutes and had a phasic component. Within the application interval of 20 minutes, the samples reached a constant plateau higher than the basal level. The observed effect was reversed after a washout. Samples treated with ddH<sub>2</sub>O instead of FTY720 showed a decrease in tone over time ( $0.4\%$  ddH<sub>2</sub>O:  $-4.5\% \pm 2.5\%$ ,  $n = 9$  and  $1.3\%$  ddH<sub>2</sub>O:  $-5.0\% \pm 2.7\%$ ,  $n = 9$ ). When comparing FTY720 treated with ddH<sub>2</sub>O-treated muscle strips, [FTY720]  $10 \mu\text{mol L}^{-1}$  increased the tone by 7% and [FTY720]  $100 \mu\text{mol L}^{-1}$  by 14% (sum of the bars, Figure 2B). Figure 3A shows the aggregated concentration-contraction data of measured fundus strips in Krebs solution and in Krebs solution containing  $1 \mu\text{mol L}^{-1}$  indomethacin. The FTY720 effect did not saturate up to the highest concentration tested.

After tone had stabilized following the final concentration step to  $100 \mu\text{mol L}^{-1}$  FTY720, a contraction was induced by increasing [K<sup>+</sup>] as described above. The observed contraction was not different from that evoked in strips exposed to ddH<sub>2</sub>O instead of FTY720 (FTY720<sub>K50</sub>:  $77.5\% \pm 7.6\%$ ,  $n = 12$ ; ddH<sub>2</sub>O<sub>K50</sub>:  $89.3\% \pm 9.4\%$ ,  $n = 9$ , Figure 3B).

### 3.2 | Altered effects of FTY720 under conditions of COX inhibition

In the presence of the COX inhibitor indomethacin ( $10 \mu\text{mol L}^{-1}$ ), FTY720 retained its ability to increase tone ( $10 \mu\text{mol L}^{-1}$ :  $15.7\% \pm 4.8\%$ ,  $n = 12$ ,  $P < .01$ ;  $100 \mu\text{mol L}^{-1}$ :  $32.1\% \pm 7.7\%$ ,  $n = 12$ ,

$P < .01$ ) (Figure 4). The temporal pattern of drug responses was not changed (Figure 4A). In samples treated with ddH<sub>2</sub>O, tone decreased over time ( $0.4\%$  ddH<sub>2</sub>O:  $-6.8\% \pm 4\%$ ,  $n = 10$  and  $1.3\%$  ddH<sub>2</sub>O:  $-8.8\% \pm 5.1\%$ ,  $n = 11$ ) (Figure 4B). When indomethacin was present in the bathing solution, high-K<sup>+</sup>-evoked contractions in the presence of FTY720 were significantly stronger than time-matched vehicle controls (FTY720<sub>K50</sub>:  $96.8\% \pm 10.8\%$ ; ddH<sub>2</sub>O<sub>K50</sub>:  $65.2\% \pm 4.5\%$ ;  $n = 9$ ;  $P < .05$ ) (Figure 3B).

In contrast to the enhancing effect of indomethacin on high-K<sup>+</sup> contractions in the presence of FTY720, the time-matched vehicle control contractions were significantly weaker than those evoked in standard Krebs solution (standard Krebs solution: ddH<sub>2</sub>O<sub>K50</sub>  $89.3\% \pm 9.4\%$ ; indomethacin-containing Krebs solution: ddH<sub>2</sub>O<sub>K50</sub>  $65.2\% \pm 4.5\%$ ;  $n = 9$ ;  $P < .05$ ). Furthermore, the arithmetic mean amplitude of high-K<sup>+</sup> contractions evoked in the presence of FTY720 was higher with indomethacin in the bathing solution than in standard Krebs solution. The difference, however, failed to reach significance (standard Krebs solution + FTY720<sub>K50</sub>:  $77.8\% \pm 7.6\%$ ,  $n = 12$ ; indomethacin-containing solution + FTY720<sub>K50</sub>:  $96.8\% \pm 10.8\%$ ,  $n = 9$ ;  $P = .224$ , Figure 3B).

### 3.3 | FTY720 effects under conditions of NOS inhibition

The inhibition of NO synthesis by L-NAME abolished the gradual decrease in tone over time that was otherwise observed reliably. Compared with vehicle and time control experiments, tone dropped less and was, thus, higher in the presence of L-NAME (control with ddH<sub>2</sub>O:  $-8.8\% \pm 5.1\%$ ; control with  $100 \mu\text{mol L}^{-1}$  L-NAME:  $-0.2\% \pm 1.4\%$ ,  $n = 8$ ,  $P < .05$ ).

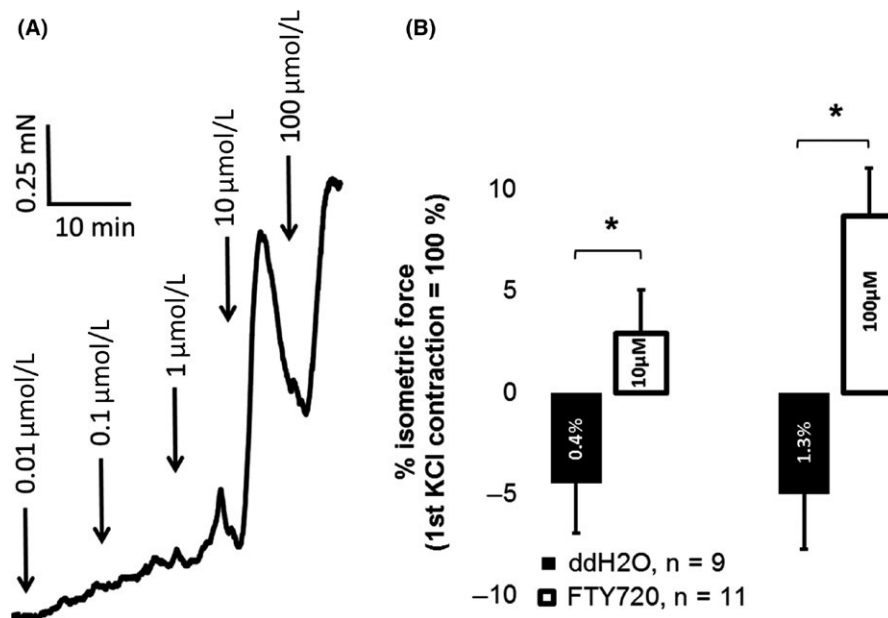


**FIGURE 2** FTY720 increases tone of circular gastric fundus strips in standard Krebs solution. A, Fundus circular smooth muscle strips in standard Krebs solution were exposed to cumulatively increasing concentrations of FTY720. A representative contractile force trace is shown. B, Fundus circular smooth muscle strips in standard Krebs solution were treated with 10 and  $100 \mu\text{mol L}^{-1}$  FTY720 or vehicle (ddH<sub>2</sub>O). The relative isometric force is expressed as the ratio of the first high-K<sup>+</sup>-induced contraction

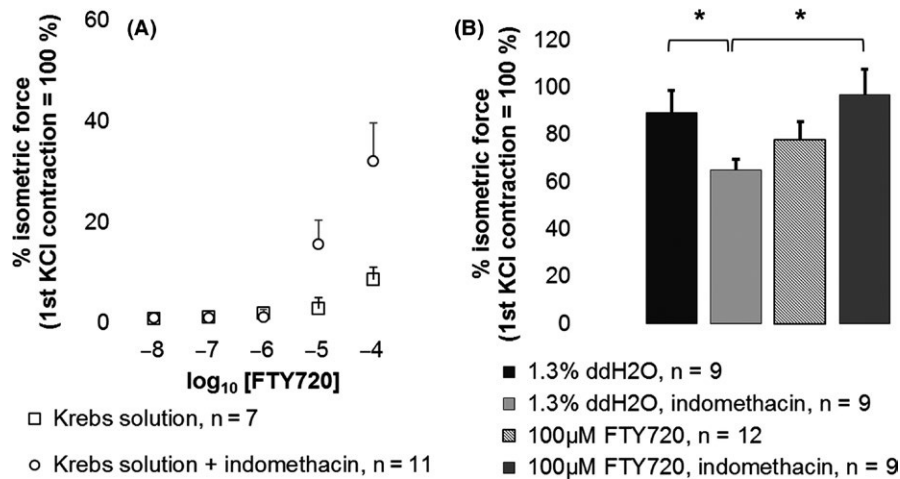


**FIGURE 3** A, Concentration-contraction data of FTY720 in standard Krebs solution and indomethacin-containing Krebs solution. Fundus circular smooth muscle strips with (n = 11) and without (n = 10) 10 μmol L<sup>-1</sup> indomethacin in the Krebs solution were exposed to increasing concentrations of FTY720. B, Effect of FTY720 on the second K<sup>+</sup>-induced contraction in standard Krebs solution vs indomethacin-containing Krebs solution. Fundus circular smooth muscle strips in indomethacin-containing Krebs solution and standard Krebs solution were treated with 100 μmol L<sup>-1</sup> FTY720 or 0.4% resp. 1.3% ddH<sub>2</sub>O followed by the addition of 50 mmol L<sup>-1</sup> KCl

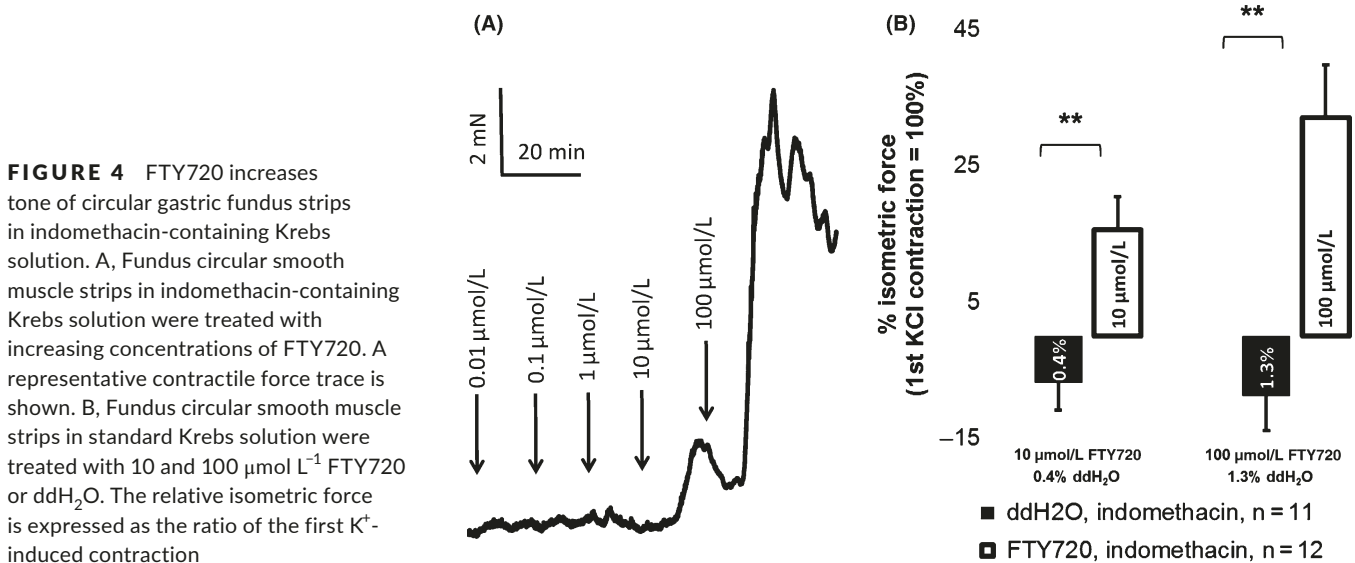


**FIGURE 4** FTY720 increases tone of circular gastric fundus strips in indomethacin-containing Krebs solution. A, Fundus circular smooth muscle strips in indomethacin-containing Krebs solution were treated with increasing concentrations of FTY720. A representative contractile force trace is shown. B, Fundus circular smooth muscle strips in standard Krebs solution were treated with 10 and 100 μmol L<sup>-1</sup> FTY720 or ddH<sub>2</sub>O. The relative isometric force is expressed as the ratio of the first K<sup>+</sup>-induced contraction

In contrast to other experimental conditions, FTY720 added in the presence of L-NAME caused a significant increase in tone already at a concentration of 1 μmol L<sup>-1</sup> (indomethacin-containing solution + L-NAME + 1 μmol L<sup>-1</sup> FTY720: 7.7% ± 1.5%, n = 8; indomethacin-containing solution + L-NAME + ddH<sub>2</sub>O: -0.5% ± 1.1%, n = 9; *P* < .05) (Figure 5). Tone with 1 μmol L<sup>-1</sup> FTY720 not only differed significantly from tone in time-matched vehicle control experiments in the presence of L-NAME, but was also different from the tone seen with 1 μmol L<sup>-1</sup> FTY720 in indomethacin-containing solution (indomethacin-containing solution ± FTY720: 1.3% ± 1.4%, n = 11). This second difference was not observed at higher concentrations of FTY720. Furthermore, the second K<sup>+</sup>-induced contraction was increased with NOS inhibition (L-NAME<sub>K50</sub>: 190.6% ± 48.4%, n = 9, *P* < .05). High-K<sup>+</sup> contractions in L-NAME-containing solution did, however, not differ between

experiments with and without FTY720 (L-NAME ± FTY720<sub>K50</sub>: 131.8% ± 28.8%, n = 6; L-NAME ± ddH<sub>2</sub>O<sub>K50</sub>: 190.6% ± 48.4%, n = 9, *P* = .79).

### 3.4 | FTY720 effects under conditions of reduced extracellular [Ca<sup>2+</sup>]

After the first K<sup>+</sup>-induced contraction, the indomethacin-containing Krebs solution was changed to a modified, Ca<sup>2+</sup>-free Krebs solution containing indomethacin 10 μmol L<sup>-1</sup> and EGTA 1 mmol L<sup>-1</sup>. At least 2 washouts with this solution were done before continuing with the next experimental steps. Under these conditions, neither FTY720 nor vehicle increased tone ([FTY720] 10 μmol L<sup>-1</sup>: -0.1% ± 0.5%, n = 10; 100 μmol L<sup>-1</sup>: 0.03% ± 0.5%, n = 10; 0.4% ddH<sub>2</sub>O: 0.5% ± 0.3%, n = 7; 1.3% ddH<sub>2</sub>O: 0.2% ± 0.1%, n = 7).

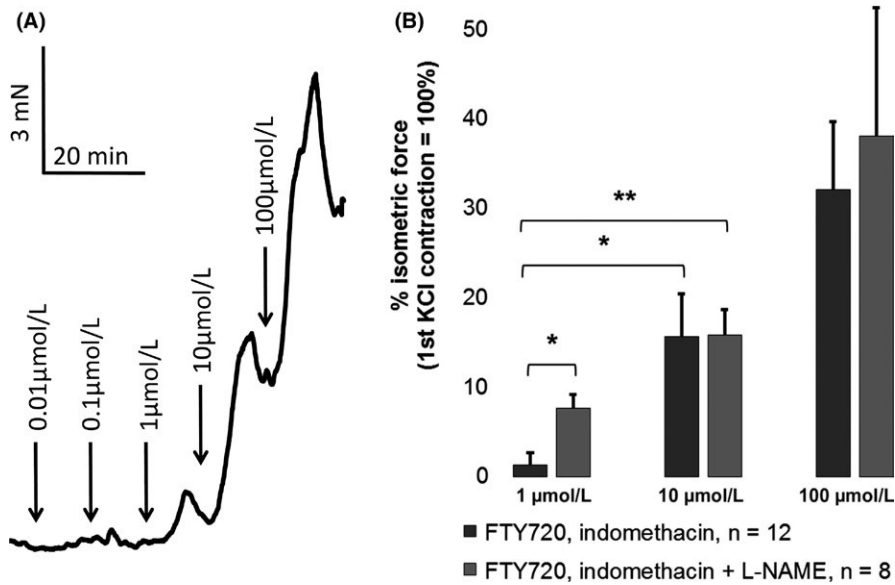


**FIGURE 5** The effect of FTY720 + L-NAME on the tone. A, Fundus circular smooth muscle strips in indomethacin-containing Krebs solution + 100  $\mu\text{mol L}^{-1}$  L-NAME were treated with increasing concentrations of FTY720. A representative contractile force is shown. B, Fundus circular smooth muscle strips in indomethacin-containing Krebs solution and indomethacin-containing Krebs solution + 100  $\mu\text{mol L}^{-1}$  L-NAME were treated with 10 and 100  $\mu\text{mol L}^{-1}$  FTY720. The maximal isometric force is expressed as the ratio of the first  $\text{K}^+$ -induced contraction

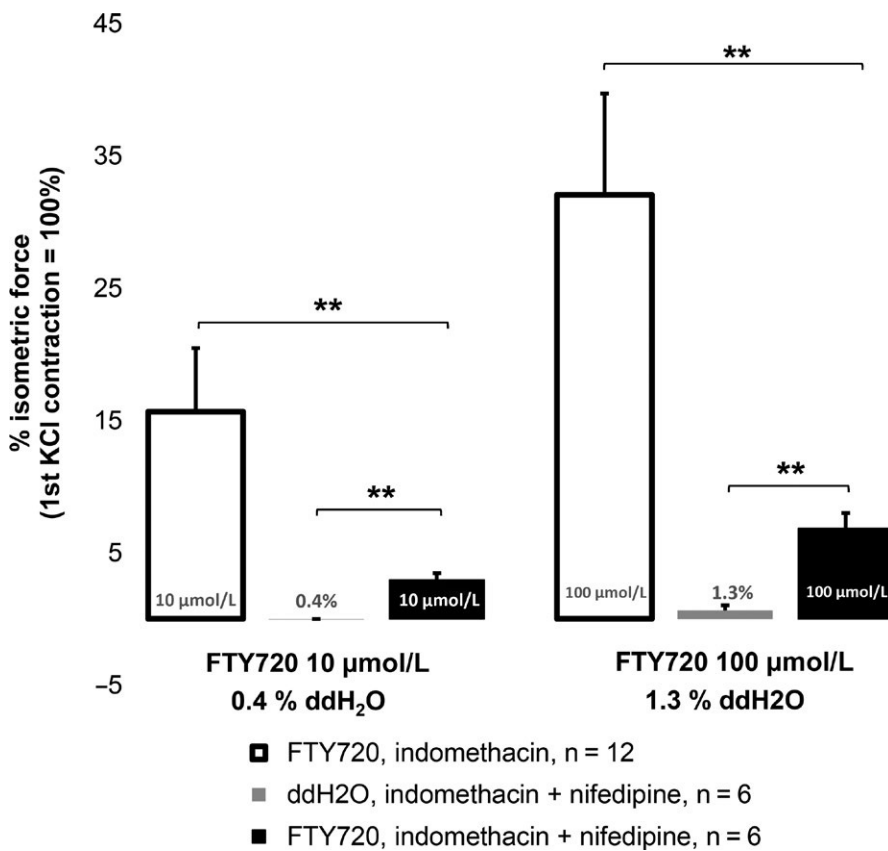


**FIGURE 6** The effect of FTY720 + nifedipine on tone. Fundus circular smooth muscle strips in indomethacin-containing Krebs solution pretreated with [nifedipine] 0.1  $\mu\text{mol L}^{-1}$  were treated with [FTY720] 10 and 100  $\mu\text{mol L}^{-1}$  or vehicle (ddH<sub>2</sub>O)

Strips treated with FTY720 and samples exposed to vehicle showed a weak contraction after KCl application in  $\text{Ca}^{2+}$ -free solution (FTY720<sub>K50</sub>: 2.3%  $\pm$  0.5%, n = 10,  $P = .526$  and ddH<sub>2</sub>O<sub>K50</sub>: 3.8%  $\pm$  2.5%, n = 7).

### 3.5 | FTY720 effects under conditions of L-type $\text{Ca}^{2+}$ channel inhibition

The inhibition of L-type  $\text{Ca}^{2+}$  channels by nifedipine (0.1  $\mu\text{mol L}^{-1}$ ) markedly reduced the FTY720 induced increase in tone (Figure 6)

and abolished high- $\text{K}^+$ -induced contractions (Figure 7). After application of FTY720, tone increased significantly compared with time-matched vehicle controls ([FTY720]10  $\mu\text{mol L}^{-1}$ : 3%  $\pm$  0.5%, n = 6; 0.4% ddH<sub>2</sub>O: -0.1%  $\pm$  0.05%,  $P < .01$ , n = 6; [FTY720] 100  $\mu\text{mol L}^{-1}$ : 6.8%  $\pm$  1.2%, 1.3% ddH<sub>2</sub>O: 0.7%  $\pm$  0.4%,  $P < .01$ , n = 6). This increase was, however, significantly less than that observed in samples not treated with nifedipine ( $P < .01$ , Figure 6).

Although there was no  $\text{K}^+$ -induced contraction in samples exposed to vehicle with nifedipine, samples treated with

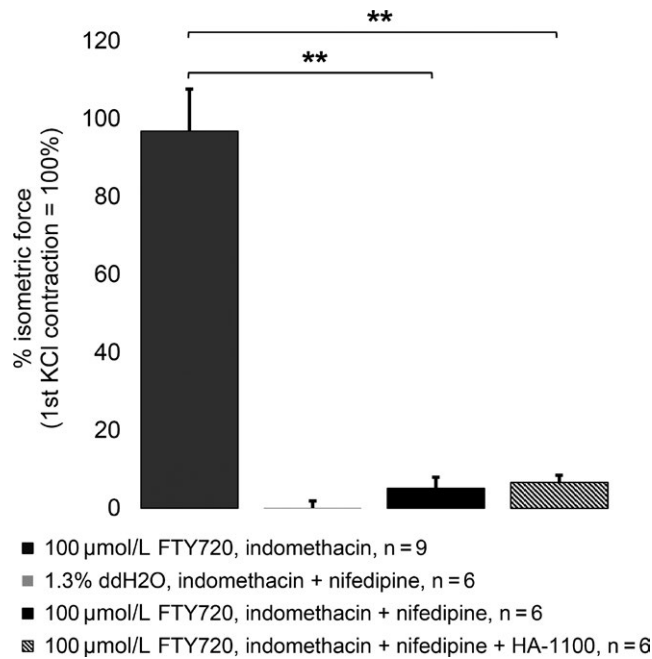


**FIGURE 7** The effect of FTY720+ nifedipine on  $K^+$ -induced contraction. Fundus circular smooth muscle strips in indomethacin-containing Krebs solution and indomethacin-containing Krebs solution +  $0.1 \mu\text{mol L}^{-1}$  nifedipine were treated with  $100 \mu\text{mol L}^{-1}$  FTY720 or 1.3% ddH<sub>2</sub>O followed by the addition of  $50 \text{mmol L}^{-1}$  KCl. Further combined experiments with  $0.1 \mu\text{mol L}^{-1}$  nifedipine +  $10 \mu\text{mol L}^{-1}$  HA-1100 were realized

FTY720 under the same conditions showed a small contraction after KCl application (FTY720<sub>K50</sub>  $5.1\% \pm 2.9\%$ ,  $n = 6$ ,  $P = .167$ , Figure 7).

### 3.6 | FTY720 effects in the presence of sphingosine receptor antagonists

To verify the specificity of effects evoked by high concentrations of FTY720, we tested for interactions with the S1PR antagonists JTE-013 (S1PR<sub>2</sub>) and suramin (S1PR<sub>3</sub>). Suramin ( $10 \mu\text{mol L}^{-1}$ ) itself did not affect tone, whereas  $1 \mu\text{mol L}^{-1}$  JTE-013 led to a slight, non-significant decrease in tone when added to indomethacin-containing Krebs solution. With both blockers, only a small increase in tone could still be observed after FTY720 application (JTE-013 + FTY720  $10 \mu\text{mol L}^{-1}$ :  $1.6\% \pm 0.3\%$ ,  $n = 6$  and  $100 \mu\text{mol L}^{-1}$ :  $5.9\% \pm 1.2\%$ ,  $n = 6$ ; suramin + FTY720  $10 \mu\text{mol L}^{-1}$ :  $4.3\% \pm 0.7\%$ ,  $n = 12$  and  $100 \mu\text{mol L}^{-1}$ :  $9.2\% \pm 1.7\%$ ,  $n = 12$ ,  $P < .05$  for each; Figure 8A). The amplitudes of high- $K^+$ -induced contractions did not differ between experiments with FTY720 and S1PR antagonists (FTY720 + JTE-013<sub>K50</sub>:  $78.9\% \pm 5.5\%$ ,  $n = 6$  and FTY720 + suramin<sub>K50</sub>:  $75.4\% \pm 5.3\%$ ,  $n = 12$ ) and those obtained with FTY720 in indomethacin-containing Krebs solution without S1PR antagonists.

### 3.7 | FTY720 effects in the presence of ROK inhibitors

The inhibition of ROK by HA-1100 led to a decrease in tone of fundus circular smooth muscle strips (Figure 8B). No significant effect of HA1100 on the  $K^+$ -induced contraction was observed in indomethacin-containing Krebs solution. The contractile effect of FTY720 was nearly nullified after preincubation with  $10 \mu\text{mol L}^{-1}$  HA-1100. There was no significant difference between the data of FTY720 ( $10 \mu\text{mol L}^{-1}$ :  $3.1\% \pm 1.8\%$ ,  $n = 6$ ,  $P = .509$  and  $100 \mu\text{mol L}^{-1}$ :  $3.8\% \pm 1.2\%$ ,  $n = 6$ ,  $P = .369$ ) and the data of samples exposed to vehicle ( $0.4\% \text{ ddH}_2\text{O}$ :  $1.8\% \pm 0.8\%$ ,  $n = 9$  and  $1.3\% \text{ ddH}_2\text{O}$ :

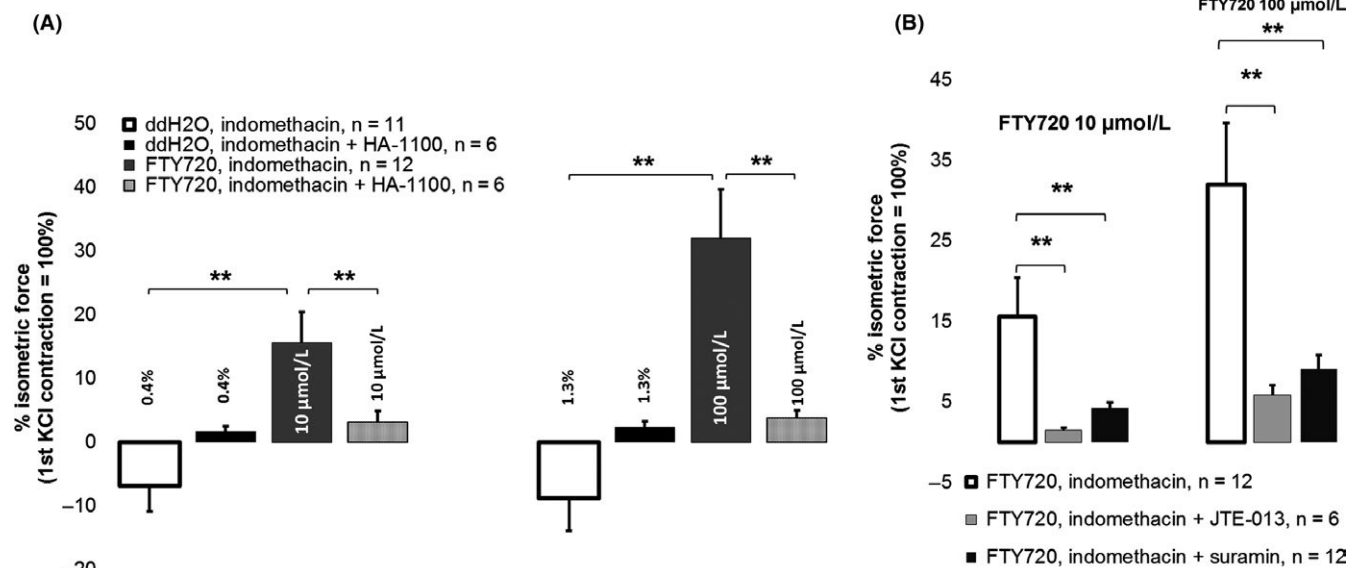


**FIGURE 8** A, The effect of FTY720 + sphingosine receptor antagonists on tone. Fundus circular smooth muscle strips in indomethacin-containing Krebs solution pretreated with [JTE-013]  $1 \mu\text{mol L}^{-1}$  or [suramin]  $10 \mu\text{mol L}^{-1}$  were treated with [FTY720] 10 and  $100 \mu\text{mol L}^{-1}$  or vehicle (ddH<sub>2</sub>O). B, The effect of FTY720 + HA-1100 on tone. Fundus circular smooth muscle strips in indomethacin-containing Krebs solution without HA-1100 and pretreated with [HA-1100]  $10 \mu\text{mol L}^{-1}$  were treated with [FTY720] 10 and  $100 \mu\text{mol L}^{-1}$  or vehicle (ddH<sub>2</sub>O)

2.4% ± 1.0%, n = 6). The pro-contractile effect of FTY720 on the second high-K<sup>+</sup>-induced contraction was not only blunted, it was even inverted by HA-1100: With FTY720 and HA-1100, the second high-K<sup>+</sup> contraction reached only half of the first K<sup>+</sup>-induced contraction (39.6% ± 8.3%, n = 6), which was significantly different from the reaction of samples treated with FTY720 and vehicle in indomethacin-containing Krebs solution without HA-1100 (74.8% ± 7.4%, n = 6, *P* < .05).

## 4 | DISCUSSION

This study gives evidence that the immune modulator FTY720 increases tone and depolarization-induced contractions of fundus circular smooth muscle strips. These results are in line with the finding that FTY720 causes an increase in intestinal motility and shortened transit times *in vivo* in a mouse model of Parkinson's disease.<sup>22</sup> They suggest that direct effects on smooth muscle may underlie the gastrointestinal side effects occurring with FTY720 in MS treatment.<sup>6</sup>

To our knowledge, the mechanism underlying the pro-contractile effects in native preparations of gastrointestinal smooth muscle has not been studied yet. For arterial vessels, it has been shown that FTY720, its metabolite FTY720-P, and its endogenous analog S1P interfere with the endothelial synthesis of prostaglandins and NO.<sup>12,16</sup> From experiments using cultured intestinal smooth muscle cells, Dragusin et al. concluded that S1P causes the contractions on intestinal smooth muscle cells in an equal manner as in the vascular system, that is, by enhancing COX activity and expression.<sup>23</sup> In fundus circular smooth muscle, inhibition of COX with indomethacin has previously been shown to reduce tone, indicating that constitutive prostaglandin release has a pro-contractile net effect.<sup>24,25</sup> Our finding that responses to high-K<sup>+</sup> were reduced in the presence of indomethacin is in line with these previous reports (Figure 3B).

In contrast to the findings in vascular smooth muscle, the FTY720 induced increase in fundus muscle tone was still observable after COX inhibition. In fact, the effect was even stronger when compared with experiments without indomethacin. Furthermore, with COX inhibition, high-K<sup>+</sup>-induced contractions were significantly enhanced by FTY720. Apparently, constitutively released prostaglandins inhibit FTY720-induced contractions, since the FTY720 effect is enhanced after inhibiting prostaglandin synthesis. In addition, FTY720 increases tone already at lower concentrations when COX is inhibited. This increased sensitivity of smooth muscle to FTY720 may be relevant in patients on FTY720 taking COX-inhibiting drugs for antithrombotic or analgesic treatment, since these could augment the gastrointestinal side effects of FTY720.

The most likely reason why our results on the role of COX and prostaglandins in mediating reactions of gastric tissue to FTY720 differ from those reported on cultured smooth muscle cells seems to be that cell culture models fail to reproduce the complexity of different cell types and their interactions which is characteristic for native intestinal smooth muscle.

This fact is also relevant when studying interactions between FTY720 and NO signaling. Our results corroborate previous reports that NO is continuously released by the enteric nitrergic neurons of the rat fundus,<sup>26</sup> since an inhibition of NO synthesis by L-NAME leads to an increase in tone and enhanced high-K<sup>+</sup>-induced contractions. If FTY720 interfered with constitutive NO synthesis, this would offer an explanation for its pro-contractile effects. We tested this by blocking NO synthesis with L-NAME and found no reduction of FTY720 effects. This virtually excludes that the tone increasing effects of FTY720 are mediated by reducing NO production. The fact that even lower concentrations (1 μmol L<sup>-1</sup>) of FTY720 produced effects when NO synthesis was blocked can be attributed to L-NAME inhibiting constitutive NO release.

To elucidate the downstream signaling pathways mediating the contractile actions of FTY720, we studied the importance of Ca<sup>2+</sup> influx and the Ca<sup>2+</sup>-sensitization through the ROK/Rho pathway for FTY720. In vascular smooth muscle, S1P-induced contractions have been reported to be highly dependent on extracellular Ca<sup>2+</sup> concentration.<sup>27</sup> Our results corroborate this dependence for FTY720 induced contractions of fundus smooth muscle. Furthermore, we assessed the contribution of Ca<sup>2+</sup> influx via voltage operated L-type Ca<sup>2+</sup> channels (VOCC) and found that FTY720 induced contractions were significantly reduced by the specific VOCC-blocker nifedipine. These findings are in line with data on the principal effects of nifedipine in gastric fundus and on its inhibition of S1P and FTY720-P mediated effects in detrusor muscle.<sup>28,29</sup>

The fact that FTY720 induced contractions are to a large part mediated by opening of VOCC implies that FTY720 leads to a depolarization of membrane potential. This may occur via potassium channel inhibition as it has been demonstrated to occur in fundus smooth muscle cells stimulated with acetylcholine or in vascular smooth muscle by S1P.<sup>30,31</sup> Besides changing intracellular calcium levels by promoting calcium influx, FTY720 increases Ca<sup>2+</sup> sensitivity via the RhoA/ROK signaling pathway: inhibition of ROK with HA-1100 lead to a decrease in the observed FTY720 effect on the tone of fundus circular smooth muscle. The interpretation of this result is, however, puzzling, since the effect of FTY720 is not just reduced but clearly reversed by HA-1100, a phenomenon that may reflect non-RhoA/ROK-specific kinase inhibiting effects.

According to data from the literature, S1P acts through a dual pathway involving both Ca<sup>2+</sup> influx and Ca<sup>2+</sup> sensitization.<sup>11,19,23</sup> Zhou and Murthy reported that S1P induced contractions in isolated muscle cells were mediated through the RhoA/ROK signaling pathway. In addition, they could show that this pathway involves the activation of S1PR.<sup>17</sup> It is established that FTY720 and its metabolite FTY720-P are potent agonists of S1P receptors as well.<sup>10</sup> The affinity to S1PR<sub>2</sub> receptor is controversial. Although Brinkmann et al. excluded, based on sphingosine kinase assays, FTY720 and FTY720-P as agonists of S1PR<sub>2</sub>, Sobel et al. assumed an interaction between FTY720 and S1PR<sub>2</sub>.<sup>10,32</sup> Our results suggest that the FTY720-induced effect on the tone is partly mediated through S1PR<sub>2</sub> interactions, since blocking S1PR<sub>2</sub> receptor leads to an 80% inhibition of the FTY720-induced increase in tone.

Another receptor subtype that is considered to be highly relevant in S1P-mediated vasoconstriction is S1PR<sub>3</sub>.<sup>33</sup> We used the S1P<sub>3</sub> inhibitor suramin to investigate the relevance of S1PR<sub>3</sub> for the contraction of fundus smooth muscle cells. By blocking S1PR<sub>3</sub>, results similar to those of S1PR<sub>2</sub> inhibition could be observed. In conclusion, both receptors seem to be involved in mediating the FTY720 on fundus smooth muscle tone. Neither S1PR<sub>2</sub> nor S1PR<sub>3</sub> are involved in the effects of FTY720 on the high-K<sup>+</sup>-induced contraction.

From the reported data, the question remains whether FTY720 itself or FTY720-P causes the observed effects. From receptor-affinity studies, it is known that FTY720-P activates S1PR<sub>1,3,4,5</sub> with EC<sub>50</sub> values in the nanomolar range<sup>10,34</sup>). In contrast, the affinity of non-phosphorylated FTY720 to S1PR is low (S1PR<sub>1,5</sub>) or seems to be lacking at all (S1PR<sub>2,3</sub>).<sup>34</sup> A direct S1PR<sub>2,3</sub> activation by non-phosphorylated FTY720, therefore, seems rather unlikely. Considering that FTY720-P as the active compound, the time required for SPK<sub>2</sub>-catalyzed phosphorylation of FTY720 would explain the delay in effect onset observed in the present study. Although the activity of SPK<sub>2</sub> in rodent intestine has been reported to be low, it is known to have a steep concentration dependency in the micromolar range (K<sub>m</sub> = 24.1 μmol L<sup>-1</sup> according to Billich et al.<sup>35</sup>). The concentration dependency of FTY720 effects observed in our experiments (Figure 3A) may, therefore, reflect the higher dynamics of FTY720-P formation rather than the direct concentration dependent binding of FTY720 to S1PR. The highest plasma concentrations of FTY720 that have been observed in vivo are in the nanomolar range with peak values occurring 8 hours after administration in mice and after 36 hours in humans.<sup>10,36,37</sup> In vivo, the phosphorylation of FTY720 occurs in parallel with the slow absorption and leads to plasma concentrations of FTY720-P that exceed those of FTY720 and are suitable for S1P receptor activation.<sup>10</sup> The rate of phosphorylation of FTY720 to active FTY720-P under the ex vivo conditions of our study is not known. It can rather be supposed that the observed effects are caused by FTY720-P that is synthesized by SPHK2, which would explain the delay in effect onset. Since the reported activity of SPHK2 in rodent intestine has been reported to be relatively low with a steep concentration dependency in the micromolar range (K<sub>m</sub> = 24.1 μmol L<sup>-1</sup> according to Billich et al.<sup>35</sup>), it is likely that the concentration dependency of FTY720 effects observed in our experiments reflects the higher dynamics of FTY720-P formation with subsequent receptor binding of FTY720-P rather than the direct concentration dependent effects of FTY720 on S1PR. Another consequence of the slow absorption of FTY720 is that after ingestion, its concentration within the lumen of the stomach and the intestine can be expected to be significantly higher than the peak concentrations measured later on in plasma after the drug has been diluted within the total body fluid volume.

Taken together, these considerations and the experimental results presented in this work show that FTY720 causes increases in gastric smooth muscle tone and contractility ex vivo. These effects may also underlie the gastrointestinal side effects observed

in patients. The fact that COX inhibition increases tissue sensitivity to FTY720 may rise special interest toward intestinal complications in patients taking non-steroidal anti-inflammatory drugs (NSAIDs) for symptomatic treatment of pain that is a very frequent albeit formerly underestimated symptom of MS.<sup>38</sup> Clearly, further studies are needed to clarify the active compound that is mediating the FTY720-induced contractions in this tissue.

## ACKNOWLEDGMENTS

We thank K. Porath, T. Sellmann, and A. Einsle for their technical assistance during the experimental process.

## DISCLOSURES

MK, TN and RP declare that they have no conflicts of interest related to this work. UKZ has received research grants from Genzyme and Novartis, while received speaker honoraria from Almirall, Byer, Biogen Idec, Genzyme, Merck & Co, Roche, Genzyme, and Teva.

## AUTHOR CONTRIBUTION

RP, UKZ, TN, and MK designed the research study; MK and DB performed the experiments; MK and RP analyzed and interpreted the data and wrote the manuscript; TN revised the manuscript.

## ORCID

R. Patejdl  <http://orcid.org/0000-0003-4587-4054>

## REFERENCES

- Binder BY, Williams PA, Silva EA, Leach JK. Lysophosphatidic acid and sphingosine-1-phosphate: a concise review of biological function and applications for tissue engineering. *Tissue Eng Part B Rev*. 2015;21:531-542.
- Levkau B. *Handbook of Experimental Pharmacology* (216). Cardiovascular effects of sphingosine-1-phosphate (S1P). Vienna: Springer; 2013:147-170.
- Garris CS, Blaho VA, Hla T, Han MH. Sphingosine-1-phosphate receptor 1 signalling in T cells: trafficking and beyond. *Immunology*. 2014;142:347-353.
- Rohrbach T, Maceyka M, Spiegel S. Sphingosine kinase and sphingosine-1-phosphate in liver pathobiology. *Crit Rev Biochem Mol Biol*. 2017;52:543-553.
- Sartawi Z, Schipani E, Ryan KB, Waeber C. Sphingosine 1-phosphate (S1P) signalling: role in bone biology and potential therapeutic target for bone repair. *Pharmacol Res*. 2017;125(Pt B):232-245.
- Calabresi PA, Radue E-W, Goodin D, et al. Safety and efficacy of fingolimod in patients with relapsing-remitting multiple sclerosis (FREEDOMS II): a double-blind, randomised, placebo-controlled, phase 3 trial. *Lancet Neurol*. 2014;13:545-556.
- Pitman MR, Woodcock JM, Lopez AF, Pitson SM. Molecular targets of FTY720 (fingolimod). *Curr Mol Med*. 2012;12:1207-1219.
- Payne SG, Oskeritzian CA, Griffiths R, et al. The immunosuppressant drug FTY720 inhibits cytosolic phospholipase A2 independently of sphingosine-1-phosphate receptors. *Blood*. 2007;109:1077-1085.

9. Paugh SW, Cassidy MP, He H, et al. Sphingosine and its analog, the immunosuppressant 2-amino-2-(2-4-octylphenylethyl)-1,3-propanediol, interact with the CB1 cannabinoid receptor. *Mol Pharmacol*. 2006;70:41-50.
10. Brinkmann V, Davis MD, Heise CE, et al. The immune modulator FTY720 targets sphingosine 1-phosphate receptors. *J Biol Chem*. 2002;277:21453-21457.
11. Watterson KR, Ratz PH, Spiegel S. The role of sphingosine-1-phosphate in smooth muscle contraction. *Cell Signal*. 2005;17:289-298.
12. Spijkers LJA, Alewijnse AE, Peters SLM. FTY720 (fingolimod) increases vascular tone and blood pressure in spontaneously hypertensive rats via inhibition of sphingosine kinase. *Br J Pharmacol*. 2012;166:1411-1418.
13. Guan Z, Singletary ST, Cook AK, Hobbs JL, Pollock JS, Inscho EW. Sphingosine-1-phosphate evokes unique segment-specific vasoconstriction of the renal microvasculature. *J Am Soc Nephrol*. 2014;25:1774-1785.
14. Fujii K, Machida T, Iizuka K, Hirafuji M. Sphingosine 1-phosphate increases an intracellular Ca(2 + ) concentration via S1P3 receptor in cultured vascular smooth muscle cells. *J Pharm Pharmacol*. 2014;66:802-810.
15. Hui S, Levy AS, Slack DL, et al. Sphingosine-1-phosphate signaling regulates myogenic responsiveness in human resistance arteries. *PLoS ONE*. 2015;10:e0138142.
16. Machida T, Matamura R, Iizuka K, Hirafuji M. Cellular function and signaling pathways of vascular smooth muscle cells modulated by sphingosine 1-phosphate. *J Pharmacol Sci*. 2016;132:211-217.
17. Zhou H, Murthy KS. Distinctive G protein-dependent signaling in smooth muscle by sphingosine 1-phosphate receptors S1P1 and S1P2. *Am J Physiol Cell Physiol*. 2004;286:C1130-C1138.
18. Song HJ, Choi TS, Chung FY, et al. Sphingosine 1-phosphate-induced signal transduction in cat esophagus smooth muscle cells. *Mol Cells*. 2006;21:42-51.
19. Kim YD, Han KT, Lee J, et al. Effects of sphingosine-1-phosphate on pacemaker activity of interstitial cells of Cajal from mouse small intestine. *Mol Cells*. 2013;35:79-86.
20. Nam JH, Kim WK, Kim BJ. Sphingosine and FTY720 modulate pacemaker activity in interstitial cells of Cajal from mouse small intestine. *Mol Cells*. 2013;36:235-244.
21. Huizinga JD. Gastrointestinal peristalsis: joint action of enteric nerves, smooth muscle, and interstitial cells of Cajal. *Microsc Res Tech*. 1999;47:239-247.
22. Vidal-Martínez G, Vargas-Medrano J, Gil-Tommee C, et al. FTY720/Fingolimod reduces synucleinopathy and improves gut motility in A53T mice: contributions of Pro-Brain-Derived Neurotrophic Factor (PRO-BDNF) and mature BDNF. *J Biol Chem*. 2016;291:20811-20821.
23. Dragusin M, Wehner S, Kelly S, et al. Effects of sphingosine-1-phosphate and ceramide-1-phosphate on rat intestinal smooth muscle cells: implications for postoperative ileus. *FASEB J*. 2006;20:1930-1932.
24. Milenov K, Golenhofen K. Contractile responses of longitudinal and circular smooth muscle of the canine stomach to prostaglandins E and F2alpha. *Prostaglandins Leukot Med*. 1982;8:287-300.
25. Porcher C, Horowitz B, Bayguinov O, Ward SM, Sanders KM. Constitutive expression and function of cyclooxygenase-2 in murine gastric muscles. *Gastroenterology*. 2002;122:1442-1454.
26. Curro D, Volpe AR, Preziosi P. Nitric oxide synthase activity and non-adrenergic non-cholinergic relaxation in the rat gastric fundus. *Br J Pharmacol*. 1996;117:717-723.
27. Bischoff A, Finger J, Michel MC. Nifedipine inhibits sphingosine-1-phosphate-induced renovascular contraction in vitro and in vivo. *Naunyn-Schmiedeberg's Arch Pharmacol*. 2001;364:179-182.
28. Watterson KR, Berg KM, Kapitonov D, et al. Sphingosine-1-phosphate and the immunosuppressant, FTY720-phosphate, regulate detrusor muscle tone. *FASEB J*. 2007;21:2818-2828.
29. Deitmer P, Golenhofen K, Noack T. Inhibitory effects of cicletanine on smooth muscle in comparison to those of nifedipine and sodium nitroprusside. *Naunyn-Schmiedeberg's Arch Pharmacol*. 1993;348:411-416.
30. Coussin F, Scott RH, Wise A, Nixon GF. Comparison of sphingosine 1-phosphate-induced intracellular signaling pathways in vascular smooth muscles: differential role in vasoconstriction. *Circ Res*. 2002;91:151-157.
31. Lammell E, Deitmer P, Noack T. Suppression of steady membrane currents by acetylcholine in single smooth muscle cells of the guinea-pig gastric fundus. *J Physiol*. 1991;432:259-282.
32. Sobel K, Monnier L, Menyhart K, et al. FTY720 phosphate activates sphingosine-1-phosphate receptor 2 and selectively couples to Gα12/13/Rho/ROCK to induce myofibroblast contraction. *Mol Pharmacol*. 2015;87:916-927.
33. Murakami A, Takasugi H, Ohnuma S, et al. Sphingosine 1-phosphate (S1P) regulates vascular contraction via S1P3 receptor: investigation based on a new S1P3 receptor antagonist. *Mol Pharmacol*. 2010;77:704-713.
34. Mandala S, Hajdu R, Bergstrom J, et al. Alteration of lymphocyte trafficking by sphingosine-1-phosphate receptor agonists. *Science*. 2002;296:346-349.
35. Billich A, Bornancin F, Devay P, Mechtcheriakova D, Urtz N, Baumruker T. Phosphorylation of the immunomodulatory drug FTY720 by sphingosine kinases. *J Biol Chem*. 2003;278:47408-47415.
36. Kovarik JM, Hartmann S, Bartlett M, et al. Oral-intravenous crossover study of fingolimod pharmacokinetics, lymphocyte responses and cardiac effects. *Biopharm Drug Dispos*. 2007;28:97-104.
37. Zollinger M, Gschwind H-P, Jin Y, Sayer C, Zécri F, Hartmann S. Absorption and disposition of the sphingosine 1-phosphate receptor modulator fingolimod (FTY720) in healthy volunteers: a case of xenobiotic biotransformation following endogenous metabolic pathways. *Drug Metab Dispos*. 2011;39:199-207.
38. Skierlo S, Rommer PS, Zettl UK. Symptomatic treatment in multiple sclerosis-interim analysis of a nationwide registry. *Acta Neurol Scand*. 2017;135:394-399.

**How to cite this article:** Kraft M, Zettl UK, Noack T, Patejdl R.

The sphingosine analog fingolimod (FTY720) enhances tone and contractility of rat gastric fundus smooth muscle.

*Neurogastroenterol Motil*. 2018;30:e13372. <https://doi.org/10.1111/nmo.13372>



## Clinical nutrition and gastrointestinal dysfunction in critically ill stroke patients

Robert Patejdl, Matthias Kästner, Stephan Kolbaske & Matthias Wittstock

To cite this article: Robert Patejdl, Matthias Kästner, Stephan Kolbaske & Matthias Wittstock (2017) Clinical nutrition and gastrointestinal dysfunction in critically ill stroke patients, Neurological Research, 39:11, 959-964, DOI: [10.1080/01616412.2017.1367545](https://doi.org/10.1080/01616412.2017.1367545)

To link to this article: <https://doi.org/10.1080/01616412.2017.1367545>



Published online: 22 Aug 2017.



Submit your article to this journal [↗](#)



Article views: 72



View related articles [↗](#)



View Crossmark data [↗](#)



## Clinical nutrition and gastrointestinal dysfunction in critically ill stroke patients

Robert Patejdl<sup>a</sup> , Matthias Kästner<sup>b</sup>, Stephan Kolbaske<sup>b</sup> and Matthias Wittstock<sup>b</sup>

<sup>a</sup>Department of Physiology, University of Rostock, Rostock, Germany; <sup>b</sup>Department of Neurology, University of Rostock, Rostock, Germany

### ABSTRACT

**Background:** Data on the epidemiology and risk factors of altered gastrointestinal motility (AGIM) is virtually lacking for patients suffering from non-traumatic neurologic diseases and stroke. This study investigated whether patterns of AGIM differ between patients with stroke and other severe acute brain diseases.

**Methods:** Clinical records of stroke and non-stroke patients treated at a neurological intensive care unit (ICU) were reviewed at day 1–5 and at day 10 after admission. The data was analyzed for the course of enteral/parenteral nutrition and for and for signs and symptoms of gastrointestinal dysfunction. The study included data of 76 patients, 57 with stroke (stroke group, SG) and 19 with other neurological diseases (non-stroke group, NSG).

**Results:** Basic demographic as well as clinical baseline characteristics and alimentation regime were similar in both groups. At least one sign of AGIM was seen in 33/57 (58%) SG and in 15/19 (79%) NSG patients ( $P = 0.099$ ). Regurgitation was significantly more frequent among patients from the NSG ( $P < 0.05$ ). Subjects from the NSG also spent a higher proportion of time with at least one symptom of AGIM present ( $P < 0.05$ ).

**Conclusions:** For the first time, this study investigated the prevalence of AGIM in patients suffering from severe stroke. The prevalence of disturbed gastrointestinal function was found to be high in stroke patients, but was lower than in a group of non-stroke patients with similar general disease severity and baseline characteristics.

### ARTICLE HISTORY

Received 21 December 2016  
Accepted 9 August 2017

### KEYWORDS

Stroke management;  
neurocritical care; nutrition;  
gastrointestinal motility

### Introduction

Difficulties in establishing, maintaining, and expanding enteral nutrition in critically ill patients are associated with numerous medical and surgical complications, a prolonged stay at the intensive care unit (ICU), a delay in the onset of effective rehabilitation, and increased costs [1–3].

It is known that a wide variety of pathophysiological mechanisms contribute to clinical problems in enteral nutrition during critical illness (e.g. medications used for analgesia, sedation, or antibiotic therapy [4,5], blood glucose [6], or preexisting diabetes [7], for reviews, see [8–10]). Furthermore, nutrients and liquids administered at inadequate and unnecessarily high quantities may per se contribute to the development of feeding intolerance and other complications [11]. In stroke as in any other underlying neurologic disease, alterations of the autonomic and enteric nervous system or of central nervous system structures add to the number of possible causative mechanisms of gastrointestinal impairment (GII) [12–16].

Despite the generally accepted relevance of nutritional matters in daily clinical routine for virtually all patients suffering from critical illness, only few studies

have investigated non-surgical and non-trauma patients and, to the authors' best knowledge, except for one single case report, there is no study that has assessed the complications of specific feeding strategies with special regard to stroke patients [13]. The purpose of this study was to assess the clinical epidemiology and risk factors of gastrointestinal disturbances within a sample of patients from a non-surgical neuro-ICU.

### Methods

#### Study population

The study retrospectively reviewed clinical records of the intensive care unit at the Department of Neurology, University of Rostock, between November 2013 and March 2015. The database contained 80 patients who met main inclusion criterion of at least 14 days of continuous intensive care treatment within the stated period of time. Thorough revision revealed inconsistencies regarding the documentation of nutrition and medications in the clinical files of four patients that were thus excluded from further analysis. Of the remaining 76 patients, there were 19 subjects primarily suffering from other conditions than acute stroke. All of these patients

were included in this analysis and will subsequently be designated as the non-stroke group (NSG). Fifty-seven patients with an acute vascular event as their principal diagnosis were defined as the stroke group (SG).

### Data collection and analysis

SG included patients with ischemic and hemorrhagic stroke as well as subarachnoid hemorrhage. NSG included patients suffering from any other acute neurological conditions apart from stroke.

We collected the following information from the patients' files: gender, date of birth, duration of treatment, main diagnosis, Acute Physiology And Chronic Health Evaluation II (APACHE II), in case of stroke severity assessment according to the National Institute of Health Stroke Scale (NIHSS) at the time of admission, presence of polyneuropathy, diabetes mellitus, presence of SIRS or sepsis, and health outcome (discharge to home, to another hospital, rehabilitation, or death).

To reflect the occurrence and severity of symptoms related to altered gastrointestinal function, we defined a measure representing the *cumulative alteration of gastrointestinal motility* (CAGIM) as a numeric value. Signs and symptoms integrated in the CAGIM were nausea, nasogastric tube regurgitation (defined as backward flow of gastric contents greater than 50 ml/8 h via the nasogastric tube), vomiting, constipation (four subsequent days without defecation after admission), and application of a prokinetic substance (erythromycine, domperidone, metoclopramide). Whenever one of the stated conditions was met by a patient, one point was assigned and added to the previous number. Thus, the 'CAGIM' could take values ranging from 0 to 5. The symptom 'diarrhea' was not included in the score since the available data from patient records did not allow for an unequivocal identification of patients suffering from or being untroubled from diarrhea.

The daily amounts of formula intake, total enteral fluid intake, and total volume of intravenous infusions were gathered to capture potential group differences in the administered nutrition that may account for differences in motility disorders.

### Statistical analysis

The database construction and statistical analysis were performed with LibreOffice Calc 3.6 (The Document Foundation, Berlin, Germany), MS Excel 2010 (Microsoft, Redmond, WA, U.S.A.), and SPSS 20 (IBM, Armonk, NY, U.S.A.). For quantitative data, statistical significance was analyzed with the independent two-sample *t*-test for equal variance, qualitative data were analyzed using the  $\chi^2$ -Test. Significance was set at  $P < 0.05$  for both tests. The power achieved by the statistical tests was calculated *post hoc* using G\*Power V3.1.9 (University of Dusseldorf, Germany).

### Ethics statement

This study was performed as a part of a research project concerning stroke and gastric motility disorders. The project was approved by the University Medicine Ethics Committee of the University of Rostock and assigned with the number A-2013-0025. Data are handled in accordance with national German law and the institutional standards of the University of Rostock.

## Results

### Study population

Patient demographics and basic clinical parameters of the whole sample, for the SG and NSG are given in Table 1. Both groups were comparable with respect to age, prevalence of diabetes mellitus, prevalence of systemic infection/inflammation, and general disease consciousness. Patients of the NSG had a significantly longer duration of their ICU stay and were dependent on mechanical ventilation over a longer proportion of time. NSG patients tended to have a slightly higher general disease severity as reflected by the APACHEII-score. Six of the stroke patients died during the further course of treatment, whereas four patients of the NSG deceased (10.5 vs. 21%,  $P = 0.24$ ).

Details about the diseases found in SG and NSG are given in Table 2. Thirty patients of the SG suffered from left, 6 from right hemispheric or bilateral lesions, 7 from bilateral pathology, and 12 from infratentorial ischemia or hemorrhage. The mean NIHSS of SG patients was

**Table 1.** Demographic and clinical characteristics of the whole patient sample, SG and NSG.

	SG + NSG (N = 76)	SG (N = 57)	NSG (N = 19)	P-value	Achieved power (1 - $\beta$ )
Female	33% (25)	28% (16)	47% (9)	0.121	0.62
Mean age, years (SD)	70.7 (11.5)	71.4 (11)	71.6 (12)	0.949	0.05
Mean duration of treatment, days (SD)	20.5 (7.8)	18.9 (5.8)	26.2 (10)	<b>0.0001</b>	0.95
% of days with mechanical ventilation within observation period	47%	39%	68%	<b>0.0001</b>	0.99
Diabetes mellitus	51% (39)	46% (26)	58% (11)	0.35	0.31
SIRS or Sepsis	62% (47)	60% (34)	58% (11)	0.141	0.99
Mean APACHE II (SD)	16.1 (7.5)	15.2 (7)	19.1 (8.4)	0.05	0.599
Mean GCS (SD)	9 (4.6)	9.5 (4.5)	7.9 (4.7)	0.176	0.37

Note: The *P*-value is given as a measure of clinical differences and similarities between SG and NSG.

**Table 2.** Distribution of stroke patterns and non-vascular diseases within the stroke group (SG) and non-stroke group (NSG).

Diagnosis
Stroke group (57)
• Ischemic (30)
▪ Hemispheric infarction (20)
• MCA (19)
○ right (2)
○ left (13)
○ mixed (4)
• PCA (1)
▪ Thalamic infarction (1)
▪ Brainstem Infarction (9)
• Hemorrhagic (27)
▪ Intracerebral, supratentorial (20)
• right (4)
• left (14)
• mixed (2)
▪ Intracerebral, infratentorial (3)
▪ Subarachnoid (4)
Non-stroke group (19)
• Status epilepticus (12)
• Hypoxic brain damage (2)
• AIDP (3)
• Meningoencephalitis (1)
• Epidural hematoma (1)

Note: MCA — middle cerebral artery, PCA — posterior cerebral artery, AIDP — acute inflammatory demyelinating polyneuropathy.

14.2 ± 9.7. Patients with hemorrhagic stroke had lower mean NIHSS values than those with ischemic stroke (NIHSS 10.6 ± 8.4 vs. 16.8 ± 10;  $P = 0.03$ ). No significant differences could be detected in NIHSS scores between left- and right-sided stroke or between supra- and infratentorial stroke.

### Gastrointestinal impairment

Signs and symptoms of impaired gastrointestinal functions indicated by an CAGIM greater than 0 at any time point were seen in 48 out of the 76 observed subjects (63%) and tended to be more frequent in non-stroke patients (Table 3, Figure 1).

The proportion of days within the observation period at which a CAGIM > 0 was observed was significantly higher in the NSG. In the NSG, the proportion of days with observed regurgitation in patients supplied with a

feeding tube or with vomiting in patients without a tube was significantly increased (Table 3).

There was a significant correlation between administration of opioid analgesics or noradrenaline and the occurrence of gastrointestinal dysfunction. On days with opioid administration, there was an increased probability for a CAGIM-score greater than zero within the total sample and the SG, but not the NSG (total sample: 49% with vs. 24% in patients without opioids, OR 2.03, 95%CI 1.30–3.20,  $P = 0.0017$ ; SG: 47% with vs. 21% in patients without opioids, OR 2.5, 95%CI 1.34–3.79,  $P = 0.0019$ ; NSG: 54% with vs. 50% in patients without opioids, OR 1.07, 95%CI 0.41–2.81,  $P = 0.88$ ). Feeding tube regurgitation was associated with opioid application in SG and the total sample (total: 27% with vs. 6.1% in patients without opioids, OR 4.4, 95%CI 1.29–15.23,  $P = 0.011$ ; SG: 22% with vs. 4.8% in patients without opioids; OR 4.6, 95%CI 1.01–20.83,  $P = 0.03$ ; NSG: 38% with vs. 3.1% in patients without opioids, OR 3.05, 95%CI 0.35–27.48,  $P = 0.29$ ). Patients receiving noradrenaline had an increased risk to develop any kind of GI-symptom, again in the SG and over the whole sample (total: 58% with vs. 27% without noradrenaline, OR 2.2, 95%CI 1.42–3.35,  $P = 0.0003$ ; SG: 57% with vs. 22% without noradrenaline, OR 2.2, 95%CI 1.52–4.35,  $P = 0.0004$ ; NSG: 59% with vs. 49% without noradrenaline, OR 1.22, 95%CI 0.56–2.64,  $P = 0.61$ ).

The prevalence of altered motility among patients was also correlated with blood glucose levels. In patients with at least one symptom, blood glucose levels were significantly increased when the whole sample and the SG were analyzed, whereas in the NSG, a trend without significance was seen (total sample: 11.2 ± 4.5 in patients with CAGIM > 0 vs. 8.9 ± 6.2 mmol/l in patients with CAGIM = 0,  $P < 0.001$ ; SG: 11.2 ± 4.4 in patients with CAGIM > 0 vs. 8.9 ± 6.2 mmol/l in patients with CAGIM = 0,  $P = 0.002$ ; NSG: 12 ± 4.8 in patients with CAGIM > 0 vs. 10.2 ± 6.9 mmol/l in patients with CAGIM = 0,  $P = 0.14$ ). Among the single parameters of dysmotility, blood glucose levels correlated significantly with the occurrence of regurgitation in the total sample, SG and NSG (total sample: 12.1 ± 5 in patients with vs. 9.2 ± 5.9 mmol/l in patients without regurgitation,  $P = 0.002$ ; SG: 12.1 ± 4.7 in patients

**Table 3.** Prevalence of clinical signs and symptoms of gastrointestinal impairment.

Symptom	SG	NSG	Odds ratio	95% confidence interval	P-value	Achieved power (1 – β)
CAGIM > 0	33/57 (58%)	15/19 (79%)	0.37	0.11–1.24	0.099	0.75
Patients with regurgitation at any time*	12/41 (29%)	11/18 (6%)	0.26	0.08–0.84	<b>0.021</b>	0.92
Days with CAGIM > 0	86/342 (25%)	40/114 (35%)	0.62	0.39–0.98	<b>0.039</b>	0.9
Days with regurgitation*	23/176 (13%)	23/86 (27%)	0.411	0.22–0.79	<b>0.006</b>	0.98
Days with nausea**	19/205 (9%)	2/37 (5%)	1.79	0.40–8.00	0.442	0.36
Days with vomiting***	23/166 (14%)	8/28 (29%)	0.40	0.16–1.02	<b>0.049</b>	0.95
Days on prokinetics	24/342 (7%)	13/114 (11%)	0.586	0.28–1.20	0.194	0.44
Patients with constipation****	17/57 (30%)	9/19 (47%)	0.472	0.16–1.37	0.163	0.56

Notes: \*Only for days at which the patient was supplied with a gastric or nasogastric feeding tube \*\* only for days without mechanical ventilation \*\*\* only for days at which patients were not supplied with a nasogastric or gastric tube \*\*\*\* only days one to five were considered since information on the tenth day does not allow for classification constipated/non-constipated. Odds ratio < 1 indicates lower probability of respective complication to occur in patients from stroke group (SG) compared to patients from the non-stroke group (NSG). CAGIM = Cumulative alteration of gastrointestinal motility, see methods section for details.

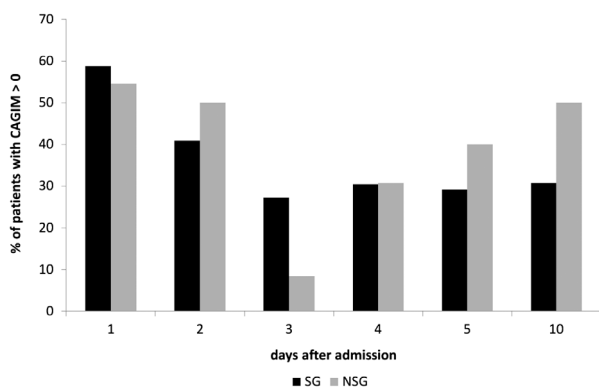


**Figure 1.** Time course of gastrointestinal impairment in patients that were unable to swallow. Cumulative alteration of gastrointestinal motility (CAGIM) was defined according to the symptoms of disturbed GI function as described in the section 'Gastrointestinal impairment' for patients of the stroke group (SG) and the non-stroke group (NSG).

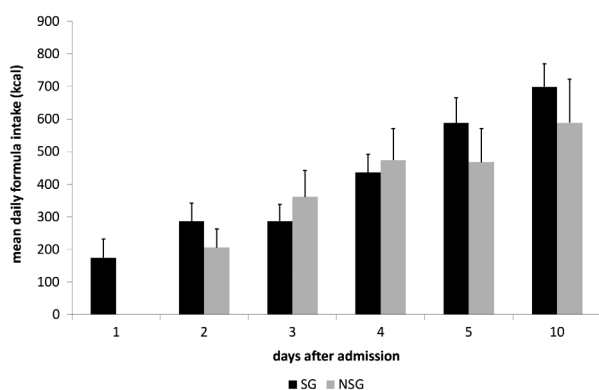


**Figure 2.** Differences in mean enteral formula intake within the observation period between patients of the stroke group (SG) and the non-stroke group (NSG). Only patients supplied with a feeding tube were included. Error bars depict standard error of mean.

with vs.  $9.3 \pm 5.9$  mmol/l in patients without regurgitation,  $P = 0.023$ ; NSG:  $13.4 \pm 5.4$  in patients with vs.  $10.2 \pm 6.45$  mmol/l in patients without regurgitation,  $P = 0.03$ ).

### Time course and characteristics of alimentation

Dysphagia and impaired consciousness in the context of severe neurological disorders were the relevant indications for enteral alimentation of patients via a gastric or nasogastric feeding tube in both groups. In all conscious patients, a swallowing test according to the Gugging Swallowing Screen protocol (GUSS) was conducted to decide whether a nasogastric tube was indicated or not [17]. When summing up the days observed within the relevant time period for all patients of both groups, it turned out that subjects from the NSG were clearly more dependent on alimentation via a feeding tube (75% vs. 51%,  $P < 0.0001$ ). Only days at which a patient of either group was supplied with a feeding tube were included in the analysis of differences of formula

intake between SG and NSG. Without this correction, formula intake of the NSG significantly outweighs that of the SG ( $307 \pm 414$  ml vs.  $219 \pm 365$  ml,  $P = 0.03$ ). After correcting for the feeding tube state of the single patients, the difference between both groups decreases and is not significant any more at any time point (Table 4 and Figure 2).

In line with this finding, both groups showed nearly identical ratios of the mean daily fluid delivered via the parenteral route and the sum of enterally and intravenously delivered fluid over the whole observation period. In patients with impaired oral food intake of whatever cause, the enteral energy delivery achieved at day 5 exceeded 1000 kcal in only one NSG and four SG patients (Table 4).

### Discussion

Our findings indicate that stroke patients do not have an increased risk of developing clinically relevant gastrointestinal motility impairment when compared to other critically ill patients with neurologic diseases.

Early enteral nutrition is generally recommended in intensive care patients with and without stroke and has been shown to reduce complications [1,18–23]. Patients included in our study received alimentation according to current guidelines with respect to overall energy, nutrient composition, and total fluid volume. Over the last years, some clinical studies found that very early enteral nutrition might not be advantageous in critically ill patients in general and also in comatose stroke patients [24–26]. On the basis of the evidence available at the time this study was conducted, enteral nutrition was started with low amounts of tea or water and formula added later on when patients did not show regurgitations, diarrhea, or severe shock.

Following the common definition (e.g. 'Feeding intolerance is present if at least 20 kcal/kg BW/day via enteral route cannot be reached within 72 h of feeding attempt' [27]), 'feeding intolerance' was thus a frequent condition within the study population irrespective of the underlying disease. This fact underlines the severity of illness and GI-dysfunction in both groups.

Despite the similarities between groups regarding severity of disease and applied alimentation, signs and symptoms differed between both groups within the early observation period between day 1 and 5, which were not detectable at day 10 anymore. Over the whole period, 57% of the stroke and 79% of the non-stroke patients suffered from at least one type of gastrointestinal symptom at least on one day (Table 3). Comparing the proportion of days with and without symptoms in both groups yielded a highly significant preponderance of GI-disturbances in the non-stroke group.

Besides the dependence on stroke or non-stroke, symptoms also correlated with parameters reflecting general disease severity and treatments with potential

**Table 4.** Characteristics of clinical nutrition for the study population.

	Stroke (N = 57)	Non-stroke (N = 19)	P-value	Achieved power (1 – $\beta$ )
<b>Nutrition</b>				
% of time with nasogastric tube (days)	51 (176/342)	75 (86/114)	<0.001	0.999
% of patients with feeding tube day 1	23 (13/57)	32 (6/19)	0.44	0.33
% of patients with feeding tube day 2	44 (25/57)	79 (15/19)	0.008	0.99
<b>Mean daily enteral*</b>				
Formula intake, all days *, ml (SD)	315 (404)	339 (414)	0.617	0.12
Formula intake day 1–5*, ml (SD)	329 (339)	345 (351)	0.750	0.09
Formula intake day 1+2*, ml (SD)	177 (240)	146 (208)	0.628	0.12
Formula intake day 3+4*, ml (SD)	311 (291)	416 (348)	0.123	0.44
Formula intake day 10*, ml (SD)	688 (530)	639 (575)	0.753	0.11
Water intake, all days *, ml (SD)	332 (256)	337 (233)	0.868	0.07
Total fluid intake, all days, ml (SD)	2415 (1509)	2605 (1421)	0.207	0.28
Energy intake, all days *, kcal (SD)	354 (420)	350 (413)	0.936	0.05
Energy intake day 5* kcal (SD)	588 (460)	476 (516)	0.407	0.16
Energy intake day 10*, kcal (SD)	716 (516)	661 (568)	0.715	0.16
<b>Mean daily intravenous</b>				
Volume intake, all days, ml (SD)	2291 (1223)	2546 (1168)	0.051	0.63
[%] of total energy intake, all days (SD)	67 (33)	73 (30)	0.071	0.62
[%] of total energy intake day 1+2 (SD)	75 (35)	81 (31)	0.346	0.26
[%] of total energy intake day 3+4 (SD)	69 (31)	74 (25)	0.382	0.18
[%] of total energy intake day 10 (SD)	52 (33)	58 (39)	0.553	0.15
<b>Mean [%] of enteral from total fluid intake</b>				
day 1–5 (SD)	26 (23)	24 (24)	0.492	0.44
day 1+2 (SD)	23 (23)	21 (24)	0.449	0.17
day 3+4 (SD)	24 (23)	23 (24)	0.934	0.07
day 10 (SD)	28 (21)	25 (22)	0.495	0.18
	36 (23)	34 (23)	0.817	0.10
<b>No. of patients reaching enteral energy delivery of at least 1000 kcal at</b>				
Day 5**	4/35	1/40	0.563	0.37
Day 10**	7/40	4/18	0.671	0.40

Notes: Values are given as the arithmetic mean of intake over the indicated time period. \*Only for patients supplied with a gastric or nasogastric feeding tube.

adverse effects on the intestine. For the whole study sample, noradrenaline application and elevated blood glucose were associated with an increased risk for feeding tube regurgitation. In addition, opioids increased the combined risk for developing any type of AGIM.

Limitations of this study include the rather small patient number, the heterogeneous disease severity in the SG when compared to the NSG as reflected by the higher proportion of patients receiving mechanical ventilation and complete gastric tube feeding in the latter as well as the strong preponderance of supratentorial strokes. The small sample size was addressed by choosing appropriate statistical measures, but made it impossible to detect small- and medium-sized effects as well as differences within subgroups of the SG regarding the lateralization, localization, and size of lesions. This aspect is of particular interest and should be addressed in future studies, since a growing body of evidence supports a role of localization for the development of autonomic dysfunction [12]. Nevertheless, despite the small sample size and the accordingly low-power, significant differences between stroke and non-stroke patients were detected.

Besides the finding that stroke patients in general seem to have no relevantly increased risk of developing AGIM when compared to other patients on the neurologic ICU, the practically most important result of this study addresses the time point on which stroke patients develop GI-disturbances. Our data indicate that this is

most frequently around the third day of hospitalization. Until day two, the incidence of AGIM is actually even lower than in patients suffering from other severe diseases. Monitoring of gastric function and — if indicated — prokinetic treatment and slowing down the rate of daily formula application should be considered around this time. Further systematic studies on the interrelation of early enteral alimentation and gastrointestinal disturbances are highly warranted to establish a fundamental for adequate feeding strategies and avoiding harm that may be caused by inadequate alimentation in the early phase of severe stroke.

### Geolocation information

The patients included in this study came from the city of Rostock and its surroundings in the federal state of Mecklenburg-Vorpommern.

### Disclosure statement

All authors declare that there are no conflicts of interest related to this work.

### ORCID

Robert Patejdl  <http://orcid.org/0000-0003-4587-4054>

## References

- [1] Cangelosi MJ, Auerbach HR, Cohen JT. A clinical and economic evaluation of enteral nutrition. *Curr Med Res Opin.* 2011;27:413–422. DOI:10.1185/03007995.2010.545816
- [2] Braga M, Gianotti L, Gentilini O, et al. Early postoperative enteral nutrition improves gut oxygenation and reduces costs compared with total parenteral nutrition. *Crit Care Med.* 2001;29:242–248.
- [3] Sand J, Luostarinen M, Matikainen M. Enteral or parenteral feeding after total gastrectomy: prospective randomised pilot study. *Eur J Surg = Acta Chir.* 1997;163:761–766.
- [4] Nguyen NQ, Chapman MJ, Fraser RJ, et al. The effects of sedation on gastric emptying and intra-gastric meal distribution in critical illness. *Intensive Care Med.* 2008;34:454–460. DOI:10.1007/s00134-007-0942-2
- [5] Nassar AP, Jr, da Silva FMQ, de Cleve R. Constipation in intensive care unit: incidence and risk factors. *J Crit Care.* 2009;24:630.e9–12. DOI:10.1016/j.jcrc.2009.03.007
- [6] Horowitz M, Edelbroek MA, Wishart JM, et al. Relationship between oral glucose tolerance and gastric emptying in normal healthy subjects. *Diabetologia.* 1993;36:857–862.
- [7] Samsom M, Bharucha A, Gerich JE, et al. Diabetes mellitus and gastric emptying: questions and issues in clinical practice. *Diabetes/Metab Res Rev.* 2009;25:502–514. DOI:10.1002/dmrr.974
- [8] Stupak DP, Abdelsayed GG, Soloway GN. Motility disorders of the upper gastrointestinal tract in the intensive care unit: pathophysiology and contemporary management. *J Clin Gastroenterol.* 2012;46:449–456. DOI:10.1097/MCG.0b013e31824e14c1
- [9] Aderinto-Adike AO, Quigley EMM. Gastrointestinal motility problems in critical care: a clinical perspective. *J Dig Dis.* 2014;15:335–344. DOI:10.1111/1751-2980.12147
- [10] Nguyen T, Frenette A-J, Johanson C, et al. Impaired gastrointestinal transit and its associated morbidity in the intensive care unit. *J Crit Care.* 2013;28:537.e11–7. DOI:10.1016/j.jcrc.2012.12.003
- [11] Reid C. Frequency of under- and overfeeding in mechanically ventilated ICU patients: causes and possible consequences. *J Human Nutr Diet Off J Br Diet Assoc.* 2006;19:13–22. DOI:10.1111/j.1365-277X.2006.00661.x
- [12] Walter U, Kolbaske S, Patejdl R, et al. Insular stroke is associated with acute sympathetic hyperactivation and immunodepression. *Eur J Neurol Off J Eur Fed Neurol Soc.* 2013;20:153–159. DOI:10.1111/j.1468-1331.2012.03818.x
- [13] Liff JM, Labovitz D, Robbins MS. Profound gastroparesis after bilateral posterior inferior cerebellar artery territory infarcts. *Clin Neurol Neurosurg.* 2012;114:789–791. DOI:10.1016/j.clineuro.2011.12.042
- [14] Levy JM, McGinness C, Jaffe BM. Megacolon, hypoganglionosis, and cerebrovascular disease. *J La State Med Soc Off Organ La State Med Soc.* 2010;162:92–95.
- [15] Camilleri M. Disorders of gastrointestinal motility in neurologic diseases. *Mayo Clinic Proc.* 1990;65:825–846.
- [16] Camilleri M, Bharucha AE. Gastrointestinal dysfunction in neurologic disease. *Semin Neurol.* 1996;16:203–216. DOI:10.1055/s-2008-1040977
- [17] Trapl M, Enderle P, Nowotny M, et al. Dysphagia bedside screening for acute-stroke patients: the gugging swallowing screen. *Stroke J Cereb Circ.* 2007;38:2948–2952. DOI:10.1161/STROKEAHA.107.483933
- [18] Wirth R, Smoliner C, Jager M, et al. Guideline clinical nutrition in patients with stroke. *Exp Transl Stroke Med.* 2013;5:14. DOI:10.1186/2040-7378-5-14
- [19] Perry L, McLaren S. Nutritional support in acute stroke: the impact of evidence-based guidelines. *Clin Nutr (Edinburgh, Scotl).* 2003;22:283–293.
- [20] McArthur KS, Quinn TJ, Dawson J, et al. Diagnosis and management of transient ischaemic attack and ischaemic stroke in the acute phase. *BMJ (Clin Res Ed).* 2011;342:d1938. DOI:10.1136/bmj.d1938
- [21] Swain S, Turner C, Tyrrell P, et al. Diagnosis and initial management of acute stroke and transient ischaemic attack: summary of NICE guidance. *BMJ (Clin Res Ed).* 2008;337:a786. DOI:10.1136/bmj.a786
- [22] Dhaliwal R, Cahill N, Lemieux M, et al. The Canadian critical care nutrition guidelines in 2013: an update on current recommendations and implementation strategies. *Nutr Clin Pract Off Publ Am Soc Parenter Enteral Nutr.* 2014;29:29–43. DOI:10.1177/0884533613510948
- [23] Gramlich L, Kichian K, Pinilla J, et al. Does enteral nutrition compared to parenteral nutrition result in better outcomes in critically ill adult patients? A systematic review of the literature. *Nutrition.* 2004;20:843–848. DOI:10.1016/j.nut.2004.06.003
- [24] Reintam Blaser A, Starkopf J, Alhazzani W, et al. Early enteral nutrition in critically ill patients: ESICM clinical practice guidelines. *Intensive Care Med.* 2017;43:380–398. DOI:10.1007/s00134-016-4665-0
- [25] Prosser-Loose EJ, Paterson PG. The FOOD trial collaboration: nutritional supplementation strategies and acute stroke outcome. *Nutr Rev.* 2006;64:289–294.
- [26] Yamada SM. Too early initiation of enteral nutrition is not nutritionally advantageous for comatose acute stroke patients. *J Nippon Med Sch = Nippon Ika Daigaku zasshi.* 2015;82:186–192. DOI:10.1272/jnms.82.186
- [27] Blaser AR, Starkopf J, Kirsimagi U, et al. Definition, prevalence, and outcome of feeding intolerance in intensive care: a systematic review and meta-analysis. *Acta Anaesthesiol Scand.* 2014;58:914–922. DOI:10.1111/aas.12302

BRIEF COMMUNICATION



# Relations Between Early Neuromuscular Alterations, Gastrointestinal Dysfunction, and Clinical Nutrition in Critically Ill Patients: An Exploratory Single-center Cohort Study

Felix Klawitter<sup>1</sup>, Johannes Ehler<sup>1</sup>, Daniel A. Reuter<sup>1</sup> and Robert Patejdl<sup>2\*</sup>

© 2020 The Author(s)

## Introduction

Several pathophysiological conditions are known to promote alterations of gastrointestinal (GI) motility and malnutrition in the critically ill [1]. Among these are lesions of the central, the autonomic, the enteric, and the somatic nervous system. Nevertheless, rather few studies have addressed the hypothetical interdependence between neurological and GI complications in the critically ill [2, 3].

Patients with critical illness neuromyopathy (CINM) are commonly exposed to risk factors of GI dysfunction [4]. We hypothesize that CINM and intensive care unit-acquired weakness (ICUAW) might be independent risk factors for GI dysmotility in critically ill patients.

## Methods

Data were derived from a current prospective observational study including patients  $\geq 18$  years with a sequential organ failure assessment (SOFA) score  $\geq 8$  on three consecutive days within the first five days after intensive care unit (ICU) admission by analyzing medical reports for parameters related to nutrition and GI function (ClinicalTrials.gov: NCT02706314, local ethics board identifier A 2016-0016). The study protocol is summarized in Fig. 1.

## Assessment of Early Critical Illness Neuromyopathy (eCINM) and Intensive Care Unit-acquired Weakness (ICUAW)

On study day 3 and 10, electroneurography (ENG) was performed by recording compound motor action potentials (CMAP) from the abductor digiti minimi (ADM) and the extensor digitorum brevis (EDB) muscles and sensory nerve action potentials (SNAP) from radial and sural nerves. A CINM-typical alteration was stated when CMAP amplitude was below 4 mV and SNAP amplitude was smaller than 7.5  $\mu$ V for the radial and 10  $\mu$ V for the sural nerve. When less than four of the recording sites gave amplitudes above the stated cutoff values, the patient was classified early CINM (eCINM) positive. ICUAW was diagnosed if the Medical Research Council sum score (MRCSS) was  $< 48$  points [5]. When MRCSS could not be assessed the ICUAW status was stated based upon neurological examination and second ENG (Fig. 1).

## Assessment of GI function and Clinical Nutrition

Over 14 days, we analyzed data on swallowing function assessed by a fiberoptic endoscopic swallowing evaluation (FEES), peroral nutrient supplementation, the extent of calories delivered via a feeding tube and the duration of feeding tube dependence, the gastric residual volume (GRV), and the frequency of bowel movements. To estimate confounding effects, plasma glucose concentration, and administered doses of opioids, laxatives and prokinetic drugs were analyzed. Measurements of GRV were standardized according to local nursing guidelines with nasogastric tubes all of the same type and diameter.

\*Correspondence: robert.patejdl@uni-rostock.de

<sup>2</sup> Oscar Langendorff Institute of Physiology, University Medical Center Rostock, Gertrudenstraße 9, 18057 Rostock, Germany  
Full list of author information is available at the end of the article

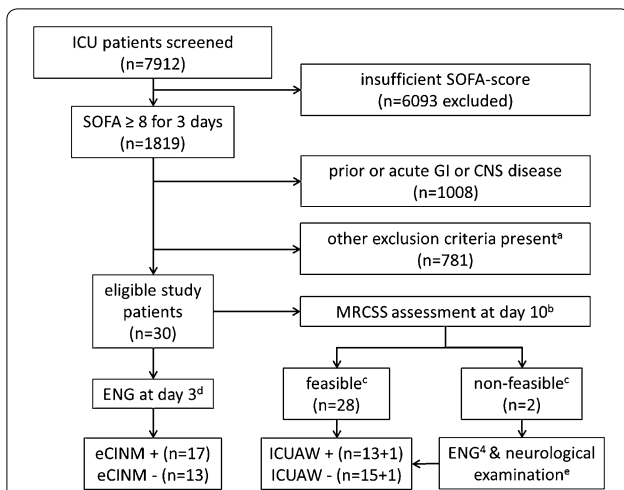


**Fig. 1** Selection of patient sample and classification of patients as eCINM± and ICUAW±. a: Exclusion criteria were: any pre-existing neuromuscular impairment or gastrointestinal disease of any kind, gastrointestinal surgery prior to ICU admission or within the following 14 days after admission to the ICU, high-dose glucocorticoid treatment (i.e., more than 300 mg of methylprednisolone or equivalent doses of other steroids), prior treatment at another ICU for more than 24 h, missing informed consent by the patient or a legal representative, participation in another clinical trial or expected imminent death. b: MRCSS is assessed by summing up strength scores graded 0–5 from each of 3 muscle groups of each extremity tested by instructing the patient to forcefully abduct the shoulder, flex the elbow, extend the wrist, flex the hip, extend the knee, and dorsiflex the foot. c: Eligibility for MRCSS testing was stated when a patient had to follow standardized requests: “Open and close your eyes”; “Look at me”; “Open your mouth and put out your tongue”; “Nod your head”; “Raise your eyebrows until I have counted to five”. d: see “methods” section for applied electrophysiological criteria of eCINM. e: Whenever MRCSS testing was not possible, patients were also classified ICUAW on day 10 if neurological examination revealed a symmetric flaccid palsy and a loss of deep tendon reflexes in all tested limb muscles

## Statistics

Statistics were done with MS-Excel 2010 (Microsoft, Redmond, WA, USA) and IBM SPSS Statistics (version 25, Chicago, IL, USA). According to the distribution of data (using Shapiro–Wilk test), Student’s *t* test or Mann–Whitney test was used for continuous variables. Chi-square test or Fisher’s exact test was used for categorical variables. Kendall’s  $\tau$  was calculated in bivariate correlations. For nonparametric analysis, we used partial rank correlations, and for two variables, a confounder corrected  $\tau$  ( $\tau_{\text{confounder}}$ ) was calculated. Statistical significance was considered at  $p < 0.05$ .

## Results

### Patient Demographics and Baseline Parameters

From 7912 patients screened initially, 30 of those (28 surgical and 2 non-surgical) that had been enrolled in the

original trial also met the additional criteria of this study (Fig. 1). At day 3, 17 patients were classified eCINM+ and 13 eCINM– according to ENG findings. With regard to the MRCSS at day 10 and the neurological examination, 16 patients were classified ICUAW+ and 14 ICUAW–. Irrespective of the classification, the different study groups were comparable in demographics and clinical baseline characteristics listed in Table 1, except for higher initial APACHE II, SOFA, and mNUTRIC scores in the group of patients classified as ICUAW+ at day 10.

### Clinical Nutrition, Motility, Laxative and Prokinetic Treatment in Relation to Neuromuscular Dysfunction

Results with regard to nutrition and GI motility are listed in Table 1. For all formed groups, the mNUTRIC score was  $>4$  and significantly higher in ICUAW+ patients, indicating high-risk for malnutrition. Concordantly, within 14 days both ICUAW+ and eCINM+ patients had fewer days with oral intake. Peroral alimentation was significantly reduced for almost all study days in ICUAW+ patients and at study day 5 in eCINM+ patients (Fig. 2a). Patients with ICUAW were longer dependent on nasogastric tubes and received more calories via tube feeding. Furthermore, none of the ICUAW+ patients received normal diet by day 14.

Mean daily GRV differed significantly in relation to the eCINM status. In ICUAW– patients, GRV was higher within the first seven days, whereas it tended to be lower in this subgroup from day 10 onwards. In contrast, mean GRV in eCINM+ patients was almost constantly equal or higher than in eCINM– patients. By individually analyzing days on mechanical ventilation, significantly more ICUAW+ patients needed nasogastric tube feeding than patients without ICUAW and the GRV was still higher in eCINM+ patients. Bowel movements were more frequently detected in ICUAW+ patients, but reduced in eCINM+ patients by analyzing days with intubation.

The duration of laxative treatment with lactulose and sodium picosulfate was significantly higher in the ICUAW+ group (lactulose: given on 63% of observation days in ICUAW+ patients vs. 40% in ICUAW–; sodium picosulfate: ICUAW+: 57%, ICUAW–: 34%,  $p < 0.001$  for both).

### Plasma Glucose, Opioids, and Narcotics in Relation To Neuromuscular Dysfunction

Mean daily plasma glucose concentrations were significantly higher in ICUAW+ and eCINM+ patients. The MRCSS, but not the number of ENG alterations, correlated significantly with the mean plasma glucose, but missed statistical significance when corrected for enteral nutrition in partial correlations (Fig. 2b–d).

**Table 1 Study population characteristics and surrogate parameters of clinical nutrition and gastrointestinal function**

Parameters	ICUAW+	ICUAW-	P value	eCINM+	eCINM-	p value
Study population characteristics						
Patient number (n)	14	16	N/A	17	13	N/A
MRCSS day 10 (n = 28)	29.3 ± 13.0	54.9 ± 4.6	<b>&lt;0.001</b>	40.6 ± 13.7	46.2 ± 18.8	0.38
Age (years)	68.2 ± 11.3	59.8 ± 15.5	0.19	67.2 ± 11.9	66.8 ± 15.9	0.94
Female	7/14	6/16	0.49	9/17	2/13	0.06
APACHE II	26.1 ± 3.5	22.9 ± 6.2	0.15	24.5 ± 5.6	24.2 ± 4.7	0.85
SOFA-score day 3	13.7 ± 3.1	9.4 ± 1.6	<b>&lt;0.001</b>	12.4 ± 3.4	10.2 ± 2.1	0.07
SOFA-score day 10	6.6 ± 3.2	3.9 ± 3.2	<b>0.004</b>	5.4 ± 3.3	4.8 ± 3.2	0.64
Patients with diabetes mellitus (n)	4/14	4/16	0.83	3/17	5/13	0.24
Surrogate parameters of clinical nutrition and gastrointestinal function						
Total observation period (days)	196	222	N/A	238	182	N/A
mNUTRIC score	7 ± 0.9	6 ± 1.6	<b>0.03</b>	4.8 ± 0.9	4.5 ± 0.9	0.39
Confirmed swallowing disorder** (n)	6/14	0/16	<b>0.005</b>	4/17	2/13	0.98
Days with nasogastric tube in situ (n)	160 (82%)	80 (36%)	<b>&lt;0.001</b>	143 (60%)	97 (53%)	0.16
Days with oral intake (n)	18 (9%)	117 (52%)	<b>&lt;0.001</b>	64 (27%)	71 (39%)	<b>0.014</b>
Patients receiving normal diet after 14 days (n)	0/14	6/16	<b>0.019</b>	2/17	4/13	0.19
Mean energy via feeding tube (kcal/day)*	1022 ± 777	205 ± 383	<b>&lt;0.001</b>	897 ± 734	830 ± 725	0.48
Days with GRV* (n)	100 (63%)	52 (65%)	0.78	99 (41%)	53 (29%)	<b>0.01</b>
Mean GRV per day (ml) *	157 ± 266	167 ± 240	0.78	194 ± 286	112 ± 189	<b>0.008</b>
Days with bowel movements (n)	82 (41%)	91 (43%)	0.92	108 (45%)	65 (36%)	0.06
Days with mechanical ventilation (n)	176 (89%)	104 (47%)	<b>&lt;0.001</b>	182 (76%)	98 (54%)	<b>&lt;0.001</b>
Days with nasogastric tube in situ (n)	143 (81%)	48 (46%)	<b>&lt;0.001</b>	139 (76%)	80 (82%)	0.37
Days with oral intake (n)	14 (8%)	29 (28%)	<b>&lt;0.001</b>	28 (15%)	15 (15%)	0.99
Mean energy via feeding tube (kcal/day)*	1017 ± 779	415 ± 470	<b>&lt;0.001</b>	906 ± 742	888 ± 722	0.85
Days with GRV* (n)	94 (61%)	18 (49%)	0.2	96 (53%)	47 (48%)	0.45
Mean GRV per day (ml)*	162 ± 267	181 ± 248	0.62	197 ± 289	117 ± 200	<b>0.03</b>
Days with bowel movements (n)	73 (41%)	45 (43%)	0.8	83 (46%)	35 (36%)	0.13
Days with endotracheal intubation	98 (50%)	50 (23%)	<b>&lt;0.001</b>	93 (39%)	55 (30%)	0.06
Days with Nasogastric tube in situ (n)	79 (81%)	35 (70%)	0.15	69 (74%)	45 (82%)	0.29
Mean energy via feeding tube (kcal/day)*	707 ± 688	358 ± 388	<b>0.01</b>	621 ± 677	596 ± 558	0.83
Days with GRV* (n)	46 (47%)	23 (46%)	0.92	41 (44%)	28 (51%)	0.42
Mean GRV per day (ml)*	94 ± 146	167 ± 254	0.14	121 ± 192	109 ± 183	0.84
Days with bowel movements (n)	28 (29%)	7 (14%)	<b>0.03</b>	21 (55%)	35 (64%)	<b>&lt;0.001</b>

Bold values indicate statistical significance

Data presented as sum or mean ± SD. Parameters indicated with "\*" are assessed only for days at which patients were supplied with a feeding tube. \*\*Number of patients with FEES-confirmed diagnosis of swallowing disorder. Patients were tested when were compliant, able to sit upright and follow specific commands  
*APACHE II* acute physiology and chronic health evaluation score II as assessed at ICU admission, *eCINM* early critical illness neuromyopathy, *GRV* gastric residual volume, *ICUAW* intensive care unit-acquired weakness, *mNUTRIC* modified nutrition risk in critically ill score, *MRCSS* Medical Research Council sum score, *SOFA* sequential organ failure assessment score

ICUAW+ and eCINM+ patients received opioids more frequently, but there was no difference in the treatment duration with sufentanil (most frequently administered opioid on 37% of all days). Patients without eCINM tended to receive sufentanil for a longer period. Administered sufentanil doses were significantly lower in ICUAW+ and eCINM+ patients.

Neither bivariate nor partial correlations (corrected for GRV) between the mean number of days at which

patients received opioids and the number of altered SNAP/CMAP sites reached significance (Fig. 2e). The same applied to the correlation between mean GRV and ENG alterations (corrected for days with opioids, Fig. 2f). In contrast, single-day GRV was correlated with the number of the patients' ENG alterations, even if corrected for sufentanil effects (Fig. 2g). There were no group differences in administered doses and application times of other opioids or narcotics.

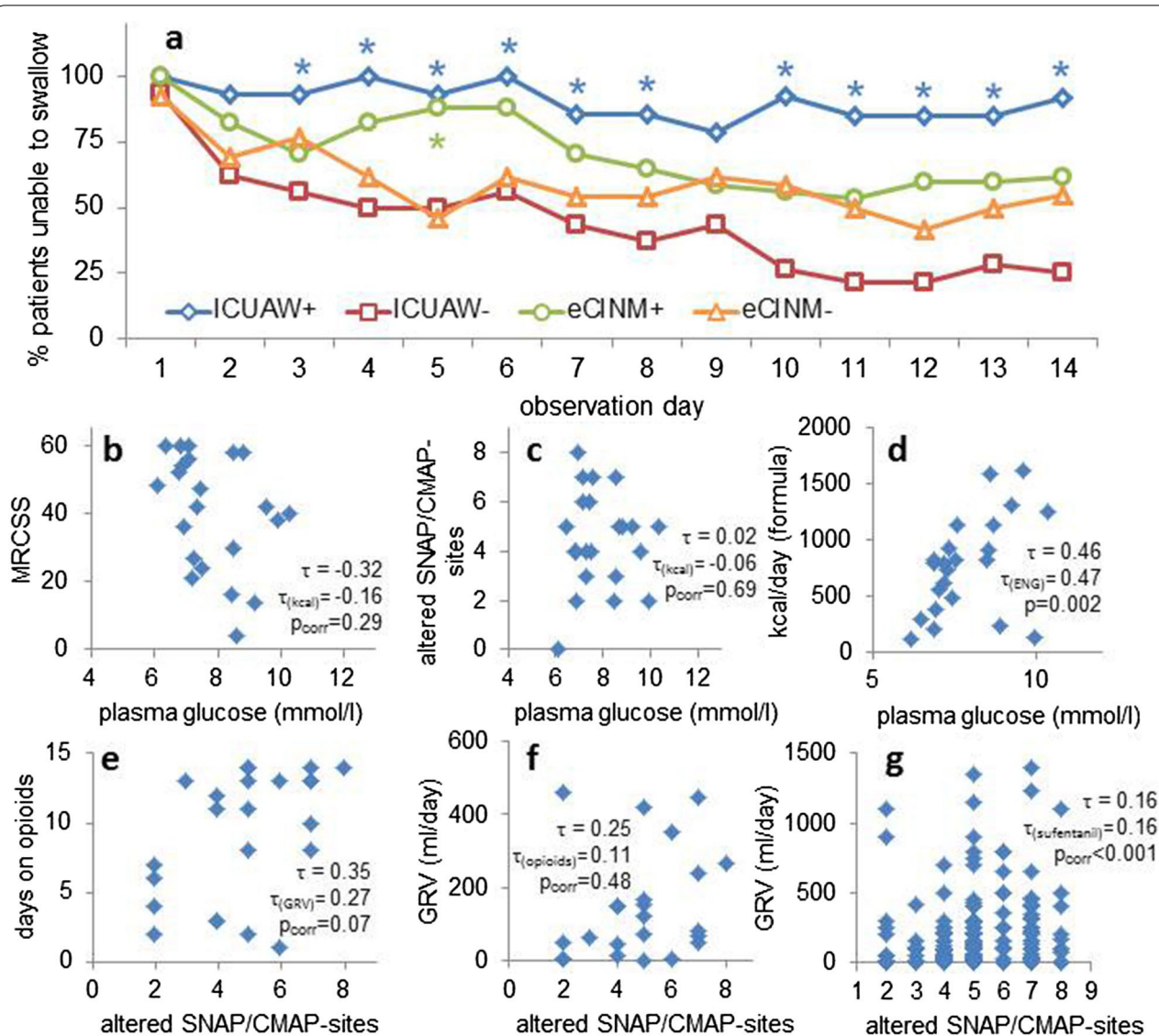


**Fig. 2 a** Changes in the percentage of patients receiving oral alimentation. The sample was divided into groups either based upon the results of muscle strength on day 10 (ICUAW ±) or depending on the results of an ENG on day 3 (CINM ±). Dots depict mean values calculated from the subsamples. Asterisks indicate significance of difference between respective groups at a level of  $p < 0.05$ . The patient numbers in each group are given in Table 1, line 1. eCINM: early critical illness neuromyopathy. ICUAW: intensive care unit-acquired weakness. **b-d** Correlations of mean daily plasma glucose levels of patients with MRCSS (**b**), the number of altered SNAP/CMAP sites in ENG (**c**) and enteral energy delivery (**d**,  $n = 22$  for all). Kendall's tau ( $\tau$ ) for the correlation of plasma glucose with MRCSS is  $> 0.299$  and thus per se significant. When corrected for energy delivered via the feeding tube, the correlation is not significant anymore. In the figures, " $p_{corr}$ " depicts  $p$  value after correction for delivered formula energy. **e-g** Correlations of the number of altered muscle/nerve recording sites on day 3 with overall opioid treatment (**e**), with GRV calculated as mean value of all GRV measured in single patients over the whole observation period (**f**) and with all single GRV values measured on sufentanil-treatment days (**g**). For mean calculations of GRV, only days when patients were supplied with a feeding tube were calculated. In the figures, " $p_{corr}$ " depicts  $p$  value after correction for GRV (**e**), for the number of days patients were on opioids (**f**), and for the administered daily dose of sufentanil (**g**). CMAP compound motor action potential. MRCSS Medical Research Council sum score. SNAP sensory nerve action potential

### Discussion

The results of this study indicate that alterations in electrophysiological parameters may be predictive for increased GRV, prolonged feeding tube dependence, less frequent bowel movements in intubated patients, prolonged opioid prescription, and decreased

sufentanil-dose demands in the later course of critical illness. When ICUAW status was assessable by day 10, ICUAW+ subjects had retrospectively suffered from more severe disease, had more often required mechanical ventilation, and had shown a prolonged dependency on tube feeding and opioids. Considering all this and the fact

that baseline SOFA and APACHE II scores were worse in this same group of patients, it seems likely that ICUAW merely reflects foregoing disease severity, whereas early CINM may predict upcoming gastrointestinal signs and symptoms independently from disease severity.

Since hyperglycemia is stated as a risk factor for ICUAW [6], increased glucose levels may either be a cause for or a consequence of ICUAW+ or eCINM+ status. As neither the MRCSS nor the number of ENG alterations was independently correlated with glucose levels (Fig. 2b, c), both findings do not support a causative role of hyperglycemia for the development of ICUAW or eCINM here.

Surprisingly, sufentanil doses were lower in ICUAW+ and eCINM+ patients by comparing days on mechanical ventilation. We hypothesize that the impairment of neuromuscular function influenced the clinical perception of opioid needs due to sensory impairment or muscular weakness with reduced pain-indicating movements. Despite our efforts to compensate opioid effects, we cannot rule out that some of the observed differences in GI function parameters are confounded by opioid exposure.

This study has some relevant limitations: First, the low number of patients resulted from our intended preselection of patients who were diseased so severely that GI and neuromuscular complications were likely to occur. This selection caused the small sample size, which limits the certainty of all stated statistical relations. Second, some of the observed effects were rather small. But although more sensitive functional tests or biomarkers might have yielded more specific results, it was our genuine interest to analyze the impact of ICUAW and eCINM on clinically accessible and relevant parameters. Third, our criteria to define eCINM were based on our monocentric reference values and differ from general definitions suggested by other groups. The decision to define own criteria was motivated by the fact that there are no generally applicable criteria for diagnosing eCINM in a cohort like ours [5].

The preliminary results of this exploratory study need verification in future studies. These may exclusively enroll critically ill surgical patients and combine the essential early electroneurographic assessment with more sensitive markers of GI function (e.g., sonographic or refractometric assessment of gastric transport) or measurement of biomarkers of nutrition and intestinal failure (e.g., prealbumin, citrulline, fatty acid-binding protein) [7]. Furthermore, we conclude that the concept of ICUAW is not suitable to study the potential relevance of neuromuscular impairment for early gastrointestinal complications of critical illness.

#### Author details

<sup>1</sup> Department of Anaesthesiology and Intensive Care Medicine, University Medical Center Rostock, 18057 Rostock, Germany. <sup>2</sup> Oscar Langendorff Institute of Physiology, University Medical Center Rostock, Gertrudenstraße 9, 18057 Rostock, Germany.

#### Acknowledgements

Open Access funding provided by Projekt DEAL.

#### Author contributions

FK, JE and RP contributed to the study conception and design and were involved in the acquisition and analysis of data. All authors contributed to the interpretation of data, drafting and revising the article and gave final approval of the version to be published.

#### Source of support

No external support was utilized for conducting this study.

#### Conflicts of interest

The authors declare that they have no conflict of interest.

#### Ethical Approval/Informed Consent

All procedures performed in studies involving human participants were in accordance with the ethical standards of the institutional and/or national research committee and with the 1964 Helsinki declaration and its later amendments or comparable ethical standards. Informed consent was obtained from all individual participants included in the study or from their legal representatives.

#### Open Access

This article is licensed under a Creative Commons Attribution 4.0 International License, which permits use, sharing, adaptation, distribution and reproduction in any medium or format, as long as you give appropriate credit to the original author(s) and the source, provide a link to the Creative Commons licence, and indicate if changes were made. The images or other third party material in this article are included in the article's Creative Commons licence, unless indicated otherwise in a credit line to the material. If material is not included in the article's Creative Commons licence and your intended use is not permitted by statutory regulation or exceeds the permitted use, you will need to obtain permission directly from the copyright holder. To view a copy of this licence, visit <http://creativecommons.org/licenses/by/4.0/>.

#### Publisher's Note

Springer Nature remains neutral with regard to jurisdictional claims in published maps and institutional affiliations.

Published online: 03 April 2020

#### References

1. Reintam Blaser A, Parm P, Kitus R, Starkopf J. Risk factors for intra-abdominal hypertension in mechanically ventilated patients. *Acta Anaesthesiol Scand.* 2011;55:607–14.
2. Rao M, Gershon MD. The bowel and beyond: the enteric nervous system in neurological disorders. *Nat Rev Gastroenterol Hepatol.* 2016;13:517–28.
3. Patejdl R, Kastner M, Kolbaske S, Wittstock M. Clinical nutrition and gastrointestinal dysfunction in critically ill stroke patients. *Neurol Res.* 2017;39:959–64.
4. Garnacho-Montero J, Madrazo-Osuna J, Garcia-Garmendia JL, et al. Critical illness polyneuropathy: risk factors and clinical consequences. A cohort study in septic patients. *Intensive Care Med.* 2001;27:1288–96.
5. Stevens RD, Marshall SA, Cornblath DR, et al. A framework for diagnosing and classifying intensive care unit-acquired weakness. *Crit Care Med.* 2009;37:S299–S308.
6. van den Berghe G, Schoonheydt K, Becc P, Bruyninckx F, Wouters PJ. Insulin therapy protects the central and peripheral nervous system of intensive care patients. *Neurology.* 2005;64:1348–53.
7. Moreira TV, McQuiggan M. Methods for the assessment of gastric emptying in critically ill, enterally fed adults. *Nutr Clin Pract.* 2009;24:261–73.